UNIVERSITY OF MINES AND TECHNOLOGY TARKWA

FACULTY OF MINERAL RESOURCES TECHNOLOGY

GEOLOGICAL ENGINEERING DEPARTMENT

A THESIS REPORT ENTITLED

GRADE AND TONNAGE RECONCILIATION OF AFC1 REEF AT KOTTRAVERCHY PIT, GOLDFIELDS GHANA LIMITED, TARKWA MINE.

BY

ALFRED KWEKU ESSUMAN

SUBMITTED IN FULFILLMET OF THE REQUIREMENT FOR THE AWARD OF THE DEGREE OF MASTER OF SCIENCE IN GEOLOGICAL ENGINEERING

THESIS SUPERVISOR

……………………………………………..

ASSOC. PROF SULEMANA AL-HASSAN

AUGUST, 2020

DECLARATION

I declare that this thesis is my own work. It is being submitted for the Master of Science (MSc) Degree in the University of Mines and Technology (UMaT), Tarkwa. It has not been produced by anyone for a degree or examination in any other University.

……………………………………   ………………………………

Candidate's Signature   Declaration Date

ABSTRACT

Reconciliation is a vital aspect of checking and measuring variation or discrepancies between variables in the mining industry since it evaluates performance in mining ore. It is therefore necessary to have a good estimation method that can predict tonnages and grades with minimal errors as much as possible.

The Afc1 reef at Kottraverchy pit has seen discrepancies in the grade and tonnage values of the ore deposit. Tonnage is underestimated and grades overestimated. This could be attributed to the method of estimation.

Goldfields Ghana Limited Tarkwa Mine uses Ordinary Kriging a linear interpolation method as their method of estimation. Though it had proved well with the Tarkwaian deposit, estimation of Afc1 reef which has highly skewed distribution produces poor reconciliation results. Multiple Indicator Kriging is one of the few non-linear estimation techniques that can cope with highly skewed or difficult distributions and addresses some of the deficiencies of the linear estimation techniques.

This research estimated the Afc1 reef using OK and MIK and compared their estimated values with the actuals.

Figures obtained from OK estimate of Afc1 for 2013 was 235,771.75t with an average grade of 0.75g/t. MIK estimates was 272,855.79t with an average grade of 0.69g/t. And Afc1 ore mined for 2013 was 276,482.73t with an average grade of 0.70g/t.

MIK was recommended as a better method for estimating Afc1 reef since its estimates compared better with the actuals.

ACKNOWLEDGEMENT

I am highly indebted to God Almighty for giving me the strength, determination and creating the chance for me to complete this thesis. I also express my heartfelt gratitude to my supervisor Assoc. Prof Sulemana Al-Hassan for supervising me through this work.

I thank the management of Goldfields Ghana Limited Tarkwa Mine for bearing part of the cost of this study and giving me the opportunity to attend this MSc Programme.

To Dr. Mrs Fiadonu my internal supervisor and Mr. David Adjei, I sincerely appreciate the time and energy you used and the advice which made this thesis worthwhile.

I thank the University of Mines and Technology, Tarkwa for affording me the opportunity to complete this thesis and making their facilities available.

To all those who supported me with advice and inputs I say thank you and may God richly bless you.

TABLE OF CONTENTS

CHAPTER 1		1
INTRODUCTION		1
1.1	Background Information	1
1.2	Statement of The Problem	1
1.3	Research Objectives	3
1.4	Expected Outcomes	3
1.5	Methods Used	3
1.6	Facilities Used	4
1.7	Thesis Organisation	4
CHAPTER 2		5
RELEVANT INFORMATION ABOUT THE MINE		5
2.1	History of the Mine.	5
2.2	Mine Ownership	5
2.3	Location and Accessibility	6
2.4	Topography	7
2.5	Drainage	8
2.6	Climate	8
2.7	Vegetation, Soil and Land Use	8
2.8	Geological Settings	8
2.8.1	The Kawere Group	10
2.8.2	The Banket Series	11
2.8.3	Tarkwa Phyllites	11
2.8.4	Huni Sandstone	12
2.8.5	Local Geology	12
2.8.6	Deposit Geology and Mineralisation	14
2.9	Mining Practices	14
2.9.1	Grade Control	15
2.9.2	Treatment Plant	15

CHAPTER 3 16
LITERATURE REVIEW 16
3.1 Introduction 16
3.2 Data Collection, Sample Analysis and Database Quality 16
3.2.1 Data Collection 16
3.2.2 Sample Analysis 16
3.2.3 Database 17
3.3 Statistical Concepts in Mineral Resource Estimation 18
3.3.1 Analysis of Data Distribution 18
I. The mean 19
II. The Median 19
III The Variance 20
IV. Skewness 20
V Kurtosis 21
VI. Coefficient of Variation(CV) 21
3.4 Data Compatibility 22
3.4.1 F-test 22
3.4.2 t- test 22
3.5 Effects of Outliers 23
3.6 Mineral Resource Estimation Methods 24
3.6.1 Classical Methods 24
3.6.2 Geostatistical Methods 26
i) Linear Estimation Methods 26
ii) Non Linear Estimation Methods 28
3.6.3 Variography 35
3.7 Model 36
3.7.1 Spherical Model 38
3.7.2 Anisotropy 41
3.7.3 Cross-Validation of Semi-Variogram Model 42
3.8 Orebody Modelling 43
3.8.1 Types of Modelling 44

CHAPTER 4 48

DATA ACQUISITION AND ANALYSIS 48

4.1 Introduction 48

4.2 Data Management 48

4.2.1 Data Acquisition 48

4.2.2 Data Validation 49

4.2.3 Data Processing 55

4.3 Combination of Data, Wireframing, Compositing and Distribution Analysis 58

4.3.1 Combination of Diamond Drill and RC Samples 58

4.3.2 Wireframe Modelling 59

4.3.2 Sample Selection and Compositing 61

4.3.4 Distribution Analysis 61

4. 4 Variogram Modelling 63

4.4.1 Variography for OK 64

4.4.2 Variography for MIK 67

4.5 Block Modelling 77

CHAPTER 5 79

RESOURCE ESTIMATION AND ANALYSIS 79

5.1 Resource Estimation 79

5.1.1 Grade estimation using the OK Method 79

5.1.2 Resource Estimation by MIK 82

5.2 Results and Discussions 86

5.2.1 Introduction 86

5.2.2 Reconciliation 90

CHAPTER 6 93

CONCLUSIONS AND RECOMMENDATIONS 93

6.1 Conclusions 93

6.2 Recommendations 93

REFERENCES 94

APPENDICES 101

LIST OF FIGURES

Figure 1.1	A Graph Comparing AFC1 Actual to OK tonnes (t) from January to December 2013	2
Figure 1.2	A Graph Comparing AFC1 Actual to OK Grade (g/t) from January to December 2013.	2
Figure 2.1	Map Showing Goldfields Ghana Limited, Tarkwa Concession (After Smith, 2012)	6
Figure 2.2	The Map of Ghana showing the location of Tarkwa (*After: Kaperta, 2001*).	7
Figure 2.3	Map of Geology of Ghana (Modified after Smidley, 1996)	10
Figure 2.4	Stratigraphic Profile of Tarkwa Orebody from West to East (After Karpeta, 2001).	13
Figure 3.1	Types of Frequency Distribution Curves	21
Figure 3.2	MIK estimate of the cumulative distribution of gold grades (After Sinclair and Blackwell, 2002).	31
Figure 3.3	Hypothetical block surrounded by nine samples for MIK (Source: Anon., 2011).	32
Figure 3.4	Cummulative Frequency Function (CFF) for MIK	34
Figure 3.5	Models with a sill (Olea, 1999).	38
Figure 3.6	A Spherical Model with its Main Components (Source: Olea, 1999)	39
Figure 3.7	Semi-variogram showing Nested Structure (After Clark, 2001).	41
Figure 3.8	Geometric anisotropy showing different ranges with the same sill and 3.8(b) Zonal anisotropy showing the same range with different sills in 3D regionalisation (Source: Dohm, 1980)	42
Figure 3.9	Cross validation scatter plot of Actual versus Estimated.	43
Figure 3.10	Cross-sectional model (Kwofie, 1993).	44
Figure 3.11	The three kinds of strings (Kwofie, 1993).	45
Figure 3.12	Triangular Wireframe (Kwofie, 1993).	45
Figure 3.13	A Three Dimensional Wireframe Models (Kwofie, 1993)	46
Figure 3.14	A typical Block Model (After Anon., 2002).	47
Figure 4.1	Plan View of Drillhole Layout of the study area.	49

Figure 4.2	Pulp Blank Samples Performance against Detection Limit 0f 0.001 g/t.	51
Figure 4.3	Coarse Blank Samples Performance against Detection Limit 0f 0.005 g/t.	51
Figure 4.4	Scatter Plot of Field Duplicates on Original Au Values	52
Figure 4.5	HARD Plot of Field Duplicate Samples	54
Figure 4.6	Plots of Assay Results of HGST OxK69 (3.58 g/t) against ±3 Standard Deviation.	55
Figure 4.7	Cross section plot of AFc1 reef digitised wireframe string along 10900 N.	60
Figure 4.8	Isometric view of modelled orebody	61
Figure 4.9	Histogram with Cumulative Frequency of 1 m composite of AFC1 Reef.	62
Figure 4.10	Log Probability Plot of the Distribution of 1 m Composites of AFc1 Deposit.	63
Figure 4.11	Afc1 Reef Omni-directional Variogram (Downhole)	64
Figure 4.12	Afc1 Reef Directional Semi-variogram Along Strike Direction.	65
Figure 4.13	Afc1 Reef Directional Semi-variogram Across Strike Direction.	65
Figure 4.14	Variogram Map of Major Mineralisation Continuity.	66
Figure 4.15	Plan View of Search Ellipsoid Derived from Variogram Map Analysis	67
Figure 4.16	Indicator Downhole Variogram for 0.5 ppm cut-off.	69
Figure 4.17	Indicator Variogram Along Strike Direction for 0.5 ppm cut-off.	70
Figure 4.18	Indicator Variogram Across Strike Direction for 0.5 ppm cut-off.	70
Figure 4.19	Indicator Downhole Variogram for 1.0 ppm cut-off.	71
Figure 4.20	Indicator Variogram Along Strike Direction for 1.0 ppm cut-off.	71
Figure 4.21	Indicator Variogram Across Strike Direction for 1.0 ppm cut-off.	72
Figure 4.22	Indicator Downhole Variogram for 1.5 ppm cut-off	72
Figure 4.23	Indicator Variogram Along Strike Direction for 1.5 ppm cut-off	73
Figure 4.24	Indicator Variogram Across Strike Direction for 1.5 ppm cut-off.	73
Figure 4.25	Scatter Plot of Actual on Predicted (Kriged) Values of OK Semi-Variogram Spherical Models	76
Figure 4.26	Scatter Plot of Actual on Predicted (Kriged) Values of Indicator Semi-Variogram Spherical Models	77

Figure 4.27	Area Mined from Kottraverchy Block Model in 2013	78
Figure 5.1	Cross –Sectional Views of Composite and OK model grades 11500 N along strike of the Orebody.	80
Figure 5.2	Cross –Sectional Views of Composite and OK model grades 4200 E across strike of the Orebody.	80
Figure 5.3	Scatter Plot of OK model and Composite grades on 11500 N along strike of the Orebody.	81
Figure 5.4	Scatter Plot of OK model and Composite grades on 4200 E across strike of the Orebody.	81
Figure 5.5	Cross –Sectional Views of In-situ Drillhole Composite and MIK Model Grades of 11500 N Along Strike Direction of the Orebody.	84
Figure 5.6	Cross –Sectional Views of In-situ Drillhole Composite and MIK Model Grades of 4200 E across Strike Direction of the Orebody.	84
Figure 5.7	Scatter Plot of MIK model and Composite grades on 11500 N along strike of the Orebody.	85
Figure 5.8	Scatter Plot of MIK model and Composite grades on 4200E across strike of the Orebody.	85
Figure 5.9	Bench by Bench Model Tonnages of OK and MIK Method against Actual Tonnes of AFC1-Reef.	87
Figure 5.10	Bench by Bench Model Grades of OK and MIK Method against Actual Grades of AFC1-Reef.	88
Figure 5.11	Scatter Plot of Bench by Bench O.K on Actual Grades of AFC1 Reef Zone	89
Figure 5.12	Scatter Plot of Bench by Bench MIK on Actual Grades of AFC1 Reef Zone	89
Figure 5.13	Grade- Tonnage Relationship of AFC1 Reef Zone	90
Figure 5.14	A Graph Comparing AFC1 Actual to OK and MIK Grade(g/t) from January to December 2013	91
Figure 5.15	A Graph Comparing AFC1 Actual to OK and MIK Tonnes (t) from January to December 2013	92

LIST OF TABLES

Table 3.1	Interval Statistics on the Data	32
Table 3.2	Chosen cut-offs applied to the sample data and their converted indicators	33
Table 3.3	Probabilities of block below an indicator	33
Table 3.4	Indicator Kriged Estimate	35
Table 3.5	Semi-variogram models.	36
Table 4.1	Certified Referenced Material Inserted in Samples	55
Table 4.2	Surpac File Structure for Survey Data	56
Table 4.3	Surpac File Structure for Collar Data	56
Table 4.4	Surpac File Structure for Geology Data	57
Table 4.5	Surpac File Structure for Assay data	57
Table 4.6	Summary of Input Data Statistics for the Orebody	58
Table 4.7	Summary of univariate statistic of 1 m gold composite for the AFc1- Reef Zone.	62
Table 4.8	Semi-variogram Parameters for OK for Afc1 Reef	66
Table 4.9	Conditional Statistics	68
Table 4.10	Afc1 Reef Indicator Variogram Parameters for MIK	74
Table 4.11	Indicator Variogram Anisotropic Factors	74
Table 4.12	Summary Statistics of OK Spherical Variogram Model Validation	75
Table 4.13	Summary Statistics of Indicator Spherical Variogram Model Validation	75
Table 4.14	Summary of Afc1 Ore Block Model Parameters.	77
Table 5.1	Estimation Parameters used for OK	79
Table 5.2	OK Resource Estimates of AFc1 Reef	82
Table 5.3	Estimation Parameters used for MIK	83
Table 5.4	MIK Resource Estimates of AFc1 Reef	86
Table 5.5	Bench by Bench Average Grades and Tonnages of OK, MIK estimates and the Actuals mined from Pit.	86

CHAPTER 1

INTRODUCTION

1.1 Background Information

Tarkwa, the administrative capital of the Tarkwa-Nsuaem Municipality (TNM) is located in the south western part of Ghana. The area has been an important mining town, which has seen mining of both Gold and Manganese for many years.

Goldfields Ghana Limited (GGL) currently undertakes a large open pit operation utilizing the selective mining method which involves the stripping of the ore from waste, in order to minimize ore loss and dilution. The company employs Ordinary Kriging (OK) method as its estimation method for the ore deposit since OK has gained much recognition and is considered as Best Linear Unbiased Estimator (BLUE).

1.2 Statement of The Problem

Goldfields Ghana Limited uses the Ordinary Kriging (OK) method as their estimation method for the ore in some part of the deposit. Linear estimation models such as OK often produce good estimates but may encounter problems estimating recoverable reserves in cases where the distribution of samples is highly skewed (Isaaks and Srivastava, 1989). Reconciliation of Afc1 reef at Kottraverchy pit has seen very significant grade and tonnage discrepancies since this method has been found to consistently overestimate grade and underestimate tonnage as shown in Fig 1.1 and 1.2 respectively. This raises the question: could there be an alternative estimation method that can improve grade and tonnages of ore blocks other than OK?

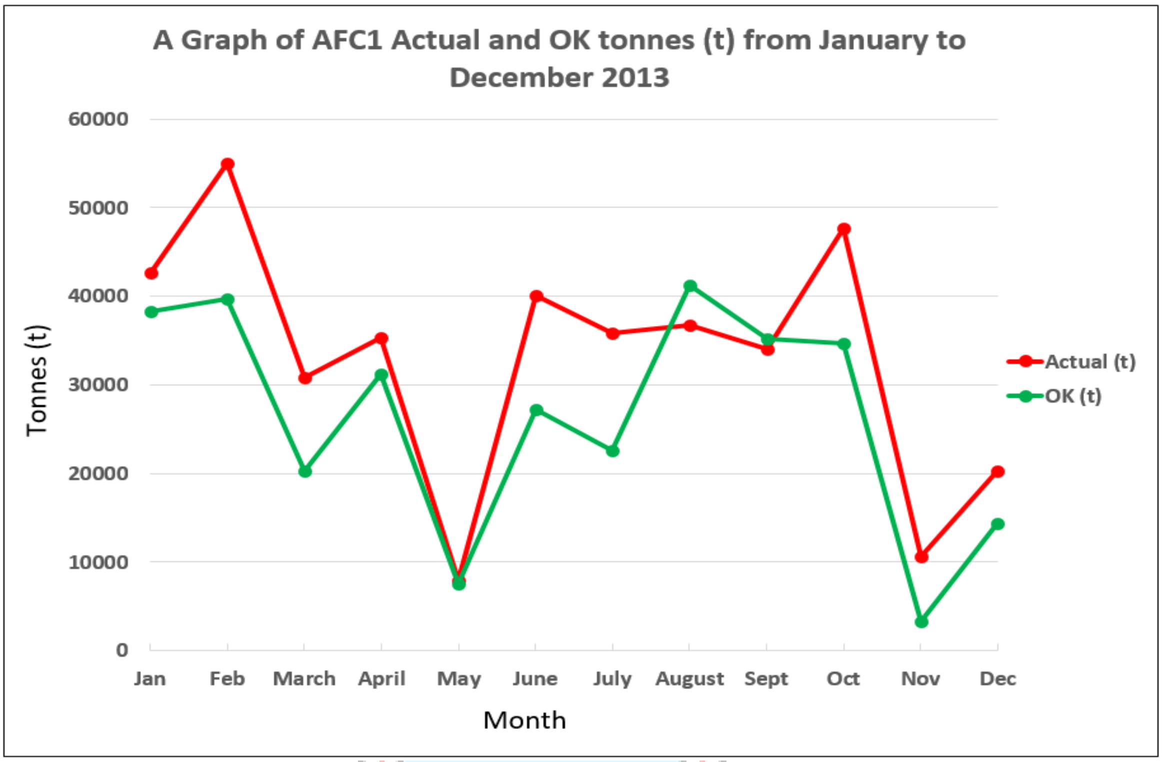

Figure 1.1 A Graph Comparing AFC1 Actual to OK tonnes (t) from January to December 2013

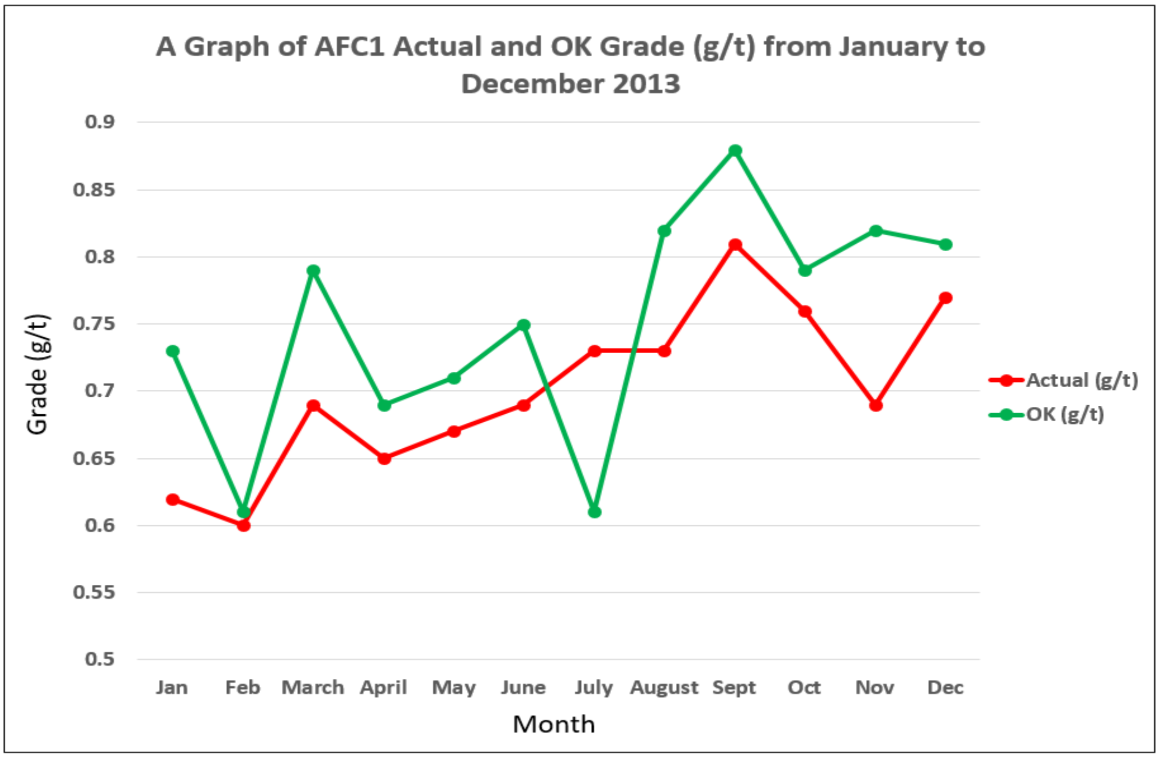

Figure 1.2 A Graph Comparing AFC1 Actual to OK Grade (g/t) from January to December 2013

Multiple Indicator Kriging (MIK) is one of the few non-linear methods of estimation technique that is able to cope with highly skewed distributions and addresses some of the deficiencies of the linear methods (Sinclair and Blackwell, 2002). It is simply the use of ordinary kriging or simple kriging to estimate a variable (e.g. grade) that has been transformed into an indicator variable. In this way, each value of the variable is transformed into zeros (0) and ones (1) depending on whether the value is above or below a given indicator threshold (cut-off). This research therefore, seeks to investigate the possibility of using the non-linear method of estimation (Multiple Indicator Kriging) to investigate whether there could be an improvement in the grade and tonnage reconciliation of the Afc1 reef at Kottraverchy pit.

1.3 Research Objectives

This research seeks to:

(a) Review the current resource estimation methods used to estimate the Kottraverchy deposit at Goldfields Ghana Limited Tarkwa mine;

(b) Employ Ordinary Kriging and Multiple Indicator Kriging for estimation of grade and tonnage to minimise the discrepancy between modelled and actual grade and tonnage on the Afc1 reef at Kottraverchy pit using the same mineralisation envelope and;

(c) Reconcile the estimates of OK and MIK with actual figures within the same wireframe model.

1.4 Expected Outcomes

It is expected that the differences in modelled and actual grades and tonnages will be minimised.

1.5 Methods Used

Methods used include:

(a) Review of relevant literature;

(b) Data acquisition of the study area and data validation;

(c) Data processing;

(d) Extraction of cross sections and digitizing of ore zones within the deposit;

(e) Creation of wireframe and modelling of the deposit including geological structures;

(f) Statistical and Geostatistical analyses of retrieved data from the wireframe model;

(g) Estimation of mineral resource by OK and MIK;

(h) Comparison of the estimates from the two estimation methods with actual production values from the same blocks.

1.6 Facilities Used

Facilities used include the following:

(a) UMaT library, computers and internet facilities.

(b) Gemcom software (Surpac 6.5.1) available at GFGL

1.7 Thesis Organisation

This project work has been divided into six (6) main chapters.

The introductory chapter is chapter 1 and it gives a broad outline of the work. Chapter 2 focuses on relevant information with regard to Goldfields Ghana Limited, Tarkwa as well as the geological settings of the area. Chapter three 3 deals with literature review of the general processes employed in mineral resource estimation. Chapter 4 covers on processes used in the resource estimation of the Kottraverchy Afc1 reef and this include data acquisition and validation, data processing and digitisation of ore zones, statistical analysis and semi-variogram analysis, wireframe and Block Modelling. Chapter five (5) dilates on the results obtained from grade interpolation and resource estimation using OK and MIK methods and the comparison of results from the two methods used. Chapter six (6), the last chapter, consist of conclusions and recommendations.

CHAPTER 2

RELEVANT INFORMATION ABOUT THE MINE

2.1 History of the Mine.

Goldfields Ghana International acquired Tarkwa Gold Mine in 1993. Historically, it was an underground gold mine and later converted to large-scale open pit mine in 1998 (Kaperta, 2001). Mining in Tarkwa dates back from the 19th century when the area was visited by C. J. Bonnat, a Frenchman in early 1877, and saw extensive artisanal workings in the vicinity of the present Tarkwa town. In 1878, Mr. Bonnat took out concessions within the Tarkwa area and started mining. The concession was then acquired by the British who operated till 1935 when the Amalgamated Banket Area Limited (ABA) bought the mining concession (Kesse, 1985). This group operated till Ghana attained independence, when the then government took over in 1961 and established Tarkwa Goldfields Limited (TGL) as one of the mines of the State Gold Mining Corporations (SGMC). The operations of TGL were characterised with mismanagement, and lack of political will on the part of the central government, to invest significantly into its operations (Karpeta, 2001). This led to its divestiture in 1993, and was thus acquired by GGL, a South African company. TGL which was essentially an underground mine was operated by GGL, until 1999 when GGL closed down all its underground operations, and concentrated only on its surface mine operations till date.

2.2 Mine Ownership

Goldfields Ghana Limited holds 90% of the issued shares after acquiring the indirect 18.9% of the issued shares belonging to IAMGOLD Cooperation and its affiliates. The government of Ghana holds a 10% free carried interest, as required by Minerals and Mining Law 2006 (Act-703). GFGL operates under seven mining leases covering a total area of approximately 207 km^2 as shown in Figure 2.1

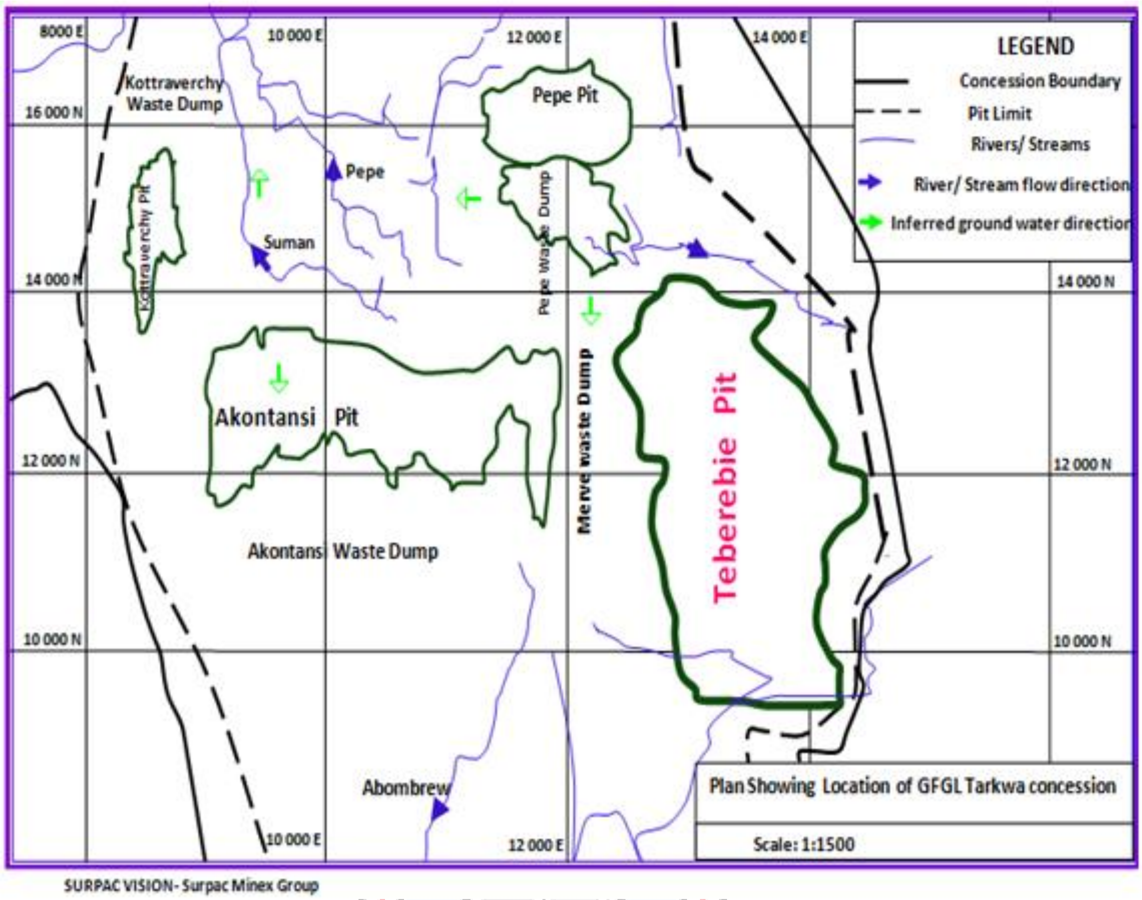

Figure 2.1 Map Showing Goldfields Ghana Limited, Tarkwa Concession (After Smith, 2012)

2.3 Location and Accessibility

Goldfields Ghana Limited (GGL) operates the Tarkwa surface mine, which forms part of the 207 km^2 Tarkwa concession and is located to the north, and northwest of the town of Tarkwa in the Western Region of Ghana. It is about 300 km by road west of Accra, the capital of Ghana, and is located on latitude 5°15’ N and longitude 2° 00’ W. GGL is about 60 km NW of the port of Takoradi on the Atlantic coast. Power is available from the Volta River Authority via an existing 161 kV power line to the mine. Figure 2.2 is a Map of Ghana showing the location of Tarkwa.

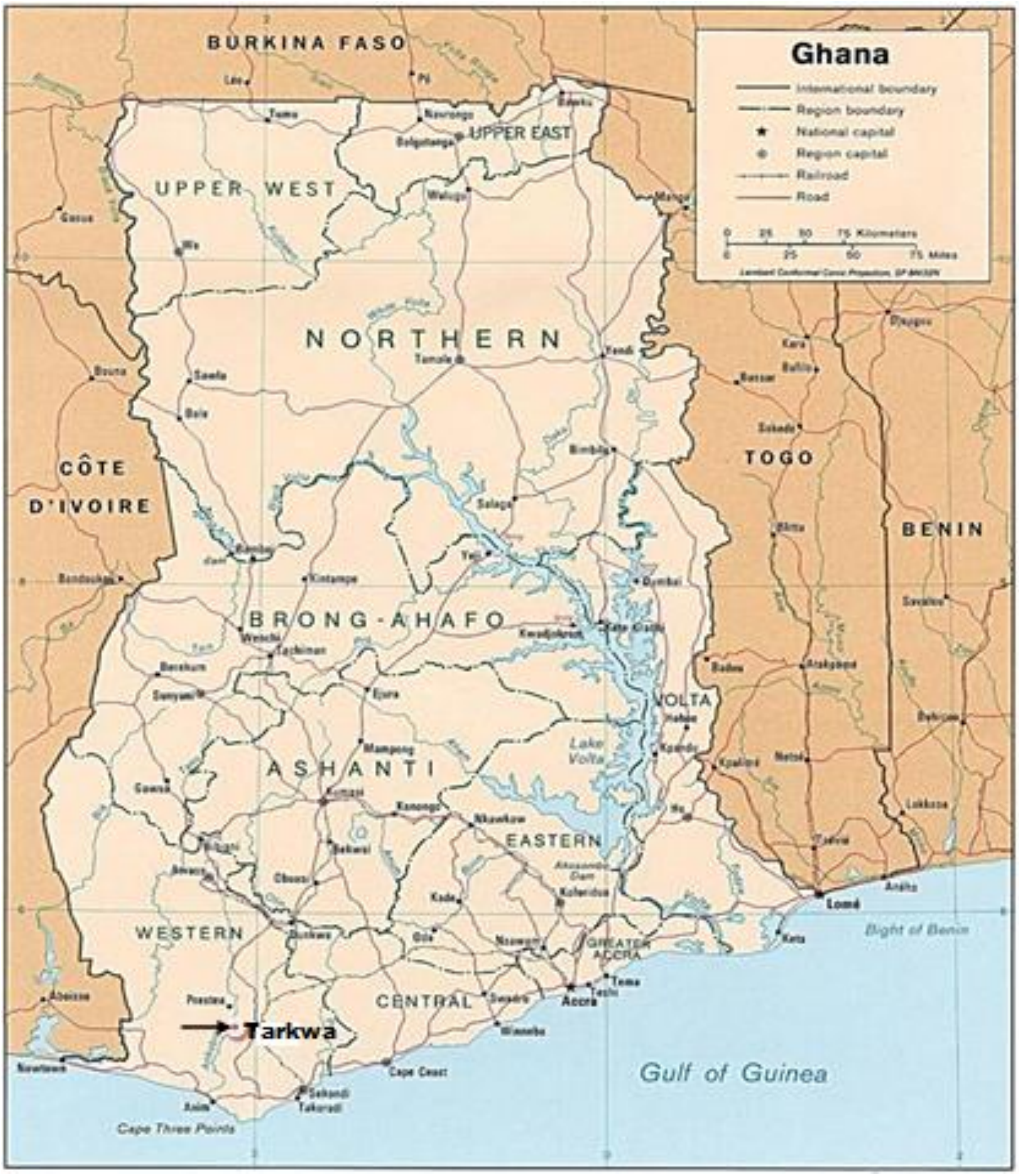

Figure 2.2 The Map of Ghana showing the location of Tarkwa (*After: Kaperta, 2001*).

2.4 Topography

The topography of the mine site is dominated by pronounced ridges and valleys. The ridges are composed of the Banket formation and phyllites with the low-lying areas dominated by sandstones/quartzites. The ridges and valleys are parallel to one another and to the general NE-SW strike of the underlying geology, a feature which lends itself to the pitching fold structures and dip and scarp slopes in the Banket Series and Tarkwa Phyllites (Wright, 1997). Transverse to the ridges and valleys are smaller valleys and gaps determined by faulting and jointing (Whitelaw, 1929). Elevations in the area range from approximately 45 m to 320 m (Karpeta, 2000). The central areas of the lease is low lying and flatter and does not show the variations in elevation typical of the southern and eastern areas near Tarkwa and Akontansi. The lowest point of the catchment area lies to the northwest of Tarkwa (Kesse, 1985).

2.5 Drainage

The drainage system comprises a number of streams that are nearly inactive in dry seasons. The concession is drained to the west of the lease. No major rivers traverse the mining area. The nearest one is the Huni River some 8 km to the northwest and flows along the concession boundary. The extreme southern portions of the lease are drained by the Bonsa River and its tributaries (Adjei, 2015).

2.6 Climate

The climatic condition in Tarkwa is typically equatorial with two main seasons. The wet season spans from April to July and from September to November whilst the dry season occurs from December to March. Mean annual rainfall is approximately 2000 mm and monthly temperatures are in the range of 21-32^0 C (Sestini, 1973). There is no major interruption to operations since climatic influence is minimal (Kaperta, 2000).

2.7 Vegetation, Soil and Land Use

The vegetation of the area can be categorised into moist semi deciduous forest mixed with tropical rain forest. But due to the activities of the population in the area, the vegetation in the vicinity of the concession has been altered to secondary forest, scrub and slash and burn farmland (Wright, 1997). The soils in the study area comprise predominantly of laterite (mainly of hydrated iron oxides with silica impurities) and red in colour with a pH of 4-5, with low organic contents. The soils are of poor fertility and highly leached due to high rainfall experienced in the area (Sestini, 1973).

2.8 Geological Settings

The Tarkwa surface mine is located almost at the southern end of the Tarkwa syncline (also called the Tarkwa Basin). The Tarkwa Basin stretches from Axim in the south to the edge of the Voltaian basin near Agogo in the Ashanti Akim District, a distance of about 250 km, and has a width of about 16 km (Kesse, 1985). The syncline rests on a folded and metamorphosed rock sequence of early Proterozoic age called the Birimian, which play host to the famous Obuasi gold deposits near Kumasi. This sequence consists of NNE-SSW trending alternations of meta-sediments and meta-volcanics called "basins" and "belts" respectively as shown in Figure 2.3

Two major tectonic (orogenic) events, within the Proterozoic era have been identified within the Birimian and Tarkwaian rocks. The first is Eburnean I orogeny (2200 - 2150 Ma) which was associated with the eruption of the Birimian mafic volcanics and intrusion of the Dixcove granitoids (Allibone *et al*., 2002) and is believed to have affected only the Birimian rocks. The second orogeny, Eburnean II resulted in the strong NE- trending structural grain associated with tight to isoclinal folding with major thrust faults, which typically separated the Birimian metasedimentary rocks from the Birimian metavolcanic rocks (Leube *et al*., 1990: and Eisenslohr and Hirdes, 1992). Eburnean II is believed to have also affected the Tarkwaian rocks based on the fact that similar styles and orientations of deformational fabrics are found within the Birimian and the Tarkwaian (Osei, 2015 and Oberthur *et al*., 1998). During the eburnean orogeny, there was upliftment and deformation of the Birimian. Accumulation of products of erosion were deposited as shallow water deltaic sediments which are believed to form the lithology of the Tarkwaian (Hirdes *et al*, 1992). The Tarkwaian consists of a thick sequence of clastic metasedimentary rocks that have suffered low grade regional metamorphism, contemporaneous or latter shearing and alteration by hydrothermal activity (Osei, 2015). Several large scale and minor faults and are well known within the Tarkwaian and a set of basic and felsic dykes also crosscut its stratigraphy (Kesse, 1985). According to Junner *et al* (1942), the Tarkwaian system can be subdivided into four stratigraphic mapable units as Kawere Group at the base, Banket Series, Tarkwa Phyllites and Huni Sandstone. The common minerals associated with the Tarkwaian include: chlorite, sericite, zoisite, calcite, quartz, lemonite and chloritoid (Kesse, 1985).

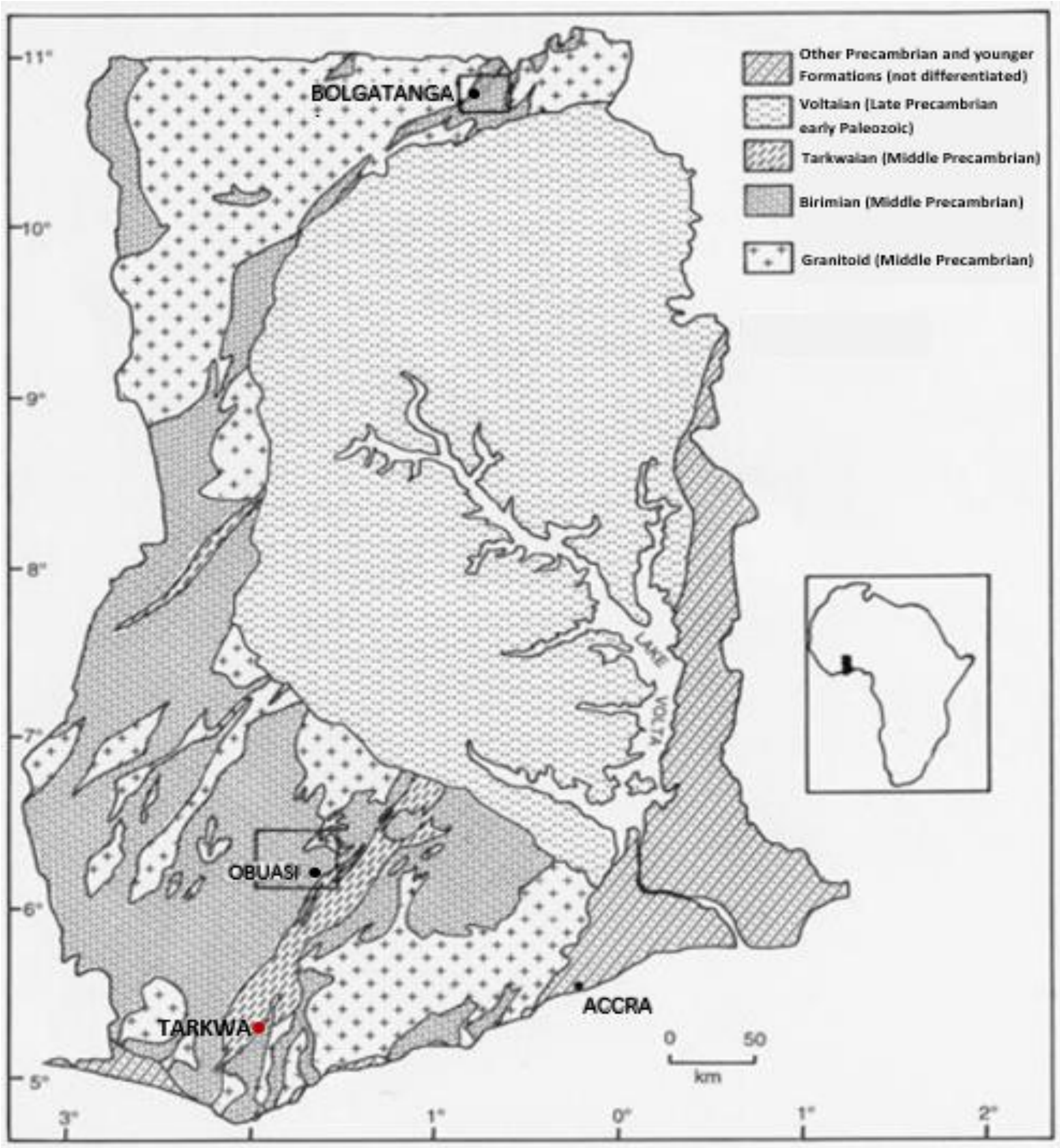

Figure 2.3 Map of Geology of Ghana (Modified after Smedley, 1996)

2.8.1 The Kawere Group

The unit consists typically of shallow water greenish-grey feldspathic quartzite, sandstone and grits, polymictic, poorly sorted large pebble conglomerate and argillites. The presence of sedimentary structures indicates fluvial origin; and, clasts of Birimian lithology indicates rocks of super group to be a partial source (Pigois et al, 2003). The quartz and grits are also normally greenish - grey in colour and it is known to be of noneconomic gold mineralisation. It varies in thickness from 250-700 m (Kesse, 1985).

2.8.2 The Banket Series

Economic gold mineralisation occurs in the Banket Series which is composed of stacked fluvial sedimentary rocks developed within a braided river system about two billion years ago (Osei, 2015). Essentially, the deposit may be described as fossil placer, in which the gold was deposited simultaneously with the sediments. This unit is about 120 m to 600 m thick and exposed in relatively open folds (Kesse, 1985). The stratigraphy of the Banket Series of the mine can be broadly divided into three units. These are;

1) Distinct barren footwall quartzite,
2) Conglomerates / pebbly quartzites and
3) An upper quartzite.

Junner *et al* (1942) identified four distinguishable reefs within the Banket Series as;

I. Breccia reef
II. Middle (West) reef
III. Basal (Main) reef
IV. Sub-basal reef

The Breccia reef is largely polymictic whiles the Basal reef is oligomitic.

The basal and middle reefs have well sorted and rounded quartz pebbles. These conglomerate reefs are gold rich and have been mined over the years.

Dykes and sills of dolerite and aplite are the main intrusive in the Banket and are spatially associated with quartz veins which occur within the sequence in the vicinity of structured discontinuities (Kesse, 1985).

2.8.3 Tarkwa Phyllites

This formation unconformably overlies the Huni sandstone and is composed of sandstones which are finely laminated and graded argillites, with interbedded green sandstone interpreted to be a lacustrine deposit. It is about 120m – 150m thick and can be divided into phylite with chloritoid and those whithout chloritoid (Sestini, 1973; Hirdes and Nunoo, 1994). Phylite with chloritoid may or may not contain pophyroblasts of carbonate whilst those without chloritoid vary from sandy to fine grained lustrous types and may contain magnetite or haematite. Colour banding effects are produced due to alterations of chlorite and sericite, and can also be due to altering sandy and fine grained material, with the latter often showing developed strain slip cleavage. (Kesse, 1985)

2.8.4 Huni Sandstone

Huni Sandstone is fine-grained, and has fairly packed angular to sub-angular grains of quartz and feldspar with variable amount of sericite, chlorite, ferrious carbonate, magnetite, and aplite (Sestini, 1973). Exposed outcrops are generally weathered and are bluish or greenish-to-pale-grey and green in colour. They exhibit distinct magnetite banding and may be cross bedded with dendritic growth of manganese oxide commonly seen microscopically (Kesse, 1985). It is interpreted to be of braided fluvial system because of its thin intercalated argillite layers (Sestini, 1973).

2.8.5 Local Geology

General Stratigraphic Structure

The Tarkwaian strata have been folded into a series of anticlines and synclines with large thrust faults separating Pepe from Akontasi East and Akontasi Ridge from Kottraverchy. Pepe, Akontasi Ridge and Kottraverchy are all situated on the north-east plunging anticlines, whilst Akontasi East on the eastern limb of Akontasi Ridge anticline (Kesse, 1985). There are evidences of reverse faults, sub-parallel to the strike which cause repetition or overlap of the reefs up to 250 meters on dip. Structural deformation extent varies across the deposit; hence, dip angles ranges from 55^0 to 35^0 in the eastern limb (away from the syncline) and flattens towards Mantraim and Pepe to approximately 18^0 to 10^0 (Karpeta, 2001, Einsenlohr, *et al*, 1992 and Kesse, 1985).

Current flow parameters indicate a flow from the east to the west hence the Tarkwain units of Tarkwa Goldfields Ghana Limited concession thickens to the west (Adjei, 2015; Karpeta, 2000). Figure 2.4 is a schematic stratigraphy of Goldfields Ghana Limited, Tarkwa.

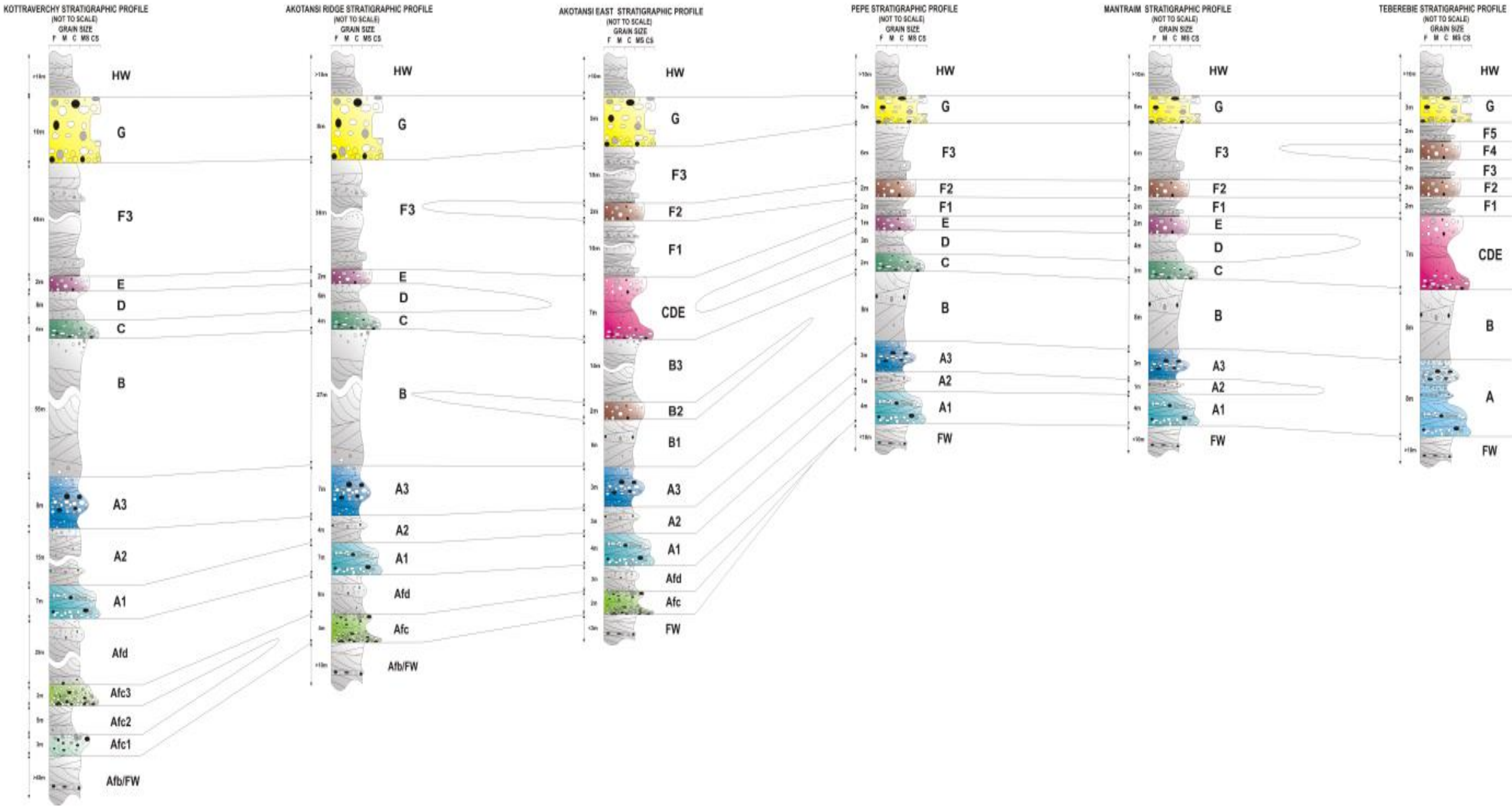

Figure 2.4 Stratigraphic Profile of Tarkwa Orebody from West to East (After Karpeta, 2001).

2.8.6 Deposit Geology and Mineralisation

The orebody is situated in the banket series which hosts gold in four specific zones or reefs which are not related to metamorphic or hydrothermal alterations (Karpeta, 2001). Mineralisation is associated with conglomerates and the gold is found within the matrix that binds the pebbles together. Concentration of gold is proportional to the pebble size, thus the bigger or well packed pebbles, the higher the gold concentration (Karpeta, 2001). Sulphide mineralisation is minimal and not associated with gold. Accessory oxides such as ilmenite, goethite, rutile, and magnetite are present as assessor minerals (Kesse, 1985). Mineralisation of the Kottraverchy, study area has been classified by Karpeta (2001) as:

A3 – reef

A1 – reef

AFC3 – reef

AFC1 – reef

2.9 Mining Practices

Goldfields Ghana Limited, Tarkwa mine is a large, open-pit gold mine that utilises selective surface mining methods to optimise the extraction of the sedimentary mineral deposits (Karpeta, 2001). The mine was owner-operated but has been sublet to Engineers and Planners and BCM who collectively operate 20 excavators, 76 dump trucks, about 24 drill rigs as well as ancillary equipment. Surveyors peg out the boundaries of the pits and the area is cleared of bush and topsoil. The topsoil is re-located for rehabilitation purposes. Reverse circulation grade control drilling is carried out, and geological models are constructed. The short-term plans and forecasts are updated with this grade control information prior to the commencement of mining (Adjei, 2015).

Currently fresh rock and transitional zones are drilled and blasted in six-metre and nine-metre lifts respectively, with excavation in three-metre flitches. At the surface mine, close geological supervision is a pre-requisite for optimising the extraction of the ore as well as keeping dilution to a minimum. Geologists monitor the mining process in the gently dipping continuous conglomerate zones as well as the more structurally complex areas such as the Akontansi Underlap, and Kottraverchy Pits. Pit geologists supervise all digging of mineral material which is classified as either ROM (Run of-the Mine) delivered to one of the two primary crushers, located on the northern section of the mine where it is either dumped directly into a crusher or stockpiled at an adjacent location for future processing. Mining operation is conducted on 24 hours per day, 7 days per week. Waste material is hauled to the nearest waste dump (Adjei, 2015).

2.9.1 Grade Control

Sampling for grade control is via reverse circulation (RC) drilling on approximately 25 m x 25 m grid pattern of which 1 m samples are taken from sample rifter and analysed using aqua regia digest with Rapid Cyanide Leach (RCL) and atomic absorption spectrometer (AAS) finish technique. Normally, vertical holes are drilled for the grade control. However, inclined holes are occasionally drilled for geotechnical purposes and also where the area is structurally complex. Holes are planned by collaboration of mine planners and geologists and the coordinates of the collars are given to surveyors for pegging and drilling. Surpac solid wireframe grade control model is developed from sectional interpretation based on grade and geology (Osei, 2015). The resultant model is used for effective short-term mining scheduling, and estimation of bench ore blocks for mining.

2.9.2 Treatment Plant

Processing of the ore utilises a convectional Carbon-In-Leach (CIL) plant with a design capacity of 12 Mtpa. Crushing is by a primary jaw crusher (toggle jaw crusher) producing feed to a secondary cone crusher which further reduces the size. The feed is transported via conveyors into Semi-Autogenous Grinding (SAG) Mill where further crushing is effected and then discharged into a Ball Mill to produce the slurry which discharges into a sump and later pumped into cyclones (Anon, 2009). The cyclone overflow travels to a thickener after which it is pumped into leach tanks. Carbon movement between the tanks is achieved by pumping carbon recovered upstream from a tank, counter current to the direction of flow of the pulp.

Gaseous oxygen and hydrogen peroxide (oxidizing agents) are added at various stages in the process to aid gold leaching. Gold is desorbed from the loaded carbon utilising a hot caustic cyanide solution. The gold-rich solution is then passed through an electro wining cell, which uses electricity to convert the gold in the cyanide solution to a metallic gold which is deposited onto steel wool for further refining into bullion bars (Osei, 2015).

CHAPTER 3
LITERATURE REVIEW

3.1 Introduction

Resource Estimation is simply the prediction of grade and tonnage of blocks of ground; and, the quality of the resource estimate depends on the quality of information used (Al-Hassan, 2011). The economic viability of a mine lies on reliable mineral resource estimate which requires an accurate 3D representation of orebody, its location, configuration and volume (Osei, 2015). Zhu *et al* (2003) stated that due to the high risk of mining projects, uncertainties in the modelled orebody geometry and estimation of properties such as grades and tonnages will have a great effect on the cash-flow and profit.

It is therefore important that investors and shareholders are protected through high quality resource model (Sinclair, 1998; Stephenson, 2002). To reliably estimate the resource of a mineral deposit, one must adopt good sampling and analytical procedures, interpret correctly the geological influence on mineralisation and select a suitable resource estimation method (Dominy *et al*., 2002).

3.2 Data Collection, Sample Analysis and Database Quality

3.2.1 Data Collection

Some of the data used in resource estimation may come from Diamond Drilling (DD), Reverse Circulation (RC) and/or Rotary Air Blast (RAB) campaigns. Before the commencement of the methods above, it is assumed that indicators of geophysical anomalies of ore at depth have been tested satisfactorily.

Rotary Air Blast (RAB), is mainly used in early exploration (mostly in geochemical sampling) since it only penetrates weathered cover over fresh rocks (Marjoribanks, 1997). Reverse Circulation Drilling and Diamond Drilling are the most popular, in that they have appreciably high rates of deeper penetration (Dzigbodi-Adjimah and Gawu, 1994). For the purpose of this work Reverse Circulation (RC) and Diamond Drill (DD) data were used.

3.2.2 Sample Analysis

In order to determine the level of mineralisation contained in large amounts of samples collected from the field, series of processes are performed on them ranging from crushing, grinding and milling to laboratory chemical analysis or other testing works (Annels, 1991). These processes can generally be grouped under two main headings of sample preparation and assaying. Sample preparation refers to the way in which a sample is treated prior to its analysis. The production of a homogeneous sub-sample, representative of the material submitted to the laboratory is the primary purpose of sample preparation (Adjei, 2015; Caldwell, 2007). Before samples are sent to the laboratory for assaying, sorting and arrangement of samples are done at a submission point.

Assaying refers to the process for determining the amount of a certain metal in an ore or alloy (Anon. 2018b). It includes a variety of analytical techniques employed to determine the value of minerals contained in a sample. According to Fitton (1997), most analytical laboratories practise one or more of the following techniques: Atomic Absorption Spectrometry, Classical Volumetric and Gravimetric analysis, Coupled Plasma Spectrometry, Fire Assay, etc. Fire assay is a standard method and provides reliable assaying for gold and silver (Anon., 2017). For the purpose of this work, all samples were analysed using aqua regia (50 g Aqua Regia with Fire Assay (FA) finish when gold grade is greater or equal to 5.0 ppm. All assay results are received electronically via e-mail so as to avoid human errors associated with data entry. Good quality assurance and quality control measures need to be established and maintained, throughout every sample preparation and assaying process so as to reduce errors in the estimation (Caldwell, 2007).

Quality Control and Quality Assurance (QAQC)

Quality control involves the observation techniques and activities used to fulfil the requirements for quality in sampling and assaying (Osei, 2015). Field duplicate samples are used to control sampling quality, coarse blanks and coarse duplicates are used in controlling preparation quality whilst pulp duplicates and Standard Reference Materials are used to control assaying quality (Armando, 2011).

When the assay results are released, graphs are drawn and analysed to check the accuracy and precision of the Laboratory.

3.2.3 Database

The quality of the information in the database is critical to the determination of reliable resource (Adjei, 2015). Every mining company needs accurate information for economic purposes. It is necessary to ensure that data for modelling and evaluation which include assays, lithology and its attributes, drill hole collar survey, etc. are well structured, captured , validated and stored securely for its integrity (Adjei 2015; Annels, 1991). In mineral resource estimation, errors can be introduced at several stages, which include poor survey pickup (ground and downhole surveys), drilling and core logging (poor recovery), geological mapping (poor quality), sampling (inappropriate method), assaying (poor preparation, contamination), modelling (lack of geological knowledge, too many assumptions on both grade and geological continuity), and grade/tonnage estimation (incorrect technique used) etc (Dowd, 1992). These combine to constitute the random component of the data variation and, thus, contribute to high nugget variance (Adjei, 2015 and Dominy, *et al*., 2002).

3.3 Statistical Concepts in Mineral Resource Estimation

Ideally, it is required that samples should have constant geometric support and that the distribution of its characteristics be normal (Annels, 1991); and, the acceptable way of ensuring equal volume of all samples within a domain is to composite the samples into equal lengths (Dowd, 1992). Normally, classical statistics may be used to obtain knowledge of the distribution function of the data. Basic statistical studies according to Noble (1992) helps in;

i. The detection of high grade or low grade outliers
ii. Identification of type of distribution

The knowledge of the overall details of the data distribution has to be gained to assist in choosing an appropriate estimation model (Al-Hassan, 2008) and these are obtained from the production of histograms and probability plots (Hayslett, 1990). The summary statistics which are used in interpreting data fall into three (3) categories: measures of location (central tendency), measures of spread (dispersion), and measures of shape (Skewness).

3.3.1 Analysis of Data Distribution

The first step in data analysis is the production of histograms and frequency distribution curves to ascertain the overall impression of the nature of the assay distribution (Al-Hassan, 2011). The visual detection and treatment of possible outliers is enhanced from a histogram plot of the data (Adjei, 2015). Due to the presence of these outliers, the arithmetic mean of assays may tend to overestimate or underestimate the mean grade of the deposit (Rendu, 1981). The important parameters deduced from the histogram and frequency plots may include: the mean, the median, the variance, the skewness, kurtosis and the coefficient of variation (Harry, 2006). Standard deviation or variance is further used to determine the spread of the data (Adjei, 2015; Davis, 1986). The larger the variance, the higher the spread of the distributions. These can be deduced according to (Marshal, 1987) from the following;

III. The mean

The mean is referred to as the average or the arithmetic mean and it is the most commonly used characteristic of a data set. It is an indication of the expected behaviour of a data set (Harry, 2006). The mean of a population is represented by the arithmetic mean of all the values of the population. According to Bronshtein (2004) and Marshal (1987), mathematically,

$$\text{Sample mean, } \bar{g} = \frac{1}{n}\sum_{i=1}^{n} g_i \quad \text{...(3.1)}$$

Where

g – grade

n – number of samples

IV. *The Median*

The median is the middle value when the values consisting of the population are listed in numerical order. It is often used when there are a few extreme values that could greatly influence the mean and distort what might be considered typical (Harry, 2006).

Mathematically, median can be expressed using the equation:

$$\text{Median} = b_i + \frac{\frac{n}{2} - f_{m-1}}{f_m} \text{ x C} \quad \text{..} \quad (3.2)$$

Where

b_i – lower boundary of the median class

n – number of observations

f_m – number of observations in the median class

f_{m-1} – cumulative frequency of the class preceding the median class

c – class interval of the median class

III The Variance

The variance describes the variability of the distribution or the spread of the data. It shows whether the values are closely bunched about the centre or widely spread. The deviations of the values from their mean value will have positive and negative values (Osei, 2015). The mean of the squares of these deviations is the variance. The square root of the variance is the standard deviation. It is obtained as:

$$\text{Sample variance, } S^2 = \frac{1}{n-1}\sum_{i=1}^{n}\left(g_i - \bar{g}\right)^2 \quad \ldots\ldots\ldots\ldots\ldots\ldots \quad (3.3)$$

Where

g_i – grade

$\bar{g}$ – mean grade

n – number of observations

$$\text{Sample standard deviation, } s = \sqrt{s^2} \quad \ldots\ldots\ldots\ldots\ldots\ldots \quad (3.4)$$

Where

S^2 – sample variance

IV. Skewness

Skewness is a measure of the asymmetry of the probability distribution of a real-valued random variable. Skewness value can be positive or negative. A negative skew indicates that the tail on the left of the probability density function is longer than the right side and the bulk of the values lie to the right of the mean whiles a positive skew also indicate that the tail on the right side is longer than the left side and the bulk of the values lie to the left of the mean (Osei, 2015). A zero value indicates that the values are relatively evenly distributed on both sides of the mean, implying symmetry, indication of a normal distribution (Sinclair and Blackwell, 2002). Mathematically, skewness is obtained using the equation below;

$$\text{Skewness} = \frac{\sum (g_i - \bar{g})^3}{ns^3} \quad \ldots\ldots\ldots\ldots\ldots\ldots \quad (3.8)$$

Where

s = the standard deviation.

n = number of samples

$\bar{g}$ = the mean

g_i = the individual assay values.

V *Kurtosis*

Kurtosis represents the amount of peakedness of the distributions. It is a measure of whether the distribution is peaked or flat relative to a normal distribution. According to Harry (2006), for Kurtosis > 3, implies that the distribution is too peaked (LEPTOKURTIC). If kurtosis = 3, the distribution is normal (MESOKURTIC) and Kurtosis < 3, means the peakedness of the distribution is low (PLATYKURTIC). Mathematically, Kurtosis is obtained using the equation:

$$\text{Kurtosis} = \frac{\sum\left(g_i - \bar{g}\right)^4}{s^4} \quad \ldots\ldots \quad (3.6)$$

These are illustrated in Figure 3.1

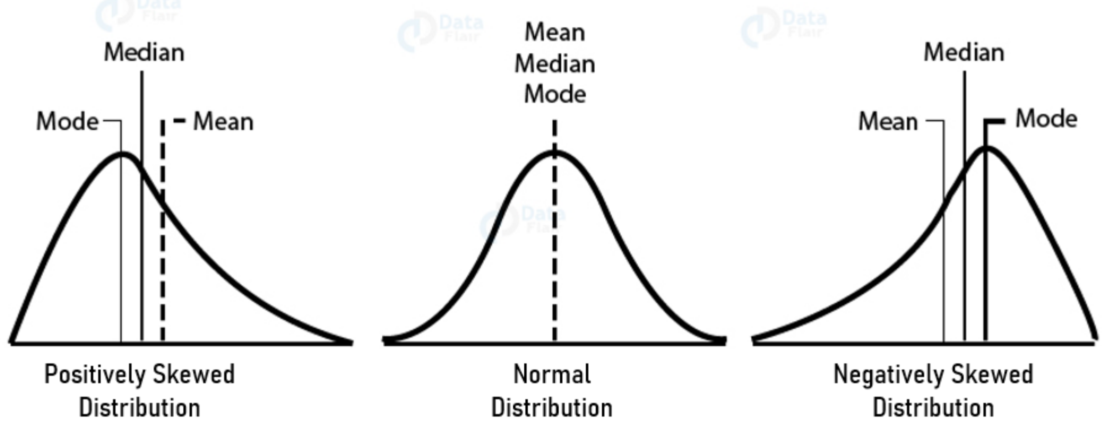

Figure 3.1 Types of Frequency Distribution Curves

VI. *Coefficient of Variation (CV)*

The coefficient of variation is used to describe the variability of the data and their subsequent suitability for use in geostatistics (Marshal, 1987). As a general rule, those distributions with a CV less than one should produce a reasonable model (Fytas et *al*., 1990). Mathematically, Coefficient of variation is expressed as:

$$\text{CV} = \frac{\sigma}{\mu} \times 100\% \quad \ldots\ldots \quad (3.7)$$

Where:

σ = standard deviation,

$\mu = mean$

3.4 Data Compatibility

If groups of samples are to be combined for statistical analysis, then they should belong to statistically similar distributions (Al-Hassan, 2008). In mineral resource estimation, the generation of variogram models require much data and may be necessary to combine different data. However, this cannot be done until it is proven that the data sets have identical distributions. F and t-test may be carried out to test the commonality of the populations through the hypothesis testing. In hypothesis testing a 'null hypothesis' (H_o) is posed which is hoped to be rejected in favour of an alternative hypothesis (H_1) (Bruce and Connell, 2003).

3.4.1 F-test

The F-test verifies the equality of variances using the F-distribution. It is expressed as the ratio of the variances of the two populations being compared (Al-Hassan, 2013).

It is obtained as,

$$F = \frac{V_1}{V_2} \qquad (3.8)$$

where, V_1 and V_2 are variances of the corresponding populations 1 and 2 respectively, and $V_1 > V_2$. The hypothesis may be stated as:

$H_o : V_1 = V_2$

$H_1 : V_1 \neq V_2$, for a given level of significance, α.

Accept H_o if $F < F_\alpha(\upsilon_1, \upsilon_2)$.

$\upsilon_1 = (n_1\text{-}1)$ and $\upsilon_2 = (n_2\ \text{-}1)$ are the degrees of freedom for samples 1 and 2 with respective sizes of n_1 and n_2. The computed 'F' value is then compared with 'F' table values found in most statistics textbooks.

3.4.2 t- test

't'-test is used for testing hypothesis about the equivalency of two sample means. It is obtained by the formula (Al-Hassan, 2013):

$$t = \frac{\left(\bar{x}_1 - \bar{x}_2\right)}{\left(\sqrt{\frac{\left(n_1 v_1 + n_2 v_2\right)}{\left(n_1 + n_2\right) - q}}\right)\left(\sqrt{\frac{1}{n_1} + \frac{1}{n_2}}\right)} \quad \text{.. (3.9)}$$

Where, $\bar{x}_1$ and $\bar{x}_2$ = Samples mean in populations 1 and 2 respectively

n_1, n_2 = number of samples in the populations 1 and 2 respectively.

v_1, v_2 = variances of the corresponding sample populations defined as in the F- test.

$(n_1 + n_2) - q =$ number of degrees of freedom, where q is the number of parameters estimated (Adjei, 2015; Kock and Link, 1970).

The hypothesis may be stated as:

$H_o : \bar{x}_1 = \bar{x}_2$

$H_1 : \bar{x}_1 \neq \bar{x}_2$, for a given level of significance, α. Accept H_0 if $t < t_{\alpha/2}$.

The computed t value is then compared with 't' table values found in most statistics textbooks.

3.5 Effects of Outliers

According to Dowd (1992), an outlier is any value which is significantly higher than or lower than its neighbours. The presence of outliers may pose problems in resource estimation. Introduction of substantial variability in estimates makes statistical parameters such as mean, variance and covariance incorrect. They may have an impact on autocorrelation measures such as experimental semi-variogram. Therefore every effort should be made to eliminate their effects in the data (Sinclair and Blackwell, 2004)

Outliers can be identified by different ways including (Dowd, 1992):

i. Physical identification
ii. Histograms
iii. Log-probability plots.

The difficulties imposed by outliers have been recognised and a variety of approaches have evolved for dealing with outliers in mineral resource estimation (Blackwell and Sinclair and Blackwell, 2002). Some of the approaches used in treating outliers according to Royle (1993) are reanalysing or top cutting to some predetermined upper limit based on experience, using an empirical cutting method tied to a histogram (95th percentile of data) and mathematical approach. In some cases, the so-called outliers may represent a separate geologic population domain in the data. In such a case, that domain is treated separately from the other domain (Krige, 1999).

3.6 Mineral Resource Estimation Methods

According to Al-Hassan (2013), resource estimation methods can be classified into classical and geostatistical methods.

3.6.1 Classical Methods

Classical methods of mineral resource estimation include, triangular method, polygonal method, cross sectional method and Inverse Distance Weighting (Al-Hassan, 2013). These have been described briefly.

Polygonal method

This method can be subdivided into angular bisector and perpendicular bisector methods. Angular bisector methods have polygons, constructed by linking drill holes with tie lines. Vertices of polygons are then obtained where three angular bisectors meet (Al-Hassan, 2013). With the perpendicular bisector method, sample points are joined by constructing tie lines. Perpendicular bisectors are then constructed and their intersection form the vertices of the polygons (Sinclair and Blackwell, 2004). Each polygon is assigned the grade in the polygon (Al-Hassan, 2013).

Triangular Method

The triangular method has three sample sites, joined to form a triangle with no sample site within. The grade, thickness and area of the triangle are then used to estimate the resource (Sinclair and Blackwell, 2004).

Cross-Sectional Method

The cross-sectional method is based on the delimitation of the zone of mineralisation by drawing envelopes or perimeters, based on specified cut-off, on sections across the orebody. The area of the ore on each section is then determined and the final volume is calculated using the distance between the sections (Al-Hassan, 2011). The area of each perimeter can be obtained using formulas such as counting squares, summing areas of ore blocks, Simpson's rule, digital planimeter, etc.

Inverse Distance Weighting Method

Inverse Distance Weighting (IDW) Method is a technique which applies a weighting factor that is based on an exponential distance function to each sample within a defined search neighborhood about the central point of a block (Al-Hassan, 2013 and Shephard, 1968). In predicting the value of an unknown, IDW assigns weights to measured values surrounding the unknown. Greater weights are assigned to the values closer to the unknown and weight diminish with increasing distance from the unknown point (Anon, 2018a). The formula according to Al-Hassan (2013) is;

$$Z_B^* = \frac{\sum Z_i \frac{1}{d_i^n}}{\sum_{i=1}^{n} \frac{1}{d_i^n}} \qquad (3.10)$$

where:

Z_B^* is the estimated variable of the block (of grade, thickness, accumulation etc.)

Z_i is the value of the sample at location i

d_i is the separation distance from point i, to the point of reference.

n is the power index. The separation distance, d_i, is expressed mathematically as:

$$d_i = \left[(\Delta X_i)^2 + (K\Delta Y_i)^2\right]^{\frac{1}{2}} \qquad (3.11)$$

Where,

ΔX_i - difference in the x coordinates of the sample and the block centre,

ΔY_i - difference in the y coordinates of the sample and the block centre,

K - geometric anisotropic ratio of the chosen ellipse axes.

$$K = \frac{\text{Major axis ellipse}}{\text{Minor axis ellipse}} \qquad (3.12)$$

The application of the anisotropic ratio, K, effectively transforms the search ellipse to a circle of radius ‘a’. Although the value of the power index 'n' can vary from zero to infinity, values between 1 and 5 are often appropriate (Vann and Guibal, 2001). Very low power can results in excessive smoothing, whiles very high power selects the nearest samples as this receives almost all the weight (Royle, 1992).

3.6.2 Geostatistical Methods

Geostatistics has been identified as the only method of estimation that recognises trends in mineralisation and spatial control and are able to link attributes from the samples to develop a spatial representation of the deposit. It has received a great deal of attention in mining industry over the few decades, as it offers varied tools and models to assess mineral resources (Krige, 1999; David, 1988). According to Kennedy (1990), the procedure for making resource estimation can be in two parts: The first part involves investigation of data by applying statistical tools after which semi variograms are developed. Results obtained are used for resource and reserve estimations. The second part involves the use of kriging.

Estimation techniques can be grouped into linear estimation methods and non-linear estimation methods (Goovaets, 1997).

ii) Linear Estimation Methods

Linear estimation methods are the most simple to use. They are based on classical parametric statistics and employ the normal or Gaussian distribution of data. These techniques include simple or ordinary kriging, and their variants (Glacken and Snowden, 2001).

Ordinary Kriging:

Ordinary Kriging has been described as best unbiased linear estimator (B.L.U.E.) because its estimates are weighted linear combinations of available data and aims at minimising error to zero and variance to the bearest minimum (Isaaks and Srivastava, 1989). It achieves this by assigning appropriate weights (coefficients) to the samples by considering the variability, continuity and anisotropy (exhibited by the semi-variogram for the variable, the geometry of the data points and the size of the block being estimated (Glacken, 1996). Every estimate comes with some amount of error. When the estimation errors are on average equal to zero, there is no systematic error. This implies that there is no consistent overestimation or underestimation. Though some blocks might be underestimated or overestimated, the estimated value is equal to the average of the true value (Al-Hassan, 2013).

If Z is the unknown grade of a block, then an estimator Z^* is determined by the generic equation:

$$Z^* = \sum_{i=1}^{n} a_i Z_i \quad \ldots\ldots\ldots\ldots\ldots\ldots\ldots\ldots\ldots\ldots\ldots\ldots\ldots\ldots\ldots\ldots \quad (3.13)$$

where,

Z_i = value of the data point (sample) within the search neighbourhood,

a_i = the corresponding weighting factors or Kriging coefficient given to sample Z_i and,

n = the number of samples used.

The minimum estimation error in Kriging is called the "Kriging variance, σ_K^2. This variance is not data dependent but rather is determined by the variogram and the sample location pattern as well as the location of the point to be estimated relative to the sample locations (Annels, 1991). For Z^* to be the best estimated value, two conditions must be met (Raymond, 1982):

i. The estimation variance must be a minimum, i.e. $\sigma_e^2 = E\{(Z^* - Z)^2\}$ is minimum; and

ii. The estimation must be unbiased, such that total weights must be equal to 1. i.e. $\sum_{i=1}^{n} a_i = 1$

With satisfactory weighting coefficients, the variance for the general unbiased linear estimator is obtained as:

$$\sigma_e^2 = \sigma_v^2 - 2\sum a_i \, \sigma_{V_{vi}} + \sum_i \sum_j a_i \, a_j \, \sigma v_i v_j \quad \ldots\ldots\ldots\ldots\ldots\ldots\ldots\ldots\ldots\ldots \quad (3.14)$$

where:

σ_e^2 = the estimation variance,

σ_v^2 = the grade of blocks,

$\sigma v_i v_j$ = covariance of grades of samples v_i and v_j.

In minimising the estimation variance, the weight, a_i such that $\sum a_i$ = 1, the derivatives of the function $F = \sigma_e^2 + 2\mu\left(\sum a_i - 1\right)$ with respect to all the unknowns (a_i's are μ) equates to zero (David, 1977).

This can be modified using the Langrange Principle in a matrix form (David, 1988) as:

[C][A] = [D] .... (3.15)

Where;

$$[C] = \begin{vmatrix} \sigma_{11} & \sigma_{12} & \cdot & \cdot & \cdot & \sigma_{1n} & 1 \\ \sigma_{21} & \sigma_{22} & \cdot & \cdot & \cdot & \sigma_{2n} & 1 \\ \cdot & \cdot & \cdot & \cdot & \cdot & \cdot & \cdot \\ \cdot & \cdot & \cdot & \cdot & \cdot & \cdot & \cdot \\ \cdot & \cdot & \cdot & \cdot & \cdot & \cdot & \cdot \\ \sigma_{n1} & \sigma_{n2} & \cdot & \cdot & \cdot & \sigma_{nn} & 1 \\ 1 & 1 & \cdot & \cdot & \cdot & 1 & 0 \end{vmatrix}; \quad [A] = \begin{vmatrix} a_1 \\ a_2 \\ \cdot \\ \cdot \\ \cdot \\ a_n \\ \mu \end{vmatrix}; \quad [D] = \begin{vmatrix} \sigma_{Vv1} \\ \sigma_{Vv2} \\ \cdot \\ \cdot \\ \cdot \\ \sigma_{Vvn} \\ 1 \end{vmatrix}$$

C = covariance among the samples,

A = weight of individual samples,

D = relationship between the sample and the block

σ_{ij} = covariance of the sample i and j,

σv_i = covariance of the block v and the sample, i,

$\sigma^2{}_v$ = variance of the grade of blocks.

μ = Lagrange multiplier.

The solution of the above matrix for the weighting coefficients, a_i, is given by:

$$[A] = [C]^{-1}[D] \quad \ldots\ldots\ldots\ldots\ldots\ldots\ldots\ldots \quad (3.16)$$

All the σ's are derived from the semi-variogram, hence the weights can be calculated. However, ordinary kriging performs poorly when the data distribution is skewed. Existence of extreme values makes estimation with linear methods difficult and produces unreliable results (Vann and Guibal, 2001).

ii) Non Linear Estimation Methods

Non-linear estimation methods are used to estimate conditional expectation and distribution of grade at a given point (Vann and Guibal, 2001). They are based on non-linear transformation of data such as the Gausian transform, indicator transform or natural log. They are able to work on highly skewed or mixed distributions of data (Glacken and Snowden, 2001). One of such non-linear estimation methods is Indicator Kriging

Indicator Kriging: Indicator Kriging is a spatial interpolation technique devised for estimating a conditional cumulative distribution function at an unsampled location. It is simply the use of ordinary kriging or simple kriging to estimate a variable (e.g. gold) that has been transformed into an indicator variable. In this way, each value of the variable is transformed into zeros (0) and ones (1) depending on whether the value is above or below a specific threshold (cut-off) value (Osei, 2015; Journel and Huijbregts, 1991). If z(x) is the value of an attribute at location x, then its indicator is defined by (Hackman, 2012; Hohn, 1988):

$$i\,(x\,;Z_c)=\begin{cases}1\text{ if } \ \mathrm{Z(x)}\geq \mathrm{Z_c}\\ 0\text{ if } \ \mathrm{Z(x)}<\mathrm{Z_c}\end{cases} \qquad \text{...} \qquad (3.17)$$

Where

i = indicator variable at location, x, for the cut-off, Z_c, and

Z(x) is the grade at location, x.

This method can be used to mitigate the effects of outliers (Al-Hassan, 2013).

The total population is divided into two groups based on the defined threshold value, Z_c. Those above Z_c (high grades) and those below Z_c (low grade). Semi-variograms are calculated and modelled for each sub-population. Semi-variograms are also calculated and modelled for the indicator values of one's (1's) and zeros (0's). After transforming the data, Semi-variogram model is determined for the newly transformed variable by any software design program such as Surpac Software program. Kriging can therefore be carried out as described for ordinary Kriging.

The result of Kriging with indicator values is to estimate a proportion, P_K that can be interpreted in two ways (Sinclair and Blackwell, 2002):

- probabilities (the probability that the grade is above the specified threshold); or
- as proportions (the proportion of the block above the specified cut-off on data support)

this can be supported by the equation: $Z^* = f(x) > Z_c$ -------------- (3.18)

where Z^* = probability of grade, Z_c = cut-off grade, f(x) = probability function.

Multiple Indicator Kriging: Multiple Indicator Kriging (MIK) involves series of cut-off values, Z_c that are chosen and semi-variograms are also calculated and modelled. This provides meaningful results in the grade/tonnage curves of blocks. For each block, the mean high and low grades are estimated separately using the respective models. The following are some steps required to carry out MIK (Hackman, 2012):

I. Construct grade map or histogram of the data set;

II. Select cut-of grades, preferably equidistant on the histogram scale

III. Transformation of the drillhole data into 0's and 1's values for every cut-off grade selected based on:

$$i\,(x\,;Z_c) = \begin{cases} 1\,\text{if}\;\; \mathrm{Z(x)} \le \mathrm{Z_c} \\ 0\,\text{if}\;\; \mathrm{Z(x)} > \mathrm{Z_c} \end{cases} \quad \text{...} \quad (3.19)$$

IV. Generation and modelling of indicator variogram separately for every cut-off

V. Ordinary Kriging is then carried out on the transformed (0, 1) values for every cut-off.

Vi. By repeating this step for every selected cut-off grade one gets an end result of cumulative probability curve as a function (i.e. cumulative frequency function, CFF) of the grade for every block. After estimating the CFF, the percentage of a block above/ below a given threshold (cut-off) can be estimated, which can also be interpreted as a percentage chance that the entire block is above/below a given threshold (cut-off).

The procedure is called Multiple Indicator Kriging (MIK), and the result is an estimate of the entire cumulative curve.

For illustration, Figure 3.2 shows an indicator kriged value for an assumed point say A with cluster of samples around it based on a threshold values of 0.75 g/t and 1.0 g/t. Thus, for a threshold of 0.75 g/t, if the kriging produces an estimate of say 0.73, it indicates that 27 % of the samples in the vicinity of A are higher while 73% are lower than 0.75g/t. Also if a threshold value of 1.0 g/t provides an estimate of another point on the cumulative curve say 0.87, then it indicates that 13 % of the samples in the vicinity of A are above 1.0 g/t whilst 87% are lower. Hence, the deference 14 % occurs in the interval between 0.75 g/t and 1.0 g/t. Repetition of this procedure for several thresholds or cut-offs leads to estimates of many points on the cumulative curve.

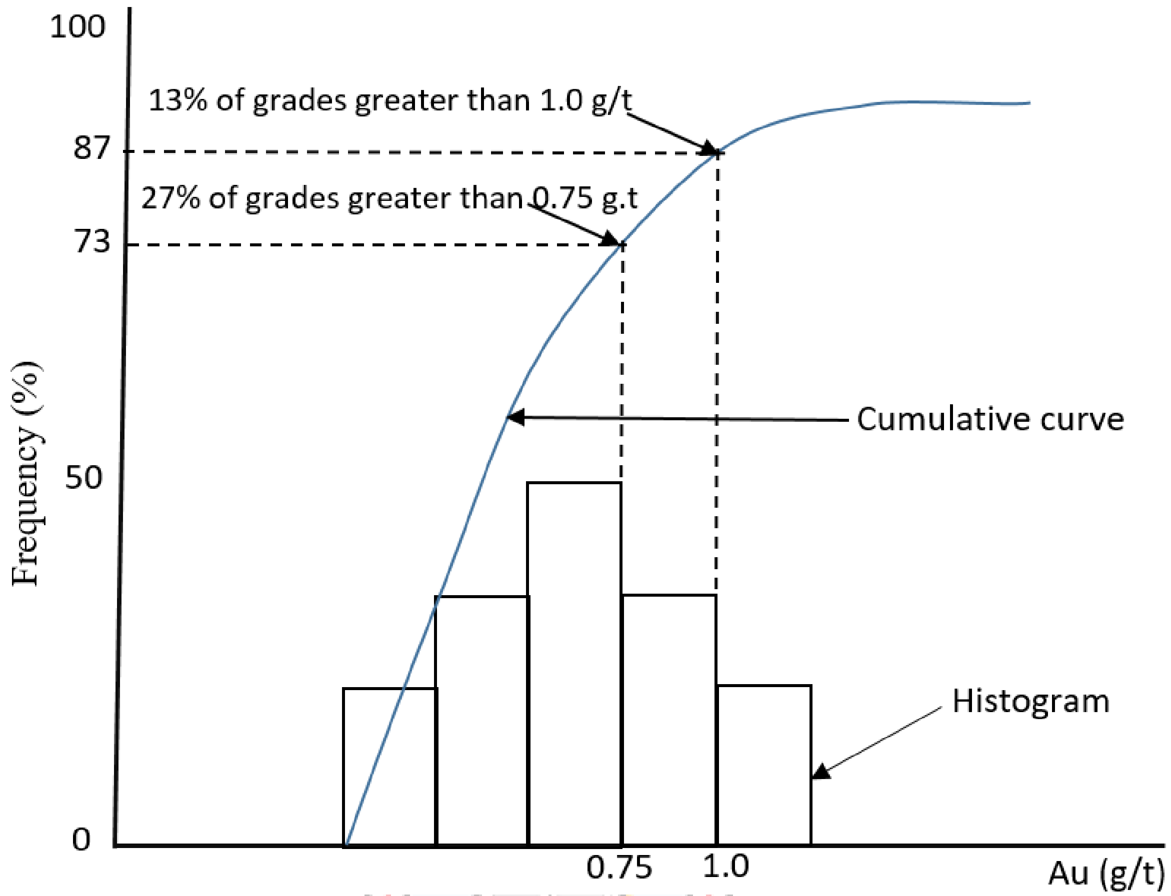

Figure 3.2 MIK estimate of the cumulative distribution of gold grades (After Sinclair and Blackwell, 2002).

The MIK estimate of the distribution of grades in a block allows the application of a cut-off to the distribution such that a proportion of the block above the cut-off and the average grade above the cut-off can be calculated. The average grade of a block can be determined from the distribution of sample grades if the average grade of each indicator interval is known. For illustration, consider a block of ore 10 mE x 10 mN x 3mRL surrounded by nine (9) samples with grades (g/t) as shown in Figure 3.3. Let's say the block is to be estimated using MIK at cut-off grades of 0.9, 1.5, 3.0 and 4.0

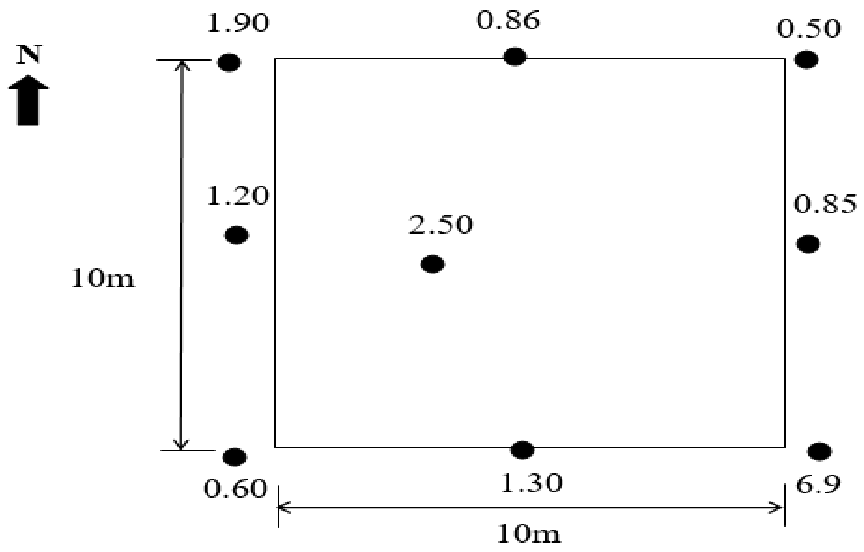

Figure 3.3 Hypothetical block surrounded by nine samples for MIK (Source: Anon., 2011).

The MIK estimates procedure for this particular block above is as follows:
The first step is to perform interval statistics on the whole data which may help to choose cut-offs by several methods such as deciles of the data (10%, 20%, 30%, ………..90%) or values near the end of the cumulative frequency to define the "upper tail of the Cumulative Density Function (95%, 97%, 99%) as for example shown in Table 3.1.

Table 3.1 Interval Statistics on the Data

Grade Interval	Mean Grade	Median Grade
0.00 – 0.90	0.67	0.62
0.90 – 1.50	1.50	1.43
1.50 – 3.00	3.10	2.84
3.00 – 4.00	5.45	4.25
> 4.00	5.99	4.85

From Table 3.1, values of 0.90, 1.50, 3.00, 4.00 and > 4.00 shall be chosen as indicator cut-offs. Alternatively, historical classified resource cut-offs can also be used as indicators, example, classification based on waste, low, medium and high grade ores (Hellman and Schofield, 2011) and then transform the data into 0's and 1's as shown Table 3.2. In this way, indicator kriging is not creating a single value for the entire block as in the case of ordinary kriging, rather describing the amount of material in the block above or below a given cut-off (Sinclair and Blackwell, 2004).

Table 3.2 Chosen cut-offs applied to the sample data and their converted indicators

Sample Values (g/t)									
Cut-off	1.90	1.20	0.60	0.86	2.50	1.30	0.50	0.85	6.90
0.90	0	0	1	1	0	0	1	1	0
1.50	0	1	1	1	0	1	1	1	0
3.00	1	1	1	1	1	1	1	1	0
4.00	1	1	1	1	1	1	1	1	0

For each cut-off, the indicator semi-variograms are calculated using the indicator values shown in Table 3.2 and modelled. At each indicator, variogram models are applied to generate weights for each sample location in order to create probabilities that the grade for the estimation location is less than the respective indicators (Boamah, 2015). For illustration, Table 3.3 shows the calculation of the probabilities below indicator threshold whiles Figure 3.4 shows the cumulative distribution curve generated by plotting the probabilities against the respective indicator threshold to produce cumulative frequency function (CFF).

Table 3.3 Probabilities of block below an indicator

	Prob (block grade < 0.90g/t)	Prob (block grade < 1.50 g/t)	Prob (block grade < 3.00 g/t)	Prob (block grade < 4.00 g/t)
	0.095 x 0	0.080 x 0	0.09 x 1	0.09 x 1
	0.14 x 0	0.12 x 1	0.18 x 1	0.15 x 1
	0.085 x1	0.08 x 1	0.10 x 1	0.13x 1
	0.25 x1	0.09 x 1	0.09 x 1	0.05 x 1
	0.20 x 0	0.20 x 0	0.05 x 1	0.10 x 1
	0.14 x 0	0.12 x 1	0.20 x 1	0.11 x 1
	0.10x 1	0.070 x 1	0.03 x 1	0.18 x 1
	0.03 x 1	0.075 x 1	0.13x 1	0.12 x 1
	0.21 x 0	0.30 x 0	0.70 x 0	0.95 x 0
Total	**0.47**	**0.56**	**0.87**	**0.93**

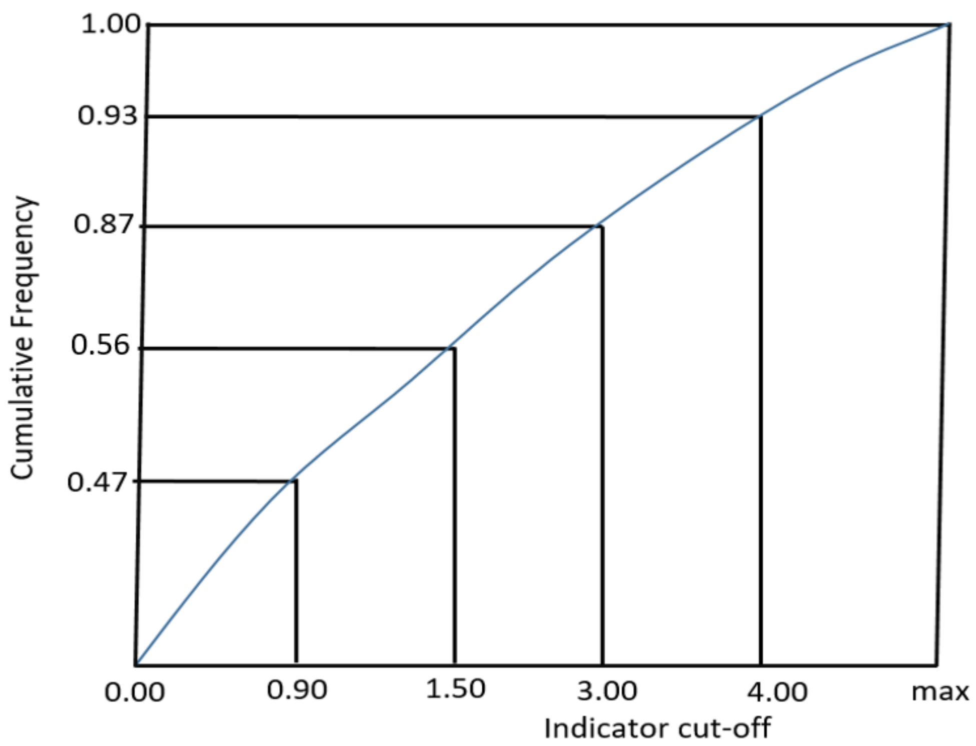

Figure 3.4 Cummulative Frequency Function (CFF) for MIK

The expected grade is the average of the distribution which is derived from weighting each interval grade (from the interval statistics of the domain data set) by the probability estimation location in that interval (Boamah, 2015). When there is a skewed tail and the mean grade of the last interval is calculated from a small set of data, the mean grade will be biased by the few extreme grades. In such situation, the median grade is believed to be a better representation of the grade conditions for the last interval and so it is used in place of the mean grade (Thomas and Snowden, 1990).

For illustration, Table 3.4 shows the block grade within grade interval and is obtained (Hellman and Schofield, 2011) as:

$$E(X) = \sum_{0}^{\infty} x\, f\,(x) \quad \ldots\ldots\ldots\ldots\ldots\ldots\ldots\ldots\ldots\ldots \quad (3.20)$$

where:
E(X) = expected grade,
x = mean grade within interval
f(x) = probability of block grade within that interval

The grade of the block is estimated as 2.36 g/t as illustrated in Table 3.4

Table 3.4 Indicator Kriged Estimate

$L_g - U_g$	Prob (x $\leq U_g$)	f(x)	$\bar{x}_i$	$\bar{x}_i$ f(x)
0.00 – 0.90	0.47	0.36	0.67	0.24
0.90 – 1.50	0.56	0.27	1.50	0.41
1.50 – 3.00	0.87	0.11	3.10	0.34
3.00 – 4.00	0.93	0.18	5.45	0.98
> 4.00	1	0.08	4.85	0.39
Total		**1**		**2.36**

Where:

$L_g - U_g$ = grade interval,

$\bar{x}_i$ = mean grade within the interval

Prob (x $\leq U_g$) = probability of block grade less than maximum grade

f(x) = probability of block grade within the interval

3.6.3 Variography

Variography is a plot of semi-variance against separation distance between samples. It represents the mean variance between sample pairs as a function of distance (lag) between them. It is used in Kriging and other estimation procedures (Clark, 1980). The experimental semi variogram, $\gamma^*(h)$ for lag distance, h, is defined as the average squared difference of values separated approximately by h, with a formulae:

$$\gamma(h) = \frac{1}{2n}\sum_{i=1}^{n}[z(x_i) - z(x_i + h)]^2 \quad \text{..} \quad (3.21).$$

where:

$Z(x_i)$ = the value of the regionalised variable at point x_i ,

n = total number of data pairs counted at each lag distance.

The importance of variography (Adjei, 2015) include:

I. It investigates how the variance of the difference of two points, belonging to the same regionalised variable Z(s), changes with varying separation distance, $|h|$

II. Model the spatial continuities of samples in order to predict differences between estimates and true values.

Good variogram analysis can provide an understanding of population and spatial information important to the production of a realistic grade or lithologic model (Al-Hassan, 2013).

3.7 Model

A model is a graphical, mathematical (symbolic), physical, representation of a concept, phenomenon, relationship, structure, system based on recorded measurements (Olea, 1999).

The objectives of a model include:

(1) To facilitate understanding of deposits and its structural complexities.

(2) To aid in decision making by simulating 'what if' scenarios,

(3) To explain, control, and predict events on the basis of measurement observations.

In general, all **models** have an information input, an information processor, and an output of expected results.

In mineral resource evaluation, variogram models can be grouped into: transition and non-transitional models (Journel and Huijbregts, 1991). Models with a finite sill, like the Gaussian, exponential, and spherical, are referred to as *transition* models whiles those without a sill like Linear, General linear and De Wijsian are *non-transitional models* (Journel and Huijbregts, 1991). Table 3.5 shows different types of theoretical semi-variograms that are likely to be encountered in nature and Figure 3.5 shows the models with a sill.

Table 3.5 Semi-variogram models.

MODEL TYPE	EQUATION	COMMENT
Spherical	$\gamma(h) = C_o + \left[1.5\left(\frac{h}{a}\right) - 0.5\left(\frac{h}{a}\right)^3\right], h < a$ $\gamma(h) = C_o + C, h \geq a$	This is the most frequent model type encountered in mining practice. It is often accompanied by a nugget effect.
Linear	$\gamma(h) = Ah + B$	The simplest model without a range.
De Wijsian	$\gamma(h) = A\ln(h) + B$	An extension of the linear model and it is encountered in cases where there is no such thing as arrange of dependence.
Exponential	$\gamma(h) = C_o + C\left[1 - \exp^{(-h/a)}\right]$	Almost similar to the spherical

		model except that it reaches its sill asymptotically and much slower than the spherical model. It is rare in the mineral deposits.
Guassian	$\gamma(h) = C_o + C\left[1 - \exp\left(-h^2/a^2\right)\right]$	The curve is parabolic near the origin and the tangent is horizontal at origin.
Parabolic	$\lambda(h) = \frac{1}{2}a^2h^2$	Observed when there is a linear drift. Its regular behaviour at the origin is seldom found in mining practice
Hole-Effect	$\gamma(h) = C\left[1 - \left(\frac{\text{sinah}}{\text{ah}}\right)\right]$	Model has a periodic behaviour, is observed when there is a succession of rich and poor zones.
Legend:	C_o = variance, C = regionalised variance, h = distance between pairs, a = range, A and B are constants, and $C_o + C$ = sill	

(Source: David (1988); Journel & Huijbregts (1991)

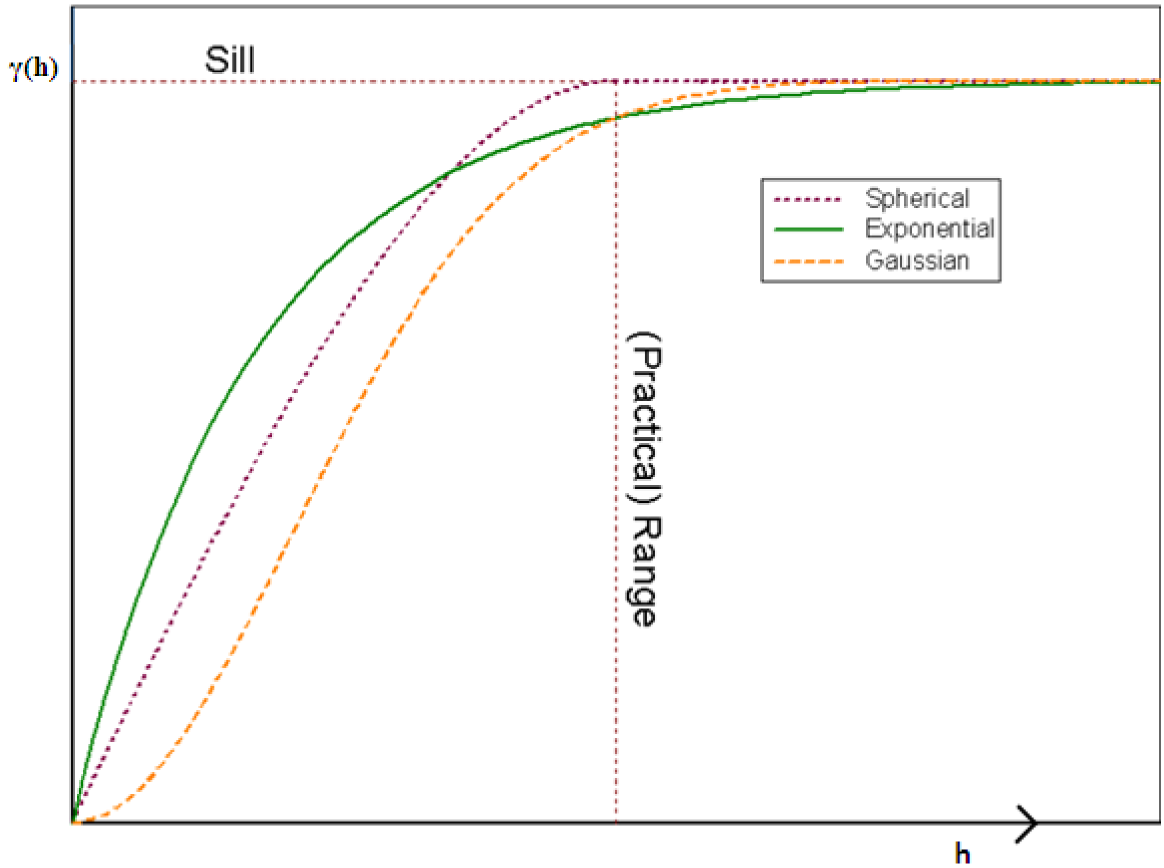

Figure 3.5 Models with a Sill (Taken from Olea *et al*., 1999).

According to (Webster and Oliver, 1993), semi-variogram model analysis consists of the experimental variogram calculated from the data by default and the variogram model fitted to the data (Figure 3.6).

3.7.1 Spherical Model

A spherical model is the one in which the semi-variogram curve rises rapidly at low lags and then gradually curves off until at a certain distance it reaches its sill and stays there even at higher lags. In fitting a spherical model to a sample variogram, it is often helpful to remember that the tangent at the origin reaches the sill about two-thirds of the range (Issaks and Srivastava, 1989). Spherical model is the most widely applied model to most ore deposits (Olea, 1999) and it was the one used for this work since it fitted the experimental variogram appropriately. Figure 3.7 shows a schematic spherical model. The spherical model is characterised as:

$$\gamma(h) = C_o + C\left[1.5\left(\frac{h}{a}\right) - 0.5\left(\frac{h}{a}\right)^3\right], h < a \quad \text{...} \quad (3.19)$$

$$\gamma(h) = C_o + C, \ h \geq a \quad \ldots\ldots\ldots\ldots\ldots\ldots\ldots\ldots\ldots\ldots\ldots\ldots\ldots\ldots\ldots\ldots\ldots\ldots\ldots\ldots(3.20)$$

where:

$\gamma(h)$ = semi variance,

C_o = nugget variance,

C = regionalised variance,

a = range of the structure and

$C_o + C$ = sill.

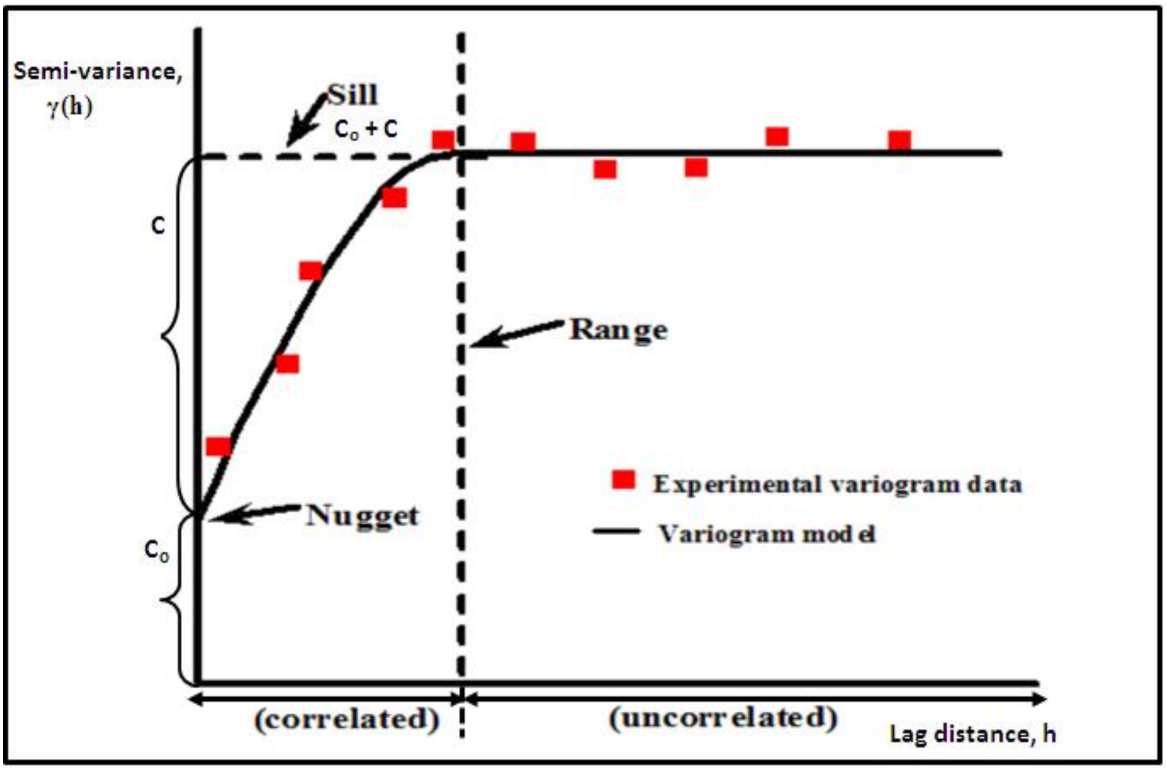

Figure 3.6 A Spherical Model with its Main Components (Source: Olea, 1999)

The components of a semi-variogram are described below:

i. Nugget Variance (C_o): The nugget variance is the value of $\gamma(h)$ at zero distance on the semi-variogram. It indicates grade variability over extremely small distances between data points (Al-Hassan, 2015). The nugget variance is the product of assaying and sampling errors, measurement errors (including data compilation errors) and micro-variability in the mineralisation which cannot be observed at the scale smaller than the sampling interval (Annels, 1991; Journel and Huijbregts, 1991).

ii. Regionalised variance (C): Regionalised variance (C) is the difference between the γ(h) value at which the variogram curve levels off (the sill) and the nugget variance. It represents the predictable part of variability of the regionalised variable. It is also referred to as the remaining variance which is the spatial component of the regionalisation (Annels, 1991).

iii. The Range: The range is the distance at which the semi-variogram reaches the sill and provides an indication of the distance within which there is some auto correlation between sample values in a particular direction (Snowden, 1999). Beyond this distance, there is no longer any correlation between samples, and covariance between the samples drops to zero (Annels, 1991).

iv. The sill, $(C_o + C)$: The sill is the level or plateau in the semi-variogram at which an increase in the separation distance of the samples no longer causes a corresponding increase in variance and it remains constant. The sill can be used to estimate the population variance (Barnes, 1991). The sill generally reflects the total data variance (i.e. the summation of the nugget variance and the regionalised variance) of the semi-variogram model (Cameron and Hunter, 2002).

Nested Structures

In many cases, it is not possible to fit an experimental semi-variogram with a single model. This situation can arise with the presence of more than one underlying structures in the data being considered. According to Journel and Huijbregts (1978), nested structures are commonly indicated by breaks in slope of an experimental semi-variogram as shown in Figure 3.7. It may be caused by some geological phenomenon such as alteration of strata, mixture of different grain size, different thickness and lithology, high and low grades, shear zones, etc (Journel and Huijbregts, 1978).

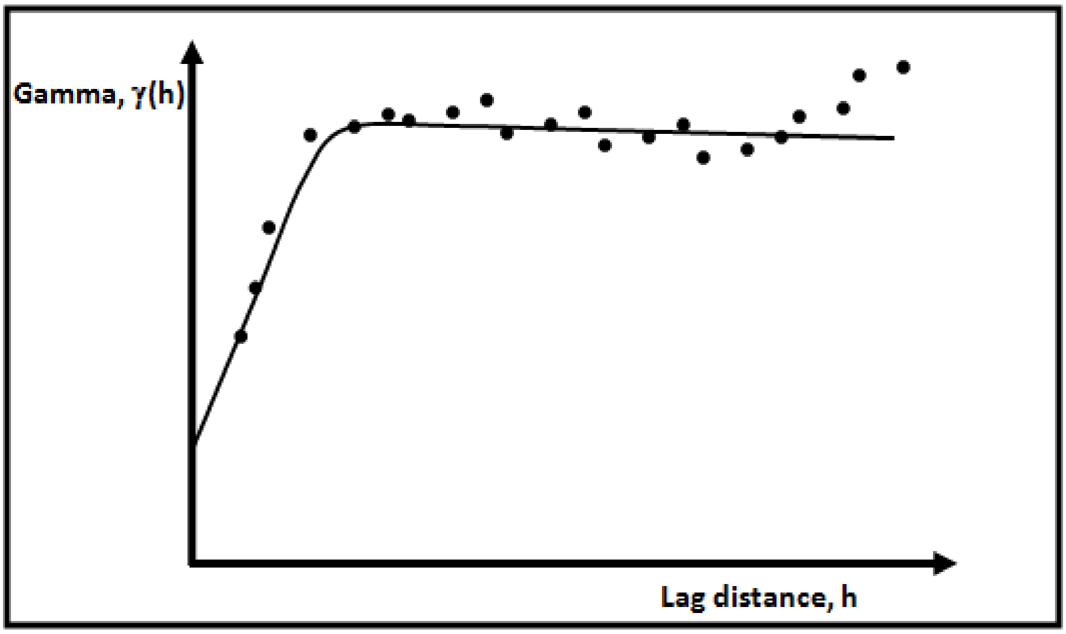

Figure 3.7 Semi-variogram showing Nested Structure (After Clark, 2001).

3.7.2 Anisotropy

Anisotropy occurs when different semi-variograms are obtained for different directions in an orebody (Clark, 2001; Annels, 1991). This means that instead of having circular zone of influence as in the isotropic case, one has an elliptical zone of influence. Many mineral deposits or orebodies are not isotropic in nature and they may have geologic explanation that can be integrated into the estimation procedure (Clark, 2001). The two common types of anisotropies recognised in mineral estimation application are Geometric and Zonal Anisotropies (Dowd, 1992).

In geometric anisotropy, illustrated in Figure 3.8a, the range varies with direction, but the sill remains constant (Lasme, 2014). In zonal anisotropy (Figure 3.8b), the range is constant whilst the sill changes with direction (Sinclair and Blackwell, 2002). Anisotropy in grade continuity can be modelled by calculating and modelling semi-variograms in three orthogonal directions. The first two directions, within the plane of mineralisation, model the direction with the longest range (major) and the direction perpendicular to that (semi-major). The minor (or vertical) direction is perpendicular to the plane of mineralisation and invariably has the shortest range (Snowden, 1999).

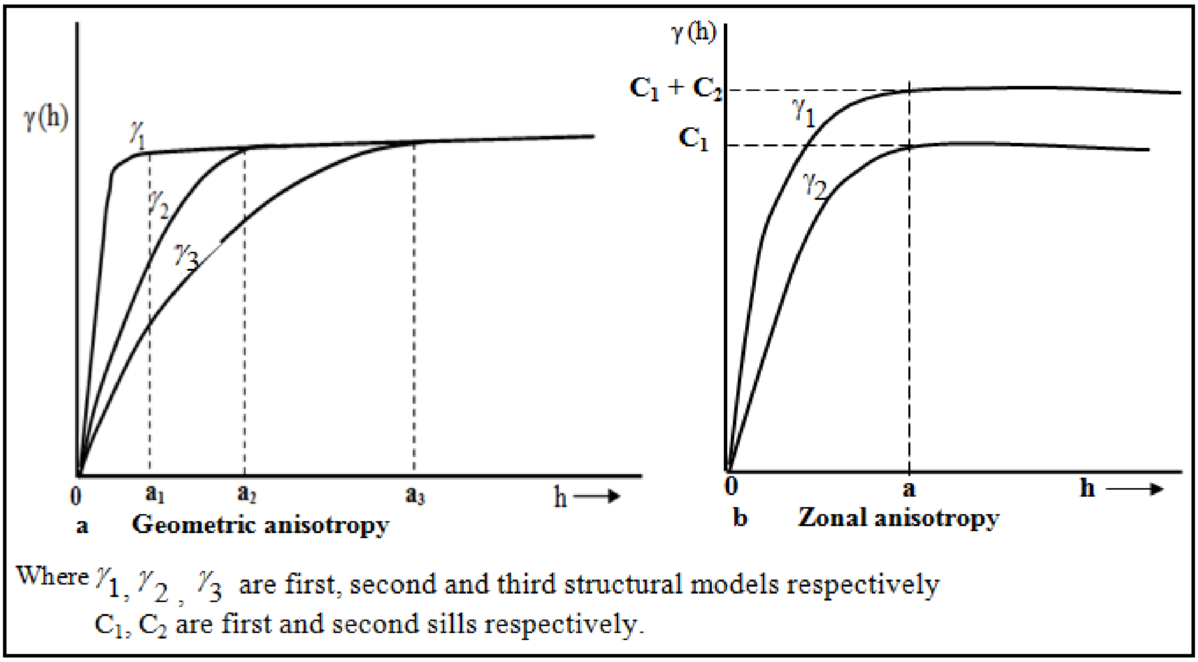

Figure 3.8(a) Geometric anisotropy showing different ranges with the same sill and 3.8(b) Zonal anisotropy showing the same range with different sills in 3D regionalisation (Source: Dohm, 1980)

3.7.3 Cross-Validation of Semi-Variogram Model

Cross validation is a widely used procedure in which point data are successively extracted individually from a data array and then estimated using the other surrounding data values. This allows for the comparison of estimated and the true values using only the information available in the sample data set (Sinclair and Blackwell, 2002). The estimated values are plotted versus the actual values and the resulting scatter plot can be evaluated (Davis, 1987). These are used to check whether semi-variogram model parameters are satisfactory or not. The conditions for a good estimate and therefore satisfactory model require that (Annels, 1991):

(i) the value of the mean algebraic error approaches zero and is not more than 1 % of the mean of all the Z_i values;

(ii) the mean absolute error should be as small as possible;

(iii) The ratio in average square error to average Kriging variance should lie in the range between 0.9 and 1.1, and be as close as possible to 1. This is one of the most important statistics to be considered when fitting the parameters;

(iv) One of the options of cross-validation is to create a scatter plot of actual against estimate. If all the estimates were perfect then all points would lie on the 45 degree line as shown in Figure 3.7. However in practice there will be a cloud of points scattered around the 45 degree line. The regression equation of actual on estimate is calculated using the standard least squares method. The equation has the format:

$$\text{actual} = c + b \times \text{estimate} \quad \text{...} \quad (3.20)$$

For perfect regression constant c (the intercept on the Y axis - actual) should be equal to zero and the slope of the line (b) equal to 1; and

(v) Also correlation coefficient produced on scatter plots of estimated and the actual values should be close to 1 and the points should lie close to the 45 ^{o} regression line as shown in Figure 3.9. This measures the strong relationship between the actual and the estimated values (Annels, 1991).

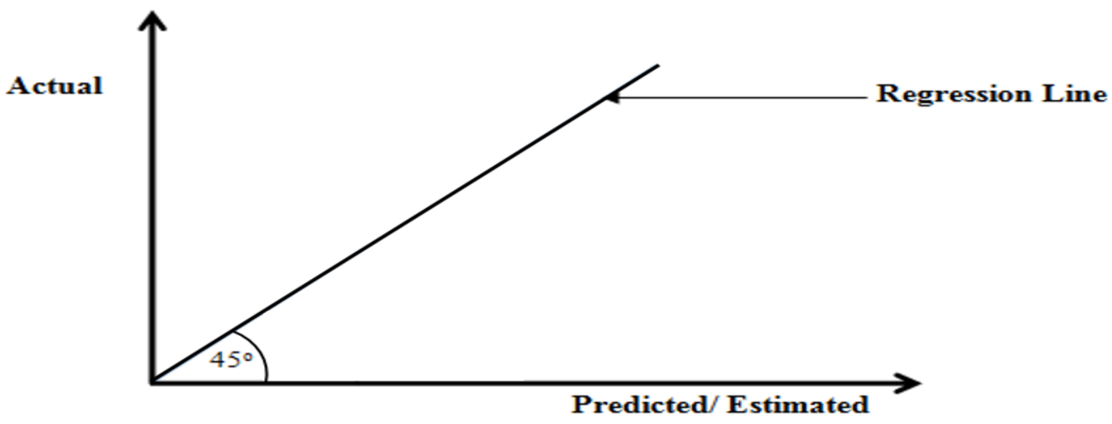

Figure 3.9 Cross validation scatter plot of Actual versus Estimated.

3.8 Orebody Modelling

The principal objective of orebody modelling is to determine the location, shape, size, structure and also to estimate the tonnage and grade of an orebody, which will assist in planning, designing and subsequent mine production. The major steps in the modelling process according to Sinclair and Blackwell (2002) are:

i. Visualisation of the deposit from drill hole data, and geologic interpretation using all other information
ii. Viewing in vertical and horizontal planes and constraining the sections
iii. Creating wireframe of deposit outlines and geologic structure
iv. Develop a 3- D solid model of the deposit
v. Extracting blocks from block model and estimates grade, tonnages, etc.

3.8.1 Types of Modelling

The different types of modelling methods exist however the most common ones (Anon, 2004) are:

1. Cross sectional modelling
2. String modelling
3. Triangular modelling
4. Wireframe modelling
5. Block Modelling

Cross-Sectional Modelling

Cross-sectional modelling is a selection of parallel dissection of the property of interest. These sections contain the geologic structure of the deposit along the section lines and the areas of mineralisation. The volume is computed using the area of sections and the distance between them. The area may be calculated by any sensible method such as counting of squares or use of planimeter. Grade can be calculated using the appropriate estimator. This method is not useful for extremely thin, irregular and lenticular orebodies (Annels, 1991). Figure 3.11 is an illustration of a cross sectional model showing section of an orebody.

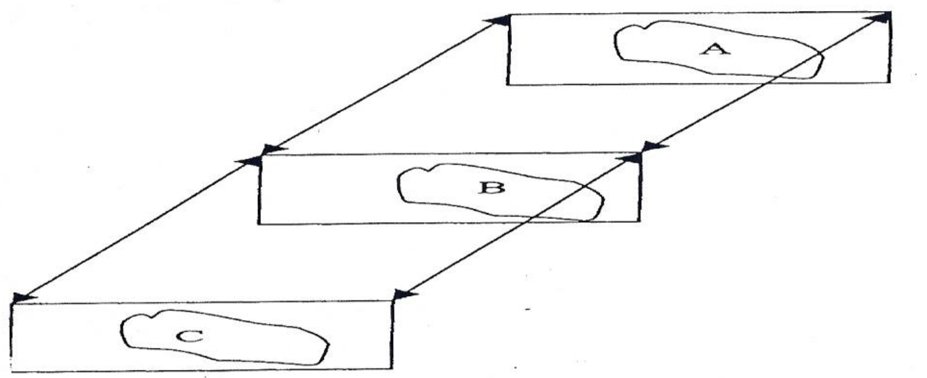

Figure 3.10 Cross-Sectional Model (Kwofie, 1993).

String Model

A String is a line joining a succession of positions in space whose X, Y, and Z are known (Points). These string lines at the surface join adjacent strings in an undulating patchwork form triangular network known as DTM. The DTM continues to undergo conventional extension by wrapping the patchwork quilt (with triangular patches) around a series of wire frames resulting in a 3- dimensional model known as a string model (Boamah, 2015).

There are three kinds of strings, namely: open string, closed string and spot height string. Figure 3.13 is an illustration of the types of strings.

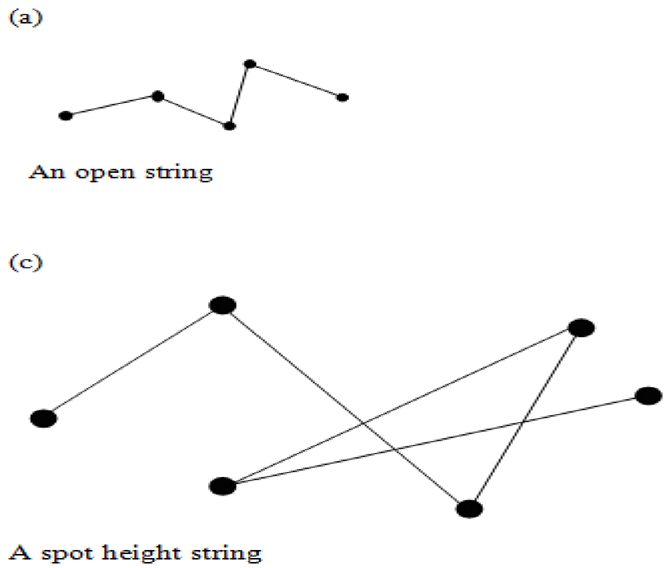

Figure 3.11 The Three Kinds of Strings (Kwofie, 1993).

Triangular Modelling

This involves the construction of triangular plates to connect all adjacent data points. This leads to a network of triangles connecting all control points together. It is mainly used for quick modelling and contouring. The triangular method uses top, bottom and midpoints of drillholes intercepts projected into a reference plane as the data points (Sides, 1997). This is illustrated in Figure 3.14

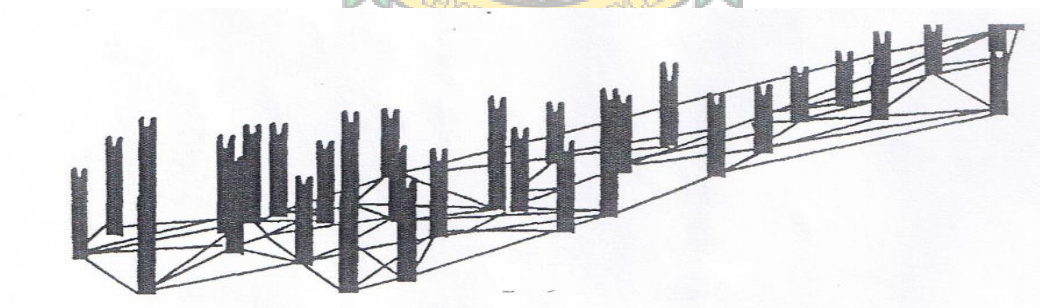

Figure 3.12 Triangular Wireframe (Kwofie, 1993).

Wireframe Modelling

Wireframe model is used almost everywhere in the mining industry and it is a method used to define geological boundaries (Boamah, 2015). It is generated by using a set of triangular lines or straight lines which are formed by linking points digitised from successive plans and cross-sections. It represents a three (3) dimensional system for the creation, modification and displaying a digital terrain model (DTM) and solid model (Kwofie, 1993). The geological interpretation from the wireframe model is usually satisfying because the geologist takes some time to analyse the sectional, plan and logging data, which is combined with surface mapping information (Boamah, 2015). Typical examples of surface wireframe and solid design structure of a 3D model are shown in Figure 3.12 (Fosu, 2012).

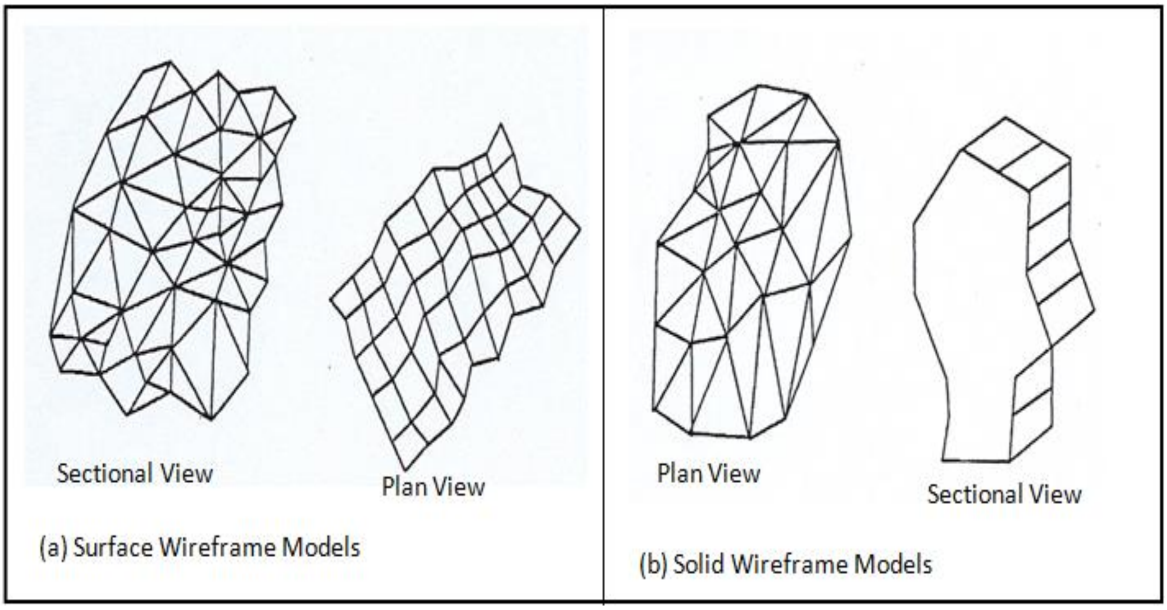

Figure 3.13 A Three Dimensional Wireframe Models (Kwofie, 1993)

Block Modelling

A resource block model is a computer-based representation of a deposit in which the geological zones are defined and filled with block, which are assigned estimated values of grades and other attributes. A resource block model is only a conceptual geological model of a deposit; however, since tonnage and grade resource estimates are derived from the block model, it is important that the key elements of the geological model such as shape, size and grades are accurately reflected in the block model (Boamah, 2015). A typical example of a block mode is shown in Figure 3.10.

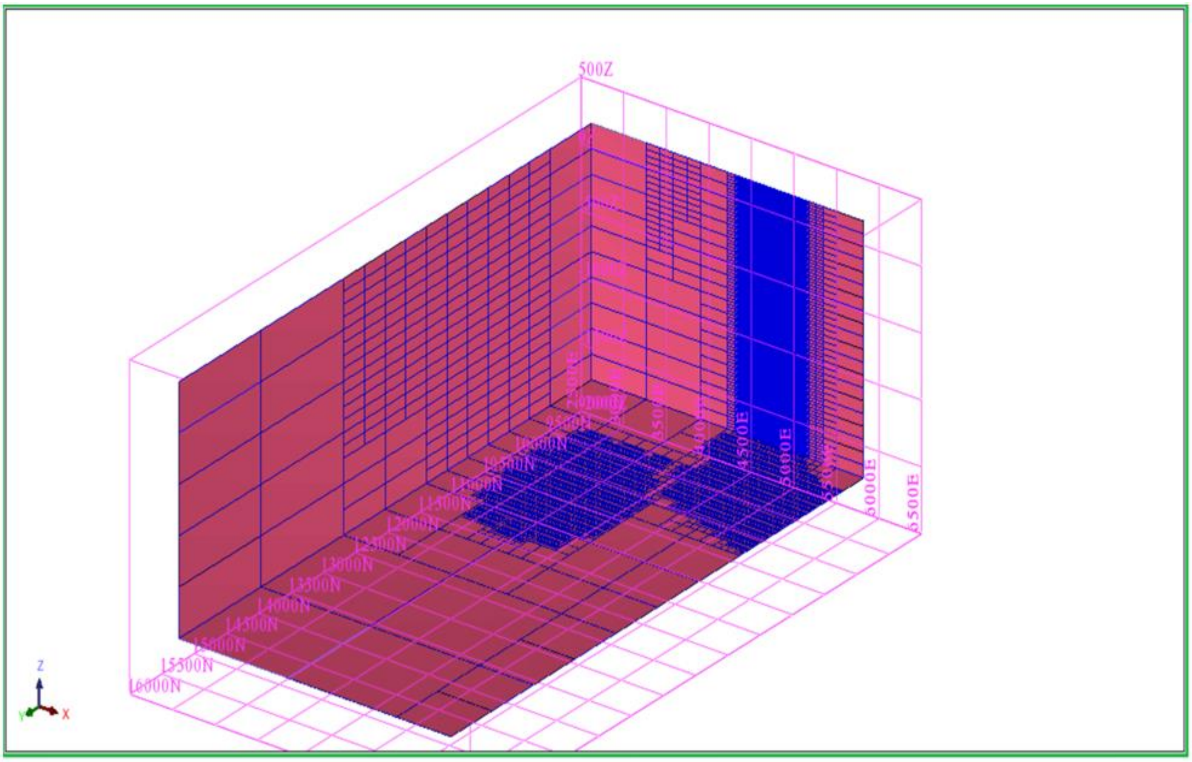

Figure 3.14 A typical Block Model (Source: Anon., 2002).

CHAPTER 4
DATA MANAGEMENT AND ANALYSIS

4.1 Introduction

In this study, the attention was focused on Afc1 at the Kottravercy pit that shares boundary with Anglogold Ashanti Iduapriem Mine (GAG) concession to the North - West called Ajopa. The data was collected from within the following area limits:

Eastings: 1150.00 E - 1875.00 E

Northings: 1100.00 N - 1650.00 N

The ore body generally strikes in the NE - SW direction and dips generally to the East between 50^{o} - 60^{o}. Drill hole secondary data was taken from the company's database and stored in C.S.V. format. The data included the collars, lithology, down-hole survey and assay. No geological structural data was available as at the time data was collected. The data was validated and subjected to statistical analysis. This was followed by direction variation analysis (variography) for both OK and MIK using the GEOVIA Surpac software, version 6.5.1. Cross validation was used to check for the validity of the variogram parameters.

Block modelling of the deposit was done after which the mineral resource was estimated by both OK and MIK using the aforementioned software. The block size was determined by the drillhole spacing (25m x 25m) and the selective mining unit (average mining width of the deposit along strike and the mining bench height in the vertical dimension, 50 x 50 x 3). The study also gathered information from the mine on the geology of the deposit and the average specific gravity value of 2.60 (as used in the mine). Results of the estimates of OK and MIK were compared with the actual mining production figures between January, 2013 and December, 2013.

4.2 Data Management

4.2.1 Data Acquisition

Data obtained from the database section of the company included collars, lithology, down-hole survey, topography and density. A total of 6,789 samples were used. It consists of 500 samples from 79 Inclined Diamond Drill Holes and 6,289 Reverse Circulation vertical samples for the resource estimation over a strike length of 500 m with an average depth of 105 m below surface. Figure 4.1 shows the drillhole layout in plan. The holes were drilled on a grid of 25 m by 25 m with occasional infill of 12.5 m. Reverse circulation holes were sampled by conventional splitting using the one stage riffle splitter at 1 m length after which the mineralised corridors were re-sampled for assaying.

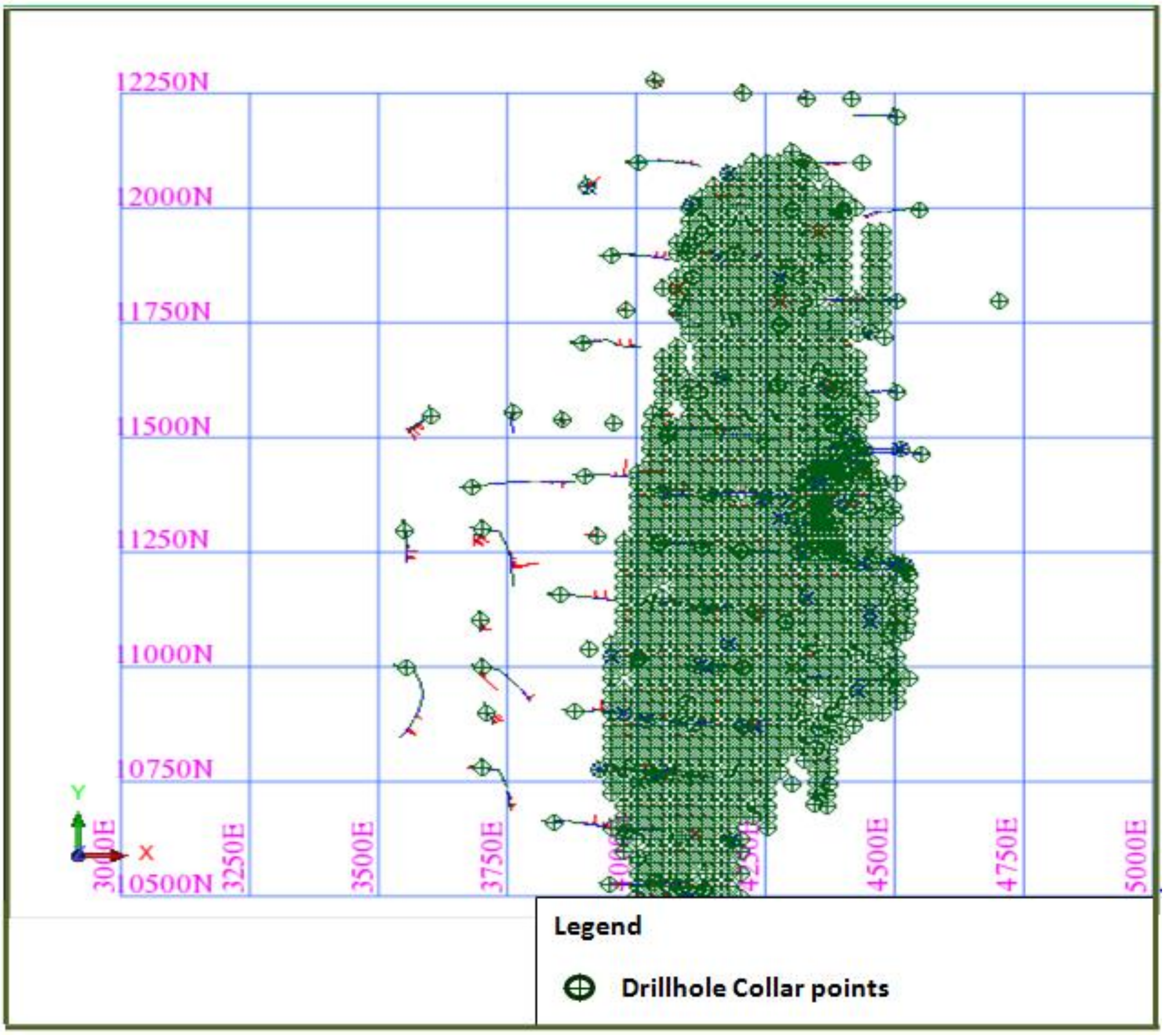

Figure 4.1 Plan View of Drillhole Layout of the Study Area.

4.2.2 Data Validation

Data validation was carried out to ensure that all errors and inconsistencies were corrected before processing. It included checking for the following:

I. Inappropriate collar coordinates

II. Inappropriate survey, lithological and assay values.

III. Interval errors/ overlaps

IV. Duplicate records

V. Typographical errors

At the end of the validation checks, no missing collar coordinates and inconsistencies were found and the data was deemed suitable to continue processing.

QAQC Reports for Kottraverchy, batches 132 to 151, 2013

Quality Assurance, Quality Control (QA/QC) were conducted on the drill-hole assay data in order to assess the quality of the assay data used for this resource work. The QAQC processes and procedures were in full compliance with Sarbanes - Oxley Act of 2002 (SOX404). Rapid Cyanide Leach and Fire Assay (FA) were the two analytical methods used to analyse for gold (au). All samples were submitted to SGS Laboratory, Tarkwa site for the period of January – September, 2013, batch 132 to 151.

For the purpose of this work, QAQC methods used was limited to pulp and coarse blank samples, field duplicate samples, certified standard reference material (SRM) samples with ± 3 standard deviation range. These were inserted into the samples as a check on precision, accuracy and contamination of the laboratory. When the analytical results returned from the Laboratory, Quality Control (QAQC) graphs were plotted to evaluate accuracy, precision and contamination index of the results. Quality Assurance Quality Control plots used for the evaluation are shown as follows:

Blanks: Blanks were used to monitor contamination of the assay results. A total number of 400 gold-barren phyllite both oxide and fresh coarse and pulp samples were used. For the purpose of this work, 5 samples above the acceptable limit of 0.001g/t for course samples and 0.005g/t for pulp samples were used as a measure of accepting the result, above these values, the results will not be accepted. Pulp and coarse blank samples submitted to the Lab had most of the results reporting around the detection limit of 0.001 and 0.005 g/t respectively and also fall within the acceptable limit of ± 3 standard deviation range as shown in Figures 4.2 and 4.3. The samples were free from contamination and thus accepted.

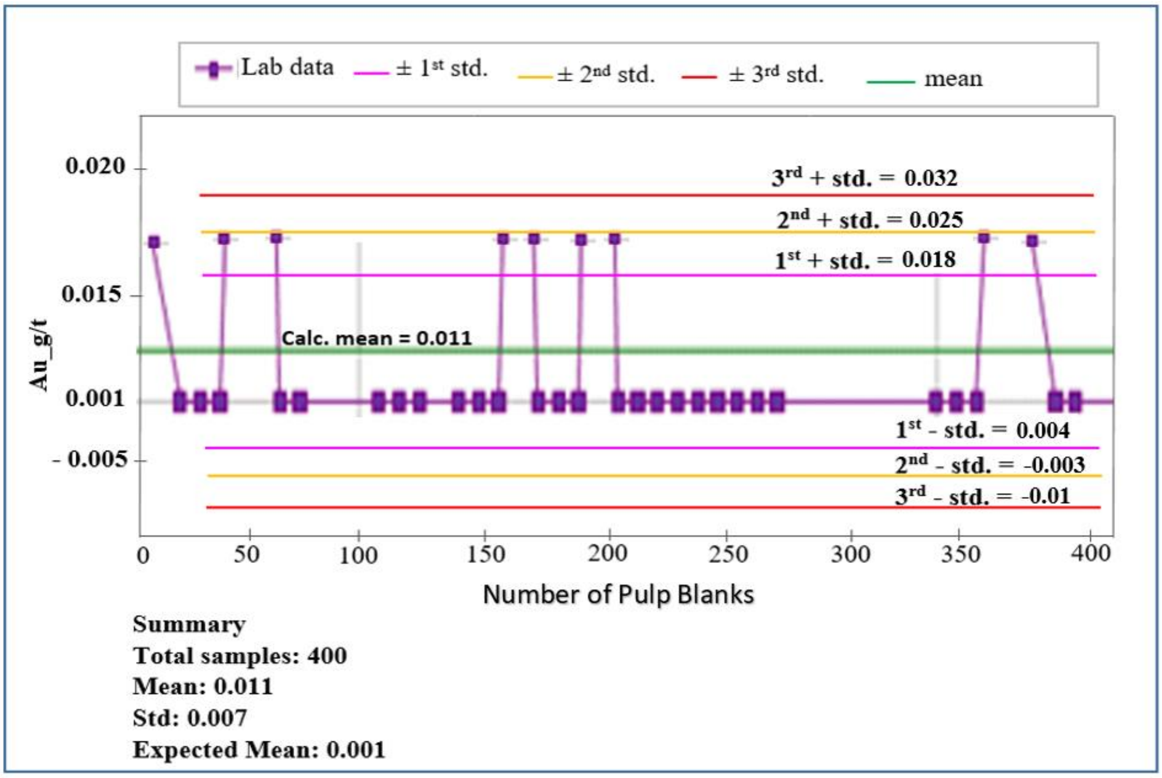

Figure 4.2 Pulp Blank Samples Performance against Detection Limit 0f 0.001 g/t.

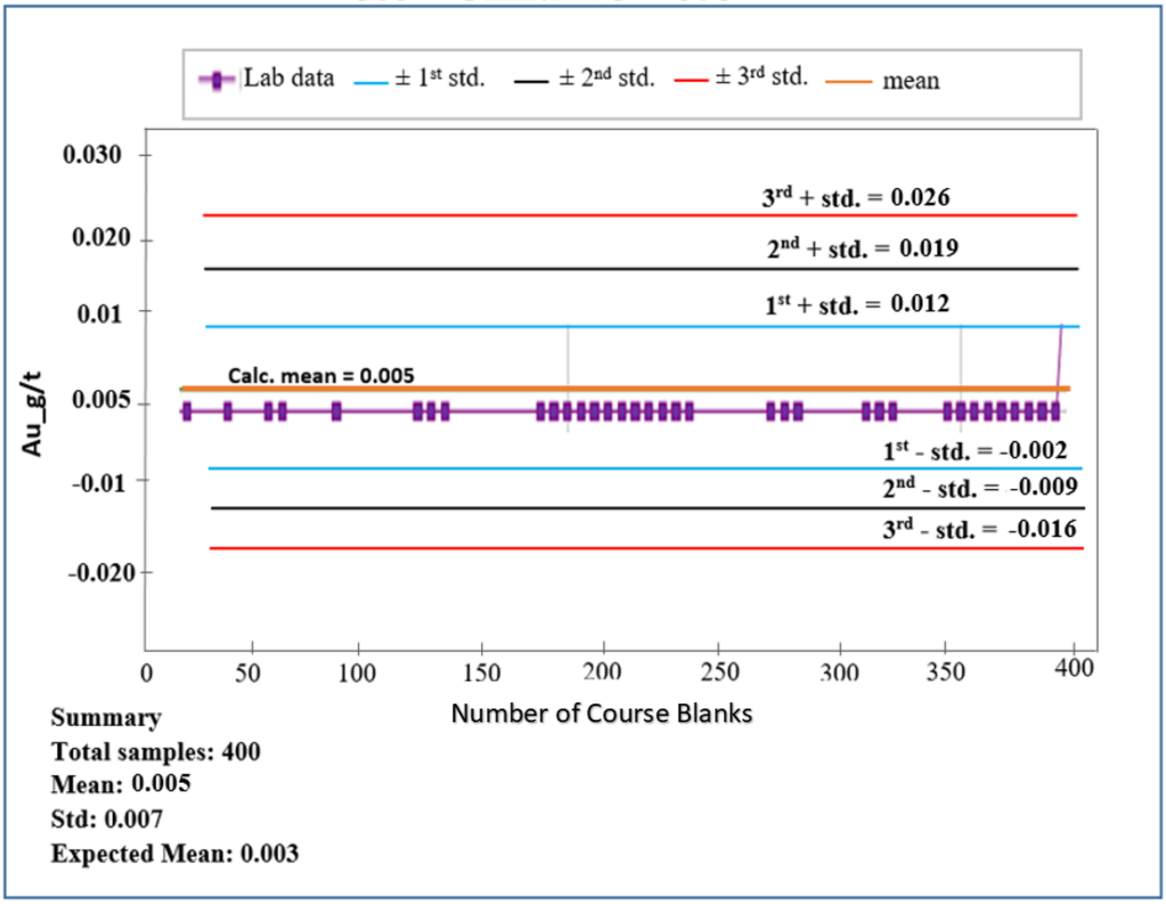

Figure 4.3 Coarse Blank Samples Performance against Detection Limit 0f 0.005 g/t.

Field Duplicates: Field duplicates were used to check whether homogeneous samples were taken or not. They provide a measure of the sample precision. A total of 586 Reverse Circulation (RC) field duplicate samples were submitted to the laboratory for assay. There was however no field duplicate taken for Diamond Drill (DD) samples since the other half core samples were being kept for geological logging and for future reference. A scatter plot of the original and the duplicate sample values produced a very good correlation coefficient of 0.98 as shown in Figure 4.4 indicating a good precision of the laboratory.

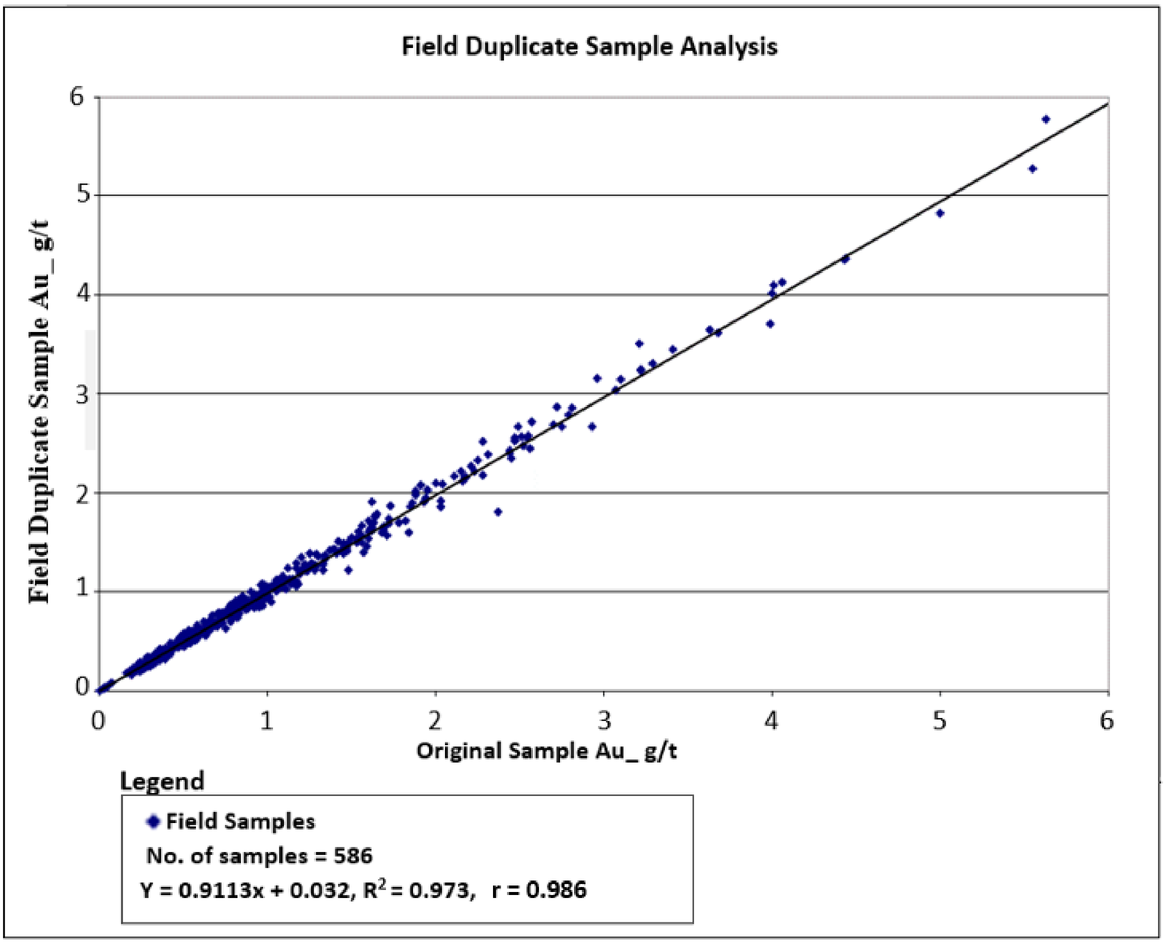

Figure 4.4 Scatter Plot of Field Duplicates on Original Au Values

The duplicate results were also subjected to Half Absolute Relative Deviation (HARD) analysis to verify a good splitting process and high precision.

The HARD was calculated from the formular according to Shaw (1997) as:

$$\text{a) } \% \text{ HARD} = \left(\frac{0.5|A-B|}{0.5(A+B)} \right) x100 \quad (4.1)$$

Where A and B are original and duplicate sample values respectively

$|A-B|$ = absolute difference between the pair values.

For illustration, % HARD of original and duplicate sample numbers CF3005 and CFD3005 respectively submitted to the Laboratory was calculated from the data below:
Sample pair: original (CF3005) = 1.7 ppm, duplicate (CFD3005) = 1.5 ppm

$$\%\text{HARD} = \left(\frac{0.5|1.7-1.5|}{0.5(1.7+1.5)}\right) \text{x} 100 = 6.3\%$$

The HARD value was then calculated for each sample pair of the 586 RC field duplicate samples that were submitted to the Lab for assay

1) The results were then ranked and the achieved % HARD value was calculated for a series of percentiles.
2) A graph was obtained where percentiles of the distribution were plotted along the X-axis and the achieved % HARD values along the Y-axis as shown in Figure 4.5. For the purpose of this work, accepted % HARD between (10 - 25 %) at 90th percentile was accepted for good splitting process and laboratory high precision (Anon., 2002).

From Figure 4.5, the Achieved Hard % was 18 %, therefore the splitting process as well as the precision of the laboratory was accepted.

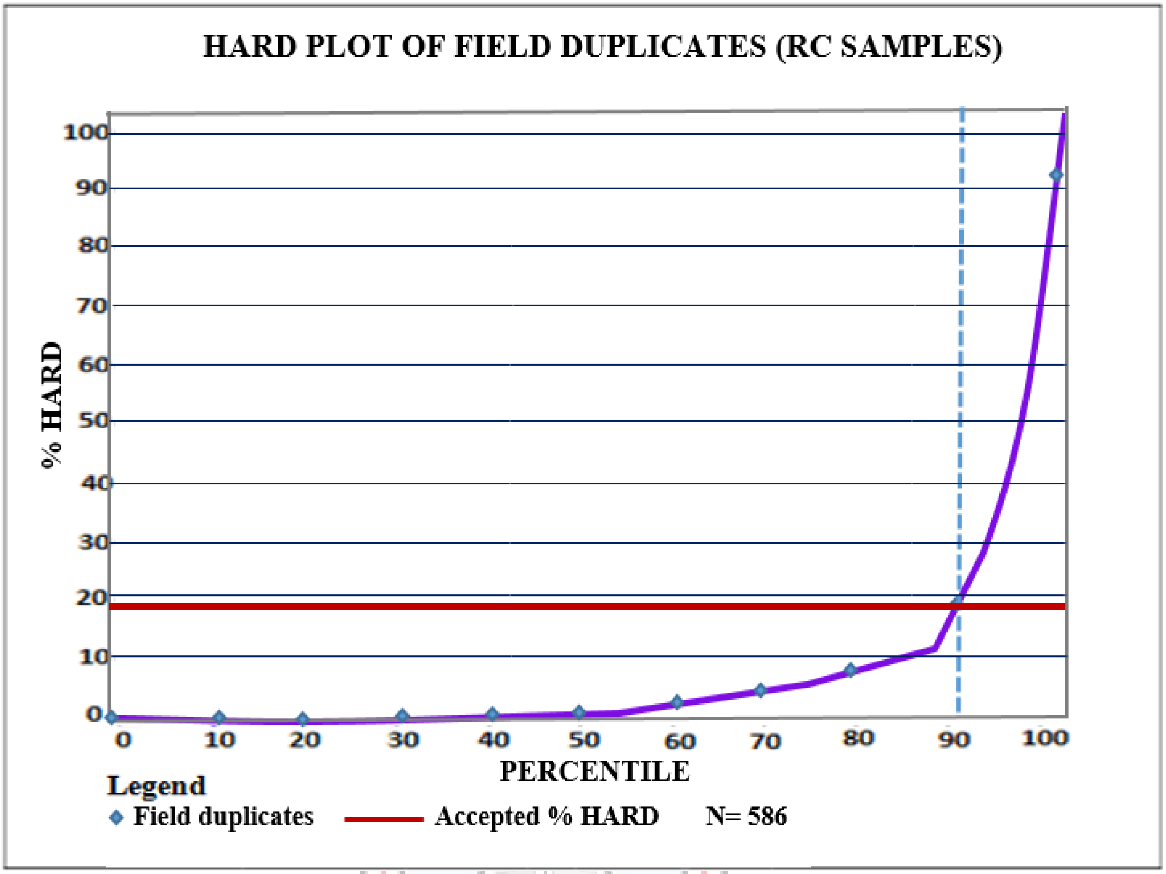

Figure 4.5 HARD Plot of Field Duplicate Samples

Certified Reference Materials– CRM: The purpose of including standard reference material was to check on the accuracy and precision of the laboratory's sample preparation and analysis protocols. SRM is a homogeneous material which has been assayed and analysed by a large number of laboratories using various techniques for assay controls. This sample has a known gold value, standard mean value, standard deviation, etc., which is used as a criterion for batch rejection (Anon, 2002).

A total of 500 standards from three (3) different grade ranges such as high grade (HGST) medium grade (MGST) and low grade (LGST) were used. Table 4.1 is a sample of SRM's used for this work and Figure 4.6 is a graphical representation of high grade standard reference material, HGST (OxK69) submitted to SGS Laboratory whiles the rest of the plots are presented in Appendix 1.

Table 4.1 Certified Referenced Material Inserted in Samples

Standard ID	Mean	Stand. Dev.	± 1st std.	± 2nd std.	± 3rd std.
HGST(OxK69)	3.58	0.072	3.65	3.72	3.80
MGST(OxG60)	1.03	0.029	1.06	1.09	1.12
LGST(OxE56)	0.61	0.016	0.63	0.65	0.66

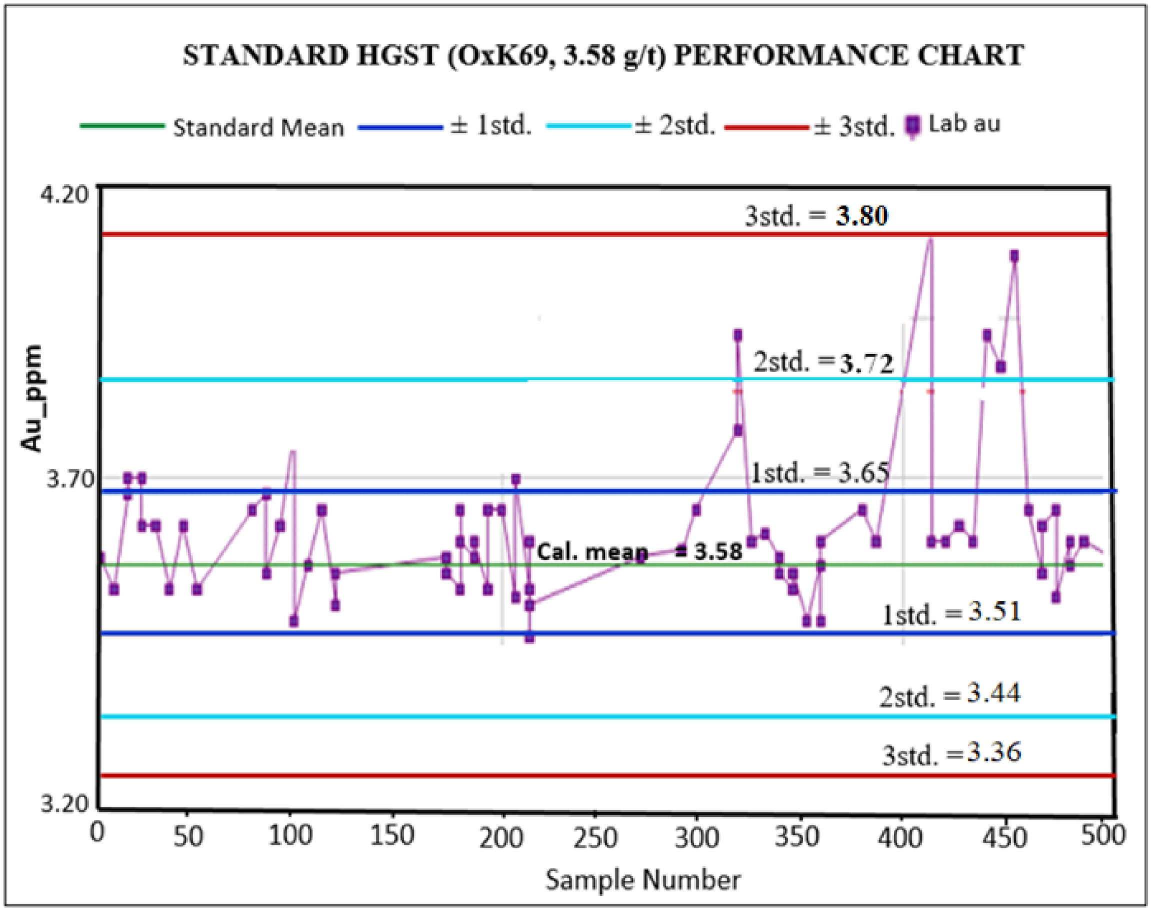

Figure 4.6 Plots of Assay Results of HGST OxK69 (3.58 g/t) against ±3 Standard Deviation.

The quality of SGS Laboratory operation was trusted and accepted since all the values used for the analysis were within the acceptable limit of ±3 standard deviation range. Data was validated and was found to be suitable for use.

4.2.3 Data Processing

The drillhole collars, survey, assay and lithology data were saved in a "comma separated format" compatible with "Surpac software", and loaded individually into the "Geovia Surpac 6.5.1 software" to generate a drillhole database. The plan view of the drillhole layout of the project area is shown Figure 4.1 and the samples of the data used for the resource estimation are shown in Tables 4.2 - 4.5.

Table 4.2 Surpac File Structure for Survey Data

Hole_id	Depth	Dip	Azimuth
CF3153	105	-90	0
CF3001	100	-90	0
CF3003	99	-90	0
CF3005	102	-90	0
CF3007	80	-90	0
CG2851	56	-90	0
CG2853	59	-90	0
CH2419	77	-90	0
CH2421	88	-90	0
GDK10	121	-45	100
GDK24	102	-46	100
GDK25	132	-50	270

Table 4.3 Surpac File Structure for Collar Data

hole_id	Eastings	Northings	Elevation	max_depth	hole_type	hole_path	Area
CF3151	4325.02	12025	92.3	98	RC	linear	Kottraverchy
CF3001	4300	11899.99	118.46	71	RC	linear	Kottraverchy
CF3003	4300	11925.03	109.83	65	RC	linear	Kottraverchy
CF3005	4300	11949.98	101.59	66	RC	linear	Kottraverchy
CF3007	4301	11975.04	93.59	95	RC	linear	Kottraverchy
CF3153	4225.11	12049.99	110.4	125	RC	linear	Kottraverchy
CG2851	4124.87	11724.98	110.75	75	RC	linear	Kottraverchy
CG2853	4125	11749.97	112.36	85	RC	linear	Kottraverchy
CH2419	4075	11325	112.32	89	RC	linear	Kottraverchy
CH2421	4075	11350	110.63	87	RC	linear	Kottraverchy
GDK10	4201.33	12009.13	103.74	207	DD	Curved	Kottraverchy
GDK24	4477.51	11718.21	101.94	83.5	DD	curved	Kottraverchy
GDK25	4522.18	11210.94	100.04	138	DD	Curved	Kottraverchy

Table 4.4 Surpac File Structure for Lithological Data

hole_id	depth_from	depth_to	lith_code	zone	Peb_size_mm	grain_size	colour	alteration	comment
CF3151	89	90	G1	Afc1		20	Dark Grey		
CF3153	90	91	S1	Afc1		15	Light Grey		
CF3001	93	94	G	Afc1		15	Dark Brown		
CF3003	76	77	G	Afc1		20	Grey		mylonite present
CF3005	77	78	G	Afc1		20	Grey	Selification present	Highly sheared
CF3007	78	79	G	Afc1		10	Dark Grey		
CG2851	88	89	S1	Afc1		10	Dark Grey		
CG2853	76	77	G1	Afc1		15	Dark Grey		
CH2419	77	78	G1	Afc1		15	Dark Grey		
CH2421	79	80	S1	Afc1		10	Dark Grey		
GDK10	75	76	G	Afc1	70	20	Dark Brown	Selification present	Dyke with mylonite
GDK24	100	101	G1	Afc1	65	15	Dark Grey		
GDK25	101	102	G	Afc1	50	20	Dark Grey		

Table 4.5 Surpac File Structure for Assay data

Batch No	Kott_2013_10-23				Au	Au	Au(F)
Method					RCL AAS	RCL AAS	FAA505
Ldectection					0.01	0.01	0.01
Udetection					1000	1000	1000
Units					ppm	ppm	ppm
hole_id	samp_id	depth_from	depth_to	samp_type	au_ppm		
CE3151	CE3151/1	89	90	Pulverised	<0.01		
CF3001	CF3001/2	90	91	Pulverised	1.09	-	
CF3003	CF3003/3	76	77	Pulverised	0.62	-	
CF3005	CF3005/4	80	81	Pulverised	2	1.77	1.82
CF3007	CF3007/5	82	83	Pulverised	0.99	-	
CF3153	CF3153/6	90	91	Pulverised	1.19	-	
CG2851	CG2851/7	88	89	Pulverised	0.89	-	
CG2853	CG2853/8	76	77	Pulverised	<0.01		
CH2419	CH2419/9	77	78	Pulverised	1.17	-	
CH2421	CH2421/10	79	80	Pulverised	0.63	-	
GDK10	GDK10/11	75	76	Hardcore	6.81	6.10	5.99
GDK24	GDK24/12	100	101	Hardcore	0.94	-	
GDK25	GDK25/13	101	102	Hardcore	1.16	-	

4.3 Combination of Data, Wireframe, Compositing and Distribution Analysis

4.3.1 Combination of Diamond Drill and RC Samples

The generation of a good variogram models requires much data. It may therefore be necessary to combine the drill hole data from the two different drilling types. For the purpose of this work, 6,289 RC samples and 500 DD samples were used. If groups of samples are to be combined for statistical analysis, then they should belong to statistically similar distributions (Annels, 1991). To investigate whether the samples produced by diamond drill (DD) and reverse circulation (RC) drilling belong to similar population statistically, F- and t-test were carried out on these two populations. The summary statistics of Input data are shown in Table 4.6

Table 4.6 Summary of Input Data Statistics for the Orebody

Data	No. of Samples	Min. (g/ t)	Max. (g/ t)	Mean (g/ t)	Variance (g/ t)^2	Standard dev. (g/t)
RC	6289	0.01	60.12	1.25	1.53	1.24
DD	500	0.01	18.15	1.18	1.82	1.35

The F-test method

The F-test was used to determine whether the RC and the DD sample data came from populations with identical variances at 5% level of significance (Davis, 1986).

The F-test calculations are presented in appendix 1 whiles the value obtained is 0.84.

For $F < F_\alpha$, H_o is not rejected.

Since the $F < F_{0.025}$ (∞, ∞), there is no enough evidence to reject the similarity of the population for RC and DD samples at 5 % level of significance. Hence the equality of the means was tested with the t-test.

The *t-test Method*

The t-test was used to test the equivalence of two means. Having proven from the F-test that the variances of the two sample types were not significantly different, the equivalence of their means was also tested using the t-test (Davis, 1986). The t-test was obtained as follows whiles the results of the test is shown in Table 4.7.

The calculated value, $t = \dfrac{\mu_{RC} - \mu_{DD}}{s_p \sqrt{\left(\dfrac{1}{n_{RC}} + \dfrac{1}{n_{DD}}\right)}}$ where S_p = pool standard deviation.

$$s_p^2 = \frac{(n_{RC} - 1)s_{RC}^2 + (n_{DD} - 1)s_{DD}^2}{(n_{RC} + n_{DD} - 2)}$$

$S_p^2 = \dfrac{(6289 - 1)(1.53) + (500 - 1)(1.82)}{(6289 + 500 - 2)}$ = 1.55. Therefore, $S_p = 1.24$

Calculated statistic; $t = \dfrac{(1.25 - 1.18)}{1.24\sqrt{\left(\dfrac{1}{6289} + \dfrac{1}{500}\right)}} = 1.21$

At 5% level of significance and for two tailed test, the tabulated value, $t_{0.025}(n_{RC} + n_{DD} - 2) = t_{0.025}(6787)$ was obtained from statistical table as $t_{0.025}(\infty) = 1.960$.
$t < t_{0.025}(\infty)$, hence H_o was not rejected.

The results of the test also indicated that there was no significant difference between the means of the distributions since calculated t value < Tabulated t value and that they came from identical populations. Hence the two samples were combined for further statistical analysis and resource estimation.

4.3.2 Wireframe Modelling

The geological interpretation of the results were done and used as guides in digitising the mineralised zones on the screen. The Afc1 zones lying close to each other were digitised. The mineralised zones were delineated using an economic cut-off grade of 0.50 g/t as used by the mine. However, few samples below 0.5 g/t but sandwiched between high grades and also with insignificant thickness (thickness less than 0.5 m) were inevitably included in the wireframe. Figure 4.7 presents a cross sectional plot of digitised wireframe string along 10900 N.

The strings created from digitising the ore zones on each section were joined to their corresponding segments in the other adjoining sections to generate a triangulated 3-dimensional wireframe solid using the "Solids-Triangulate-Between Segment and Inside segment" menus in Surpac covering the entire strike length of the project area. The solids were then validated using the "Solids-Validation-Close Open Sides for Objects" menus in

Surpac to make sure triangles forming the solids were not crossing each other. Areas with errors on the triangulated surfaces were indicated by the wireframe verification process and were duly corrected. Figure 4.8 shows a section of the three dimensional wireframe solid generated along 10900 N.

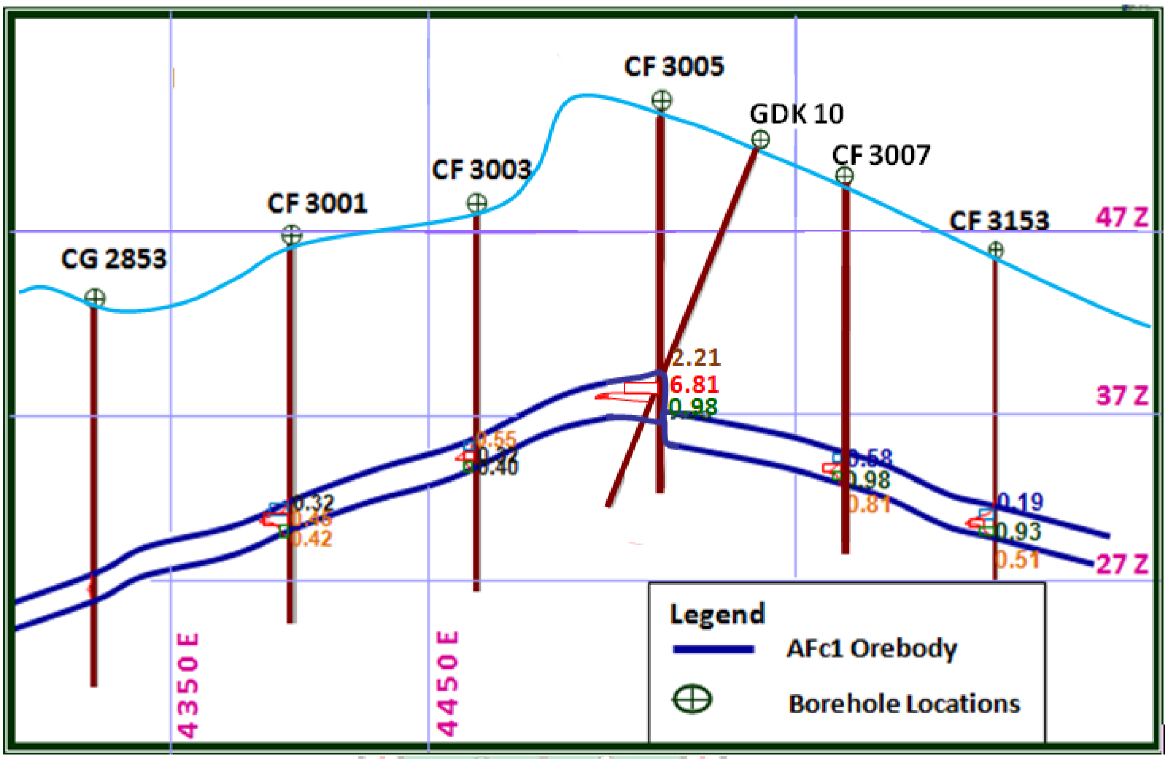

Figure 4.7 Cross Section Plot of AFc1 Reef Digitised Wireframe String Along 10900 N.

Borehole identification number CF 3005 and GDK 10 intercepts a major fault and grades along the fault has higher values than the surrounding boreholes (Figure 4.7 and Tables 4.4 and 4.5).

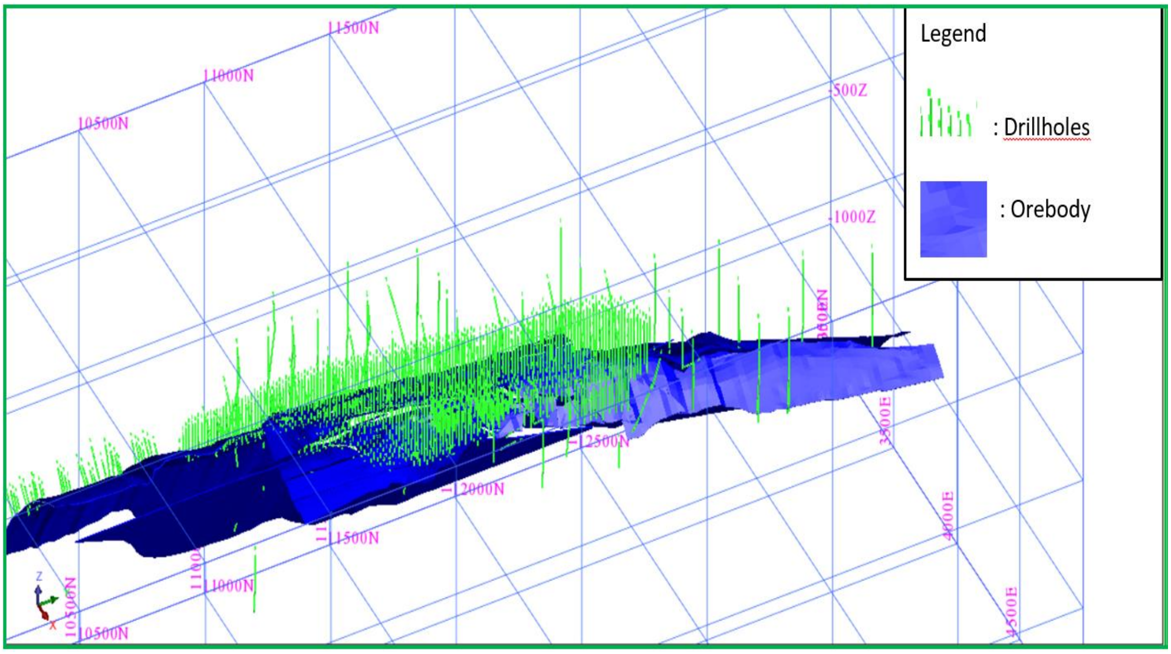

Figure 4.8 Isometric View of Modelled Orebody

4.3.2 Sample Selection and Compositing

All samples falling within the wireframe were selected and composited to 1 m downhole intervals for the entire data sets. Compositing of the drill hole data was done in order to generate uniform support to make statistical and geostatistical estimates meaningful. A threshold length of acceptance was set to 50 % so that a residual at the end of a hole within the wireframe model would not be retained if its length was less than 0.5 m. Overall, approximately 1.5 % of the samples were discarded on the basis of sample length. The generated file consisted of 6,687 composite samples.

4.3.4 Distribution Analysis

Selection of data was done, using geological and mineralogical domains. The data for the AFC1 resource analysis for the Ordinary Kriging and MIK were taken from 1 m composites. Histogram and probability plots were generated to determine types of distributions and identify outliers. Summary statistics for the 1-m composites are shown in Table 4.7 whilst Figure 4.9 shows the histogram with cumulative frequency curve. The gold mineralisation is characterised by a positively skewed distribution (Figure 4.9) as is expected for gold deposits (Davis, 1986).

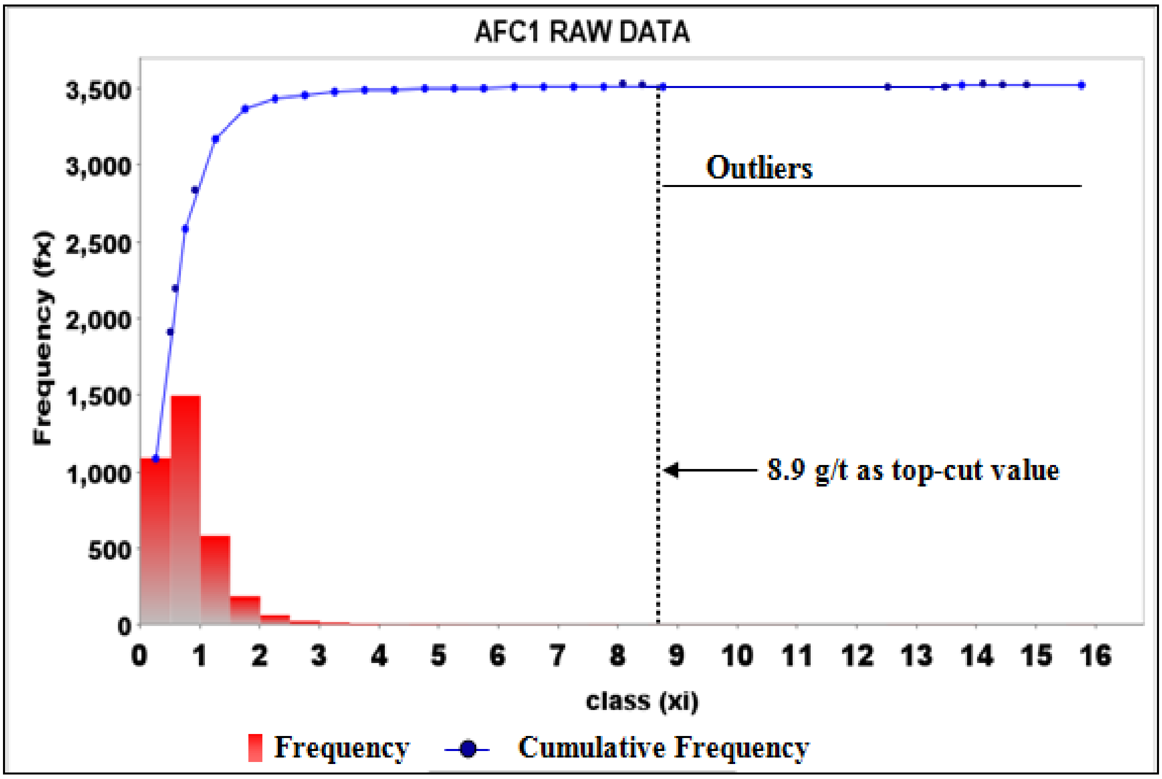

Figure 4.9 Histogram with Cumulative Frequency of 1 m Composite of AFC1 Reef.

Table 4.7 Summary of Univariate Statistic of 1 m Gold Composite for the AFc1-Reef Zone.

Statistics Raw Data	AFc1-reef Values
No. of Samples	6687
Minimum value (g/t)	0.001
Maximum value (g/t)	26.700
Mean (g/t)	0.800
Median (g/t)	0.480
Variance	6.220
Standard Dev.	2.494
Covariance (CV)	3.117
Skewness	6.407
Kurtosis	70.219

From the summary statistics (shown in Table 4.7), the coefficient of variation of 3.117 indicates moderate-to-high grade variation for the gold deposit (Bronshtein, 2004). It is an indication that few outliers may exist and estimation problems may be expected.

Outlier Analysis (Upper Cuts)

The histogram shows a positively skewed distribution (Figure 4.9). This implies that the sample population contains a large amount of low grade samples and a small amount of relatively very high grade samples, some of which may be outliers. The log probability graph (Figure 4.10) shows distinct sub-populations that confirm an indication of outliers (few high grades) in the data. At $e^{2.19}$ there is an inflexure (Figure 4.10) that indicates a change from one population to another (Bronshtein, 2004).

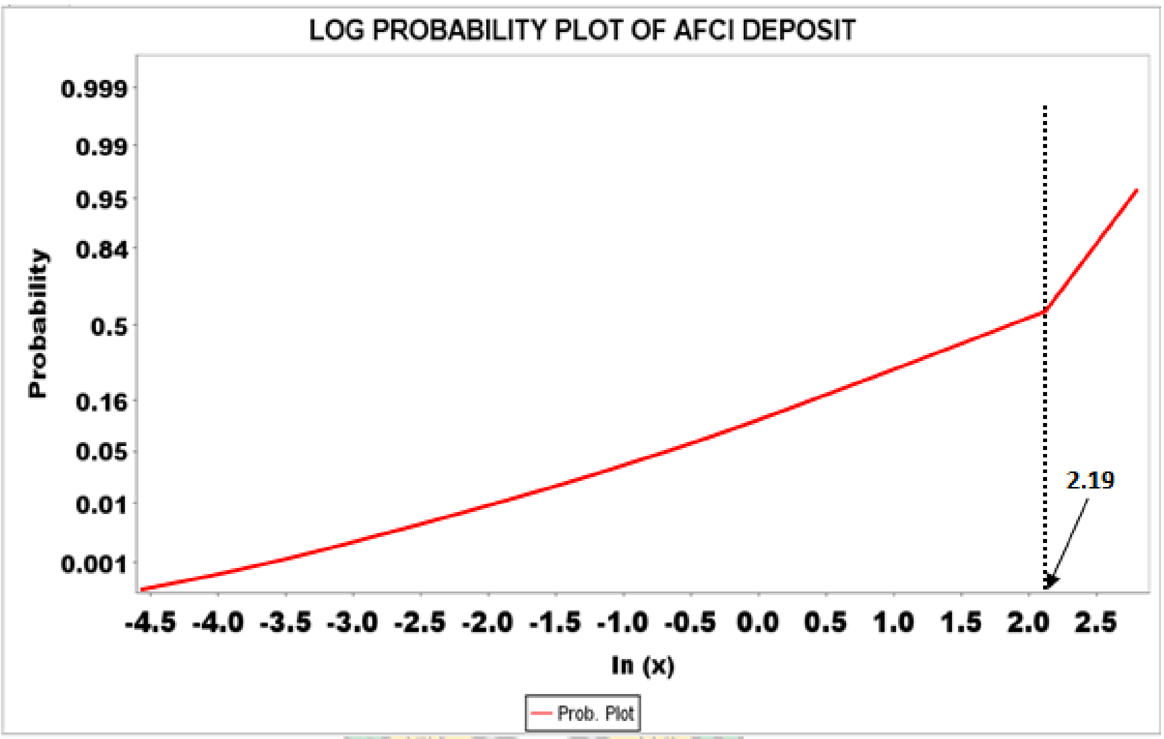

Figure 4.10 Log Probability Plot of the Distribution of 1 m Composites of AFc1 Deposit.

Upper cuts were therefore applied to limit the disproportionate influence of a few high-grade outlier samples. The $e^{2.19}$ giving a value of 8.94 was used as an upper top-cut value for the estimation. This value is evidenced in Figure 4.9. The upper cut-off grade of 8.9 g/t applied to the data prior to estimation reduced all grades above 8.9 g/t to 8.9 g/t. In all, thirteen (13) samples representing less than 1% were regarded as outliers.

4. 4 Variogram Modelling

The composited drillhole data captured within the wireframes were used for the variogram analysis for both the Ordinary Kriging (OK) and Multiple Indicator Kriging (MIK) estimation.

4.4.1 Variography for OK

An omni-directional downhole semi-variogram along azimuth of 00°, Plunge of 00°, spread of 90°, and lag spacing of 1 m was calculated and modelled (Figure 4.11). This enhanced the estimation of the nugget variance. Horizontal Directional semi-variograms were thereafter calculated and modelled with lag spacing of 12.5 m, spread of 25° and angular tolerance of 45° (to allow for adequate data capture) and a maximum lag distance of 187.5 m along strike, across strike direction of the orebody. Figures 4.12 and 4.13 show the semi-variograms along strike (which was the direction of maximum continuity) and across strike respectively. The directional semi-variogram model parameters are shown in Table 4.8

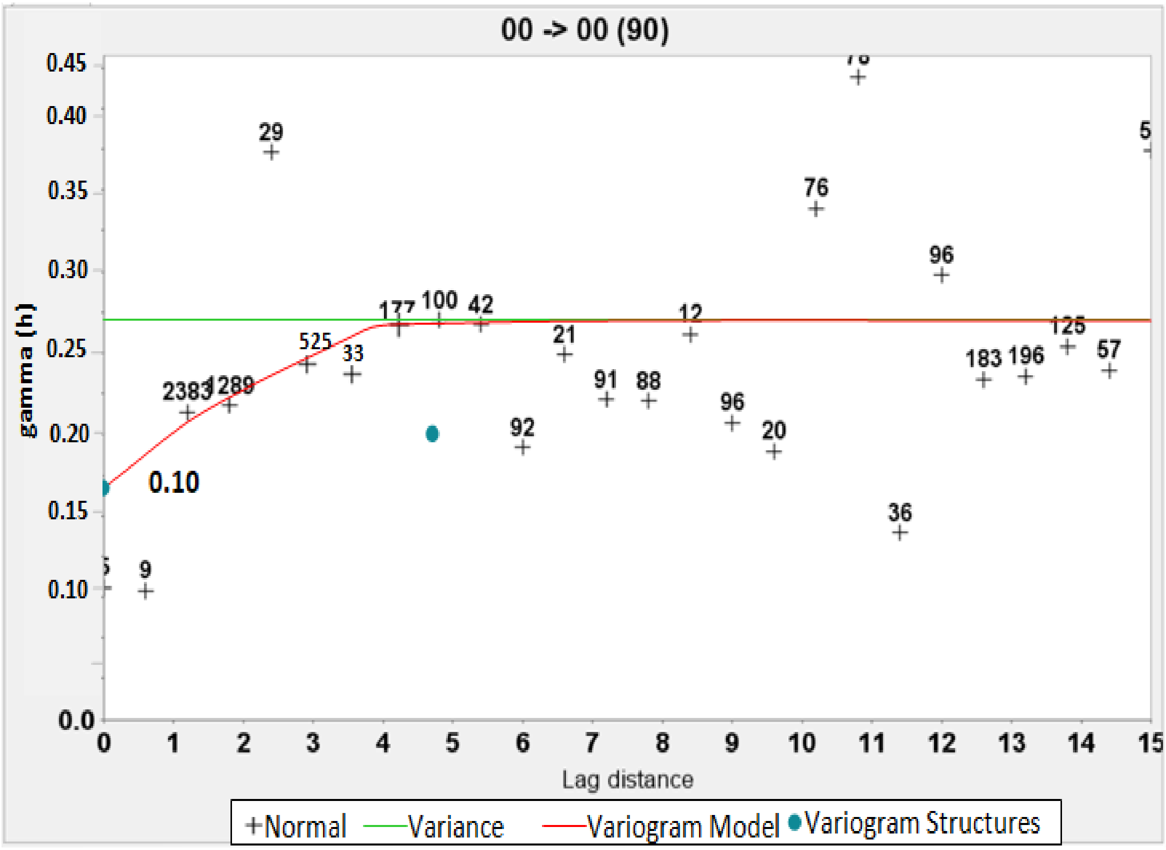

Figure 4.11 Afc1 Reef Omni-directional Variogram (Downhole)

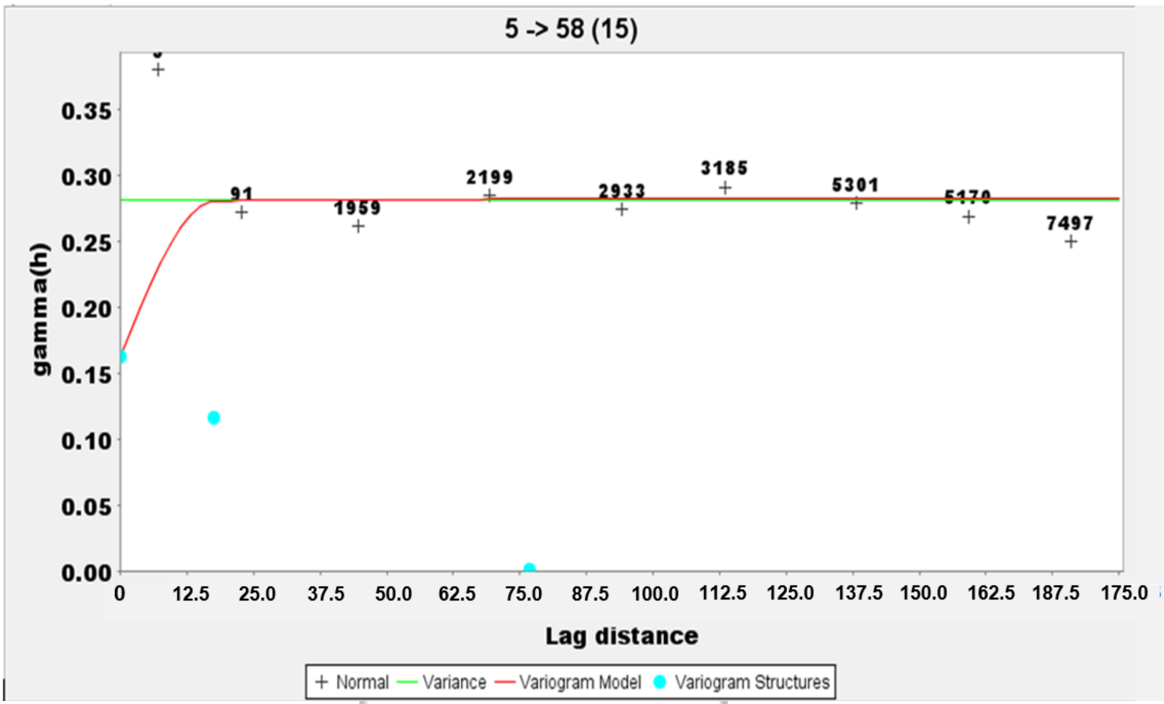

Figure 4.12 Afc1 Reef Directional Semi-variogram Along Strike Direction.

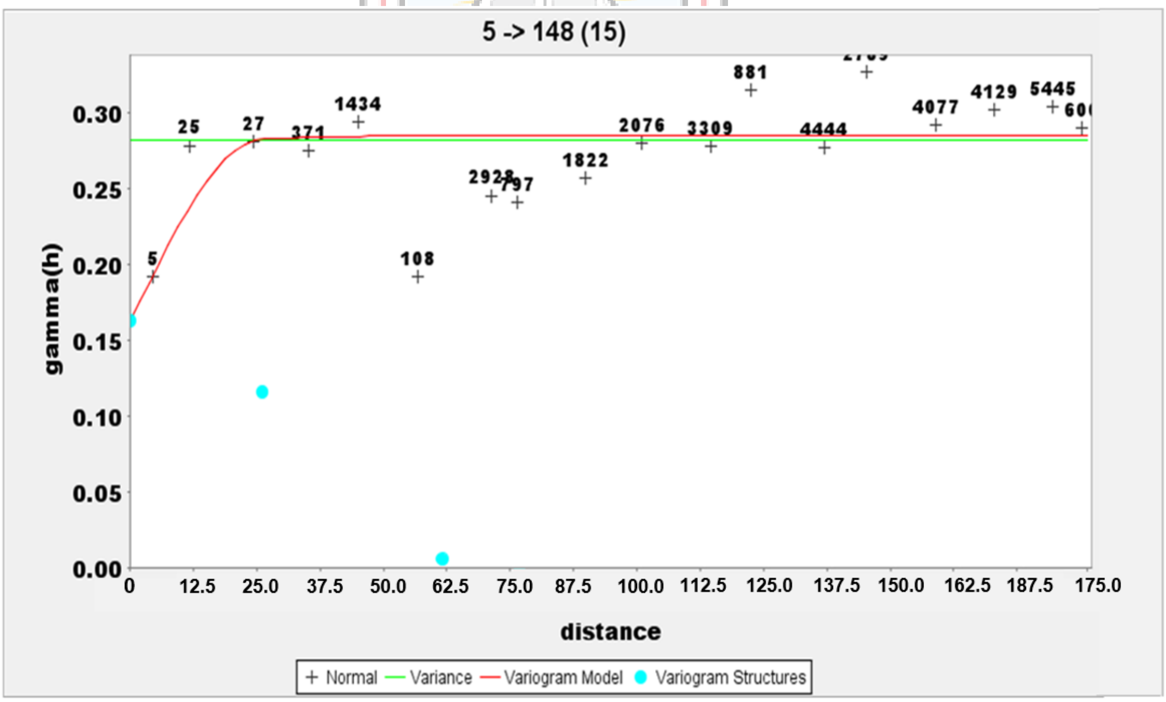

Figure 4.13 Afc1 Reef Directional Semi-variogram Across Strike Direction

OK variogram models indicates two nested structures in the plane of the orebody (Table 4.8) which may be as a result of alteration and shearing triggered by faults that controlled the mineralisation exhibiting the long range structures.

Table 4.8 Semi-Variogram Parameters for OK for Afc1 Reef

Direction	Azimuth	Co	C1	C2	a1	a2	Anisotropic Factors	
							Major / Semi-Major	Major / Minor
Downhole or Minor	0.00	0.163	0.116		4.411		1.24	17.47
Along Strike or Major	58.00	0.163	0.116	0.003	14.602	77.00		
Across Strike or Semi-Major	148.00	0.163	0.116	0.006	26.01	62.00		

During the horizontal directional variogram modelling, the variography map was generated in "Surpac -Block Model - Geostatistics -Ellipsoid visualiser tool" to aid the determination of direction of major continuity of the mineralisation. The search ellipsoid has its major, intermediate and minor radii oriented along the strike (with a steep dip of 58^{o}), across strike perpendicular to the strike (with a dip of 148^{o}) and down dip (with a dip of 0^{o}) respectively. This attributes conform to Kottraverchy structural attritudes of the orebody seen as moderate - to- steep NNE- dipping sets. Figure 4.14 and 4.15 represent a variogram map from the search ellipsoid.

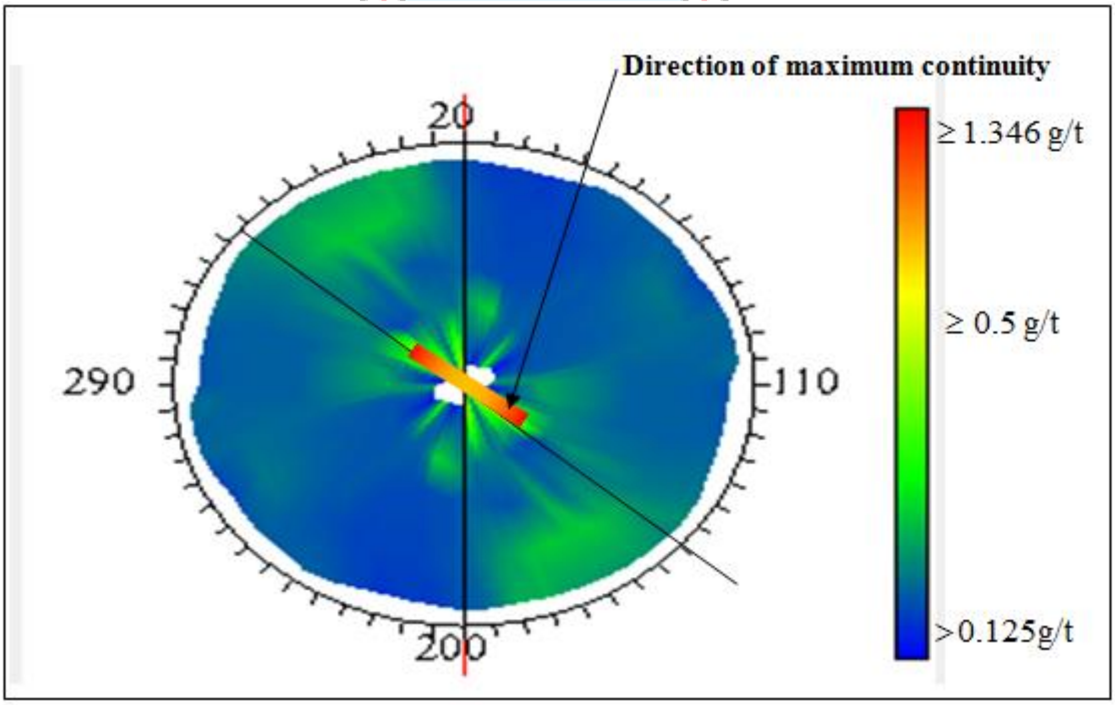

Figure 4.14 Variogram Map of Major Mineralisation Continuity.

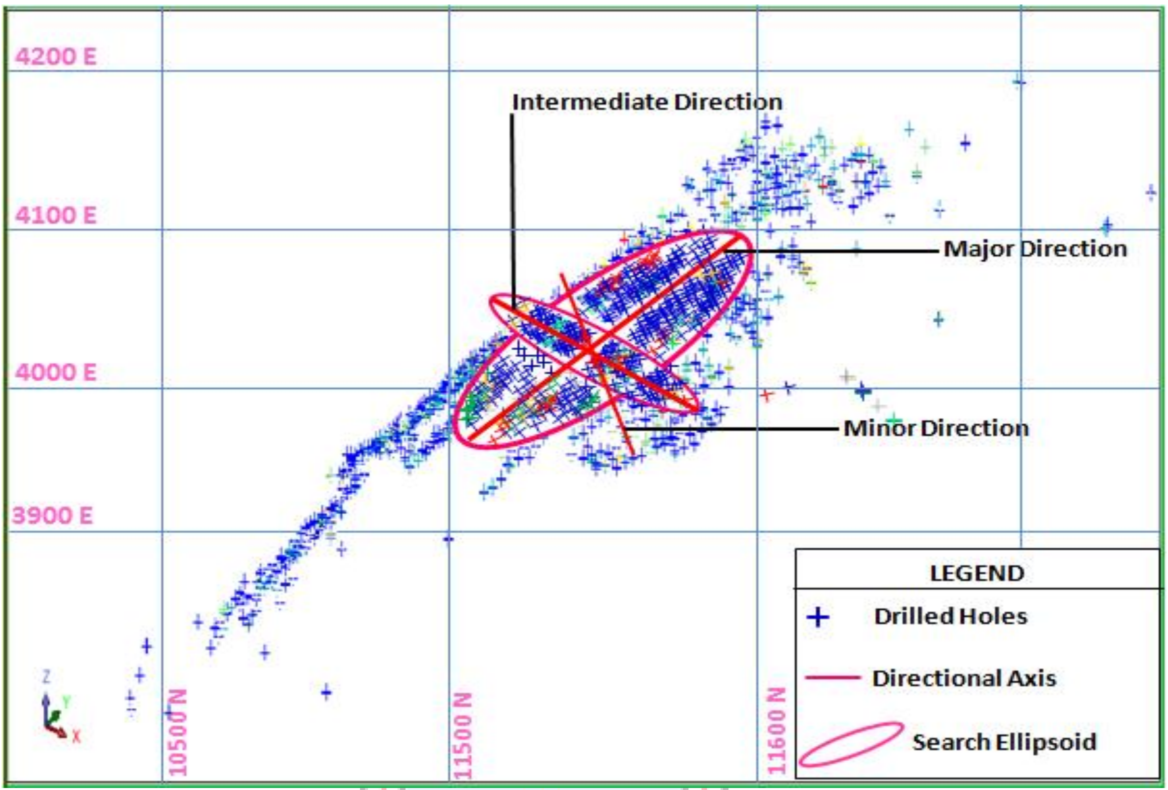

Figure 4.15 Plan View of Search Ellipsoid Derived from Variogram Map Analysis

4.4.2 Variography for MIK

A number of indicator semi-variograms were generated to study the spatial distribution of the indicators. For the MIK, seven (7) cut-offs were used: 0.5, 1.0, 1.5, 2.0, 2.5, 3.0 and 3.5 g/t. This was done using the "Surpac Basic Statistics Tool" to generate them based on the bin size of 0.5 as 0.5 g/t is the current cut-off grade of the GFGL mine. These were used as grade threshold to establish class intervals and computation of the class mean. Table 4.9 shows summaries of the conditional statistics.

Table 4.9 Conditional Statistics

Threshold	Class Count	Class Mean	Class Median	Class Relative Frequency
< 0.5	2091	0.327	0.302	0.311
0.5 - 1.0	3497	0.739	0.622	0.423
1.0 -1.5	785	1.225	1.191	0.167
1.5 - 2.0	197	1.585	1.541	0.054
2.0 - 2.5	67	2.175	2.170	0.019
2.5 - 3.0	29	2.739	2.700	0.008
3.0 - 3.5	17	3.318	3.310	0.005
≥ 3.5	4	4.920	4.080	0.003
Total				1.0

The sample values were then transformed into indicators. Sample values which were below the threshold values for each class were assigned a value of 1 and those equal to or above the threshold were assigned a value of 0 using "Perform Maths on all points of selected string menu" in Surpac. The indicator is obtained as (Hackman, 2012):

$$i(x;Z_c) = \begin{cases} 1 \text{ if } Z(x) < Z_c \\ 0 \text{ if } Z(x) \geq Z_c \end{cases} \quad \text{.......... (4.1)}$$

where

i = indicator variable at location x, for the cut-off Z_c, and

Z(x) = grade at location, x.

With the data transformed into zeros (0) and ones (1), directional indicator semi-variogram models for indicator values of 0's and 1's were calculated and modelled for each cut-off. A lag spacing of 12.5 m based on the average drill hole spacing in horizontal plane, spread of 25° with an angular tolerance of 45° and a maximum lag distance of 187.5 m were used. The directional experimental variograms were calculated and modelled along strike, across strike and downhole. Downhole indicator semi-variograms were used first to establish the nugget variances for along strike and across strike directions for each given cut-offs.

All depicted nested structures of spherical models similar to those of the OK semi-variogram models. Tables 4.10 and 4.11 show summaries of indicator variogram model parameters and anisotropic ratios for the various cut-offs whiles Figures 4.16 - 4.24 present indicator variogram models along strike, across strike and down dip for cut-off values of 0.5 g/t , 1.0 g/t and 1.5 g/t respectively. Those for other cut-off indicator models are presented in Appendix 1.

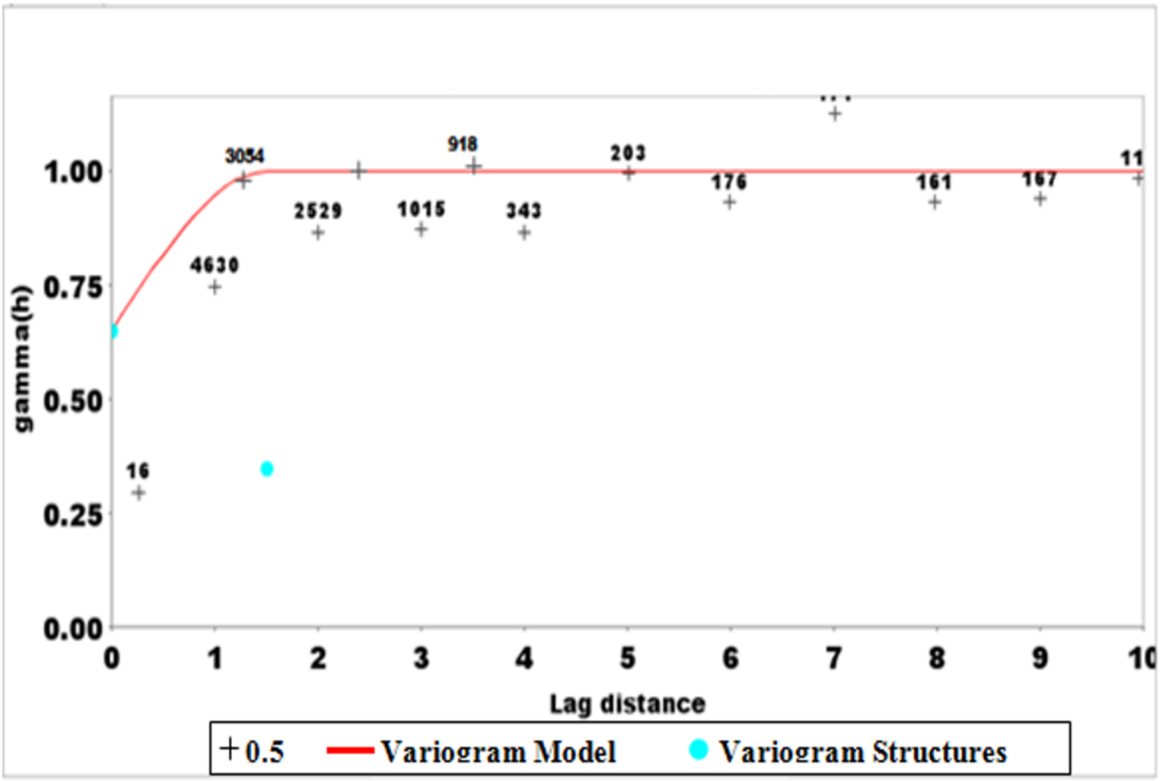

Figure 4.16 Indicator Downhole Variogram for 0.5 g/t Cut-Off.

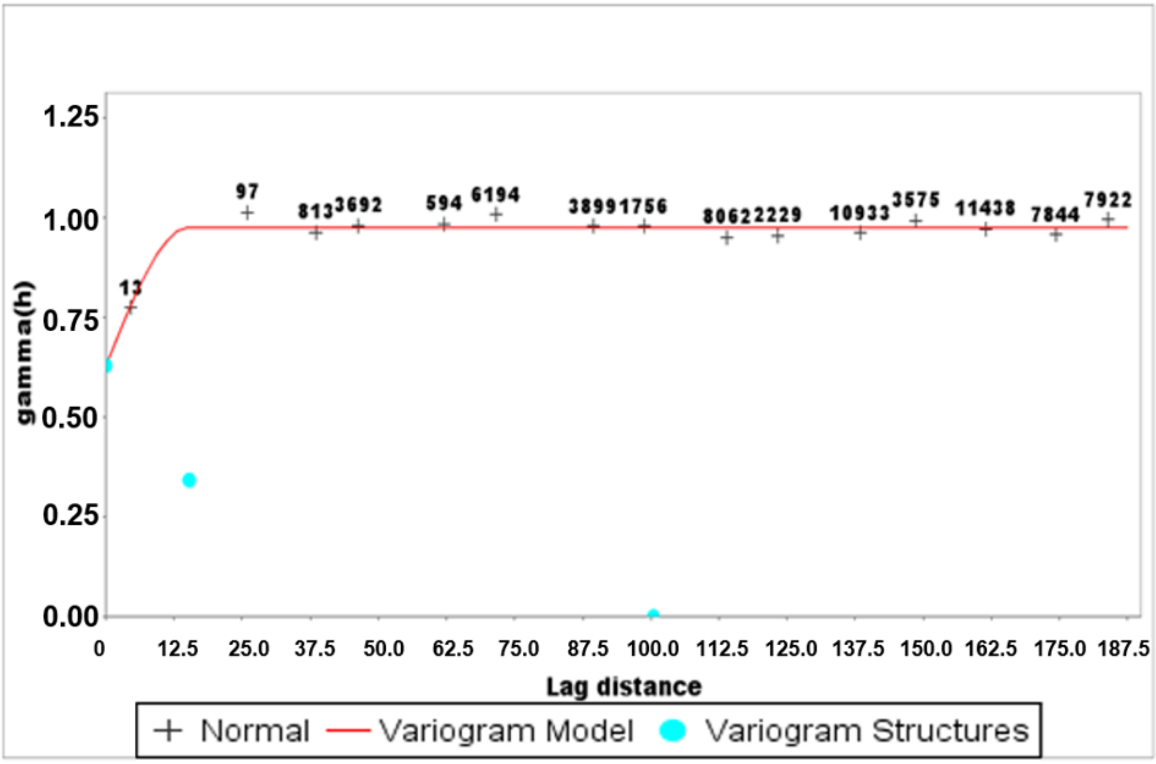

Figure 4.17 Indicator Variogram Along Strike Direction for 0.5 g/t Cut-Off.

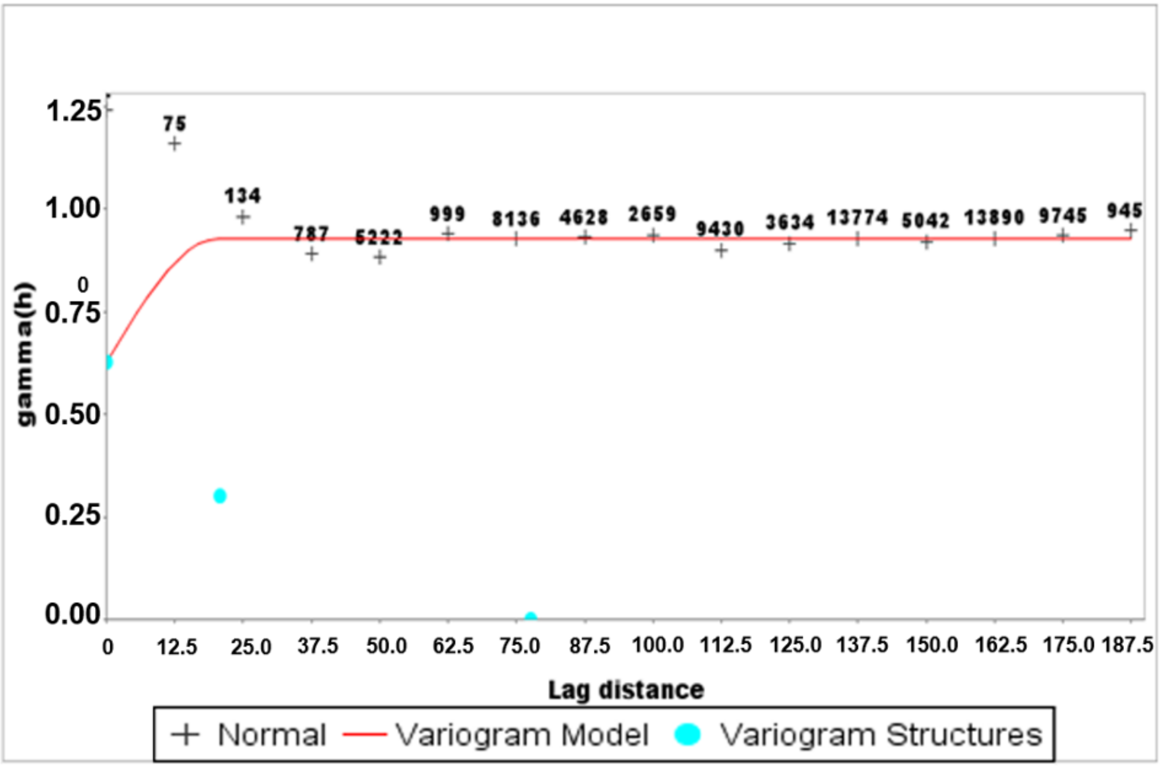

Figure 4.18 Indicator Variogram Across Strike Direction for 0.5g/t Cut-Off.

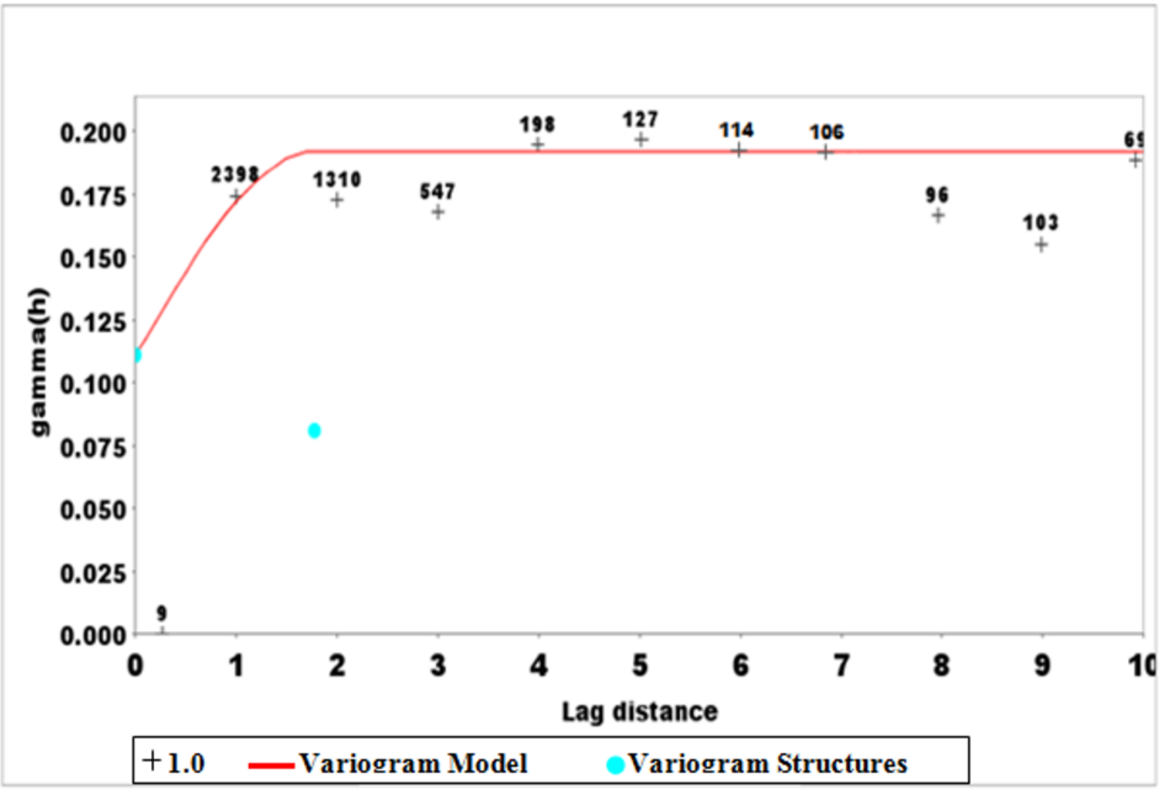

Figure 4.19 Indicator Downhole Variogram for 1.0g/t Cut-Off.

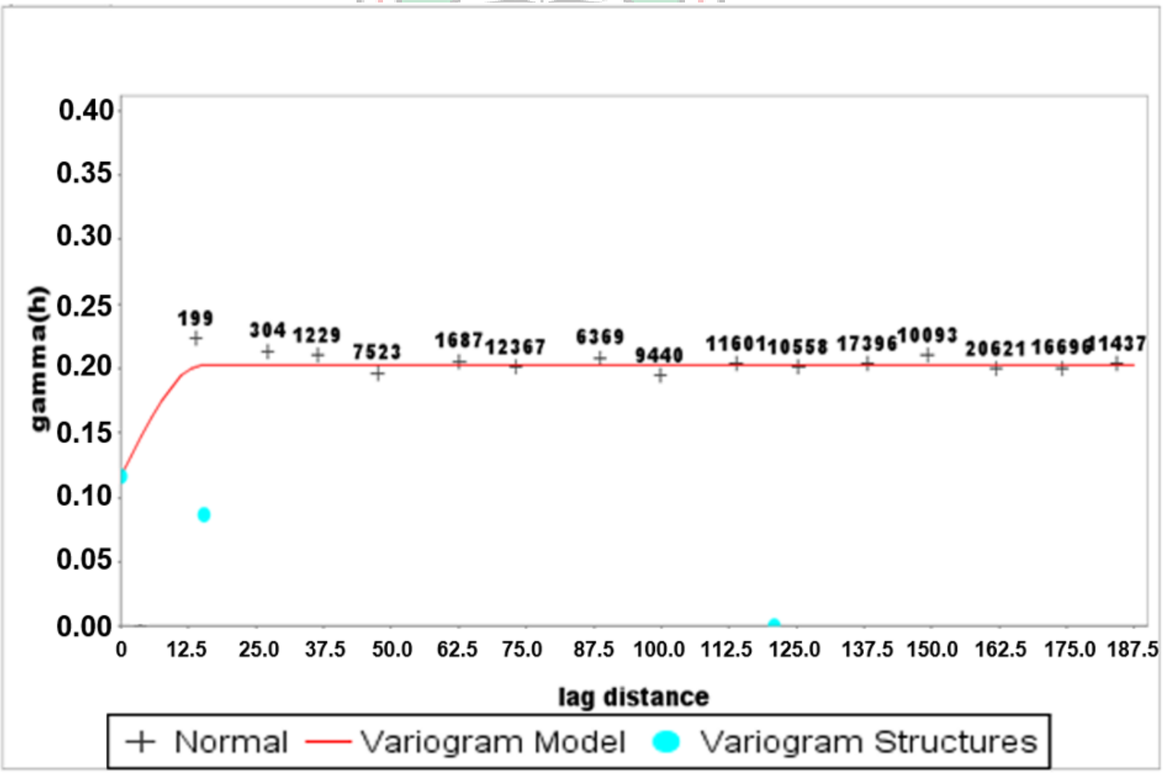

Figure 4.20 Indicator Variogram Along Strike Direction for 1.0g/t Cut-Off.

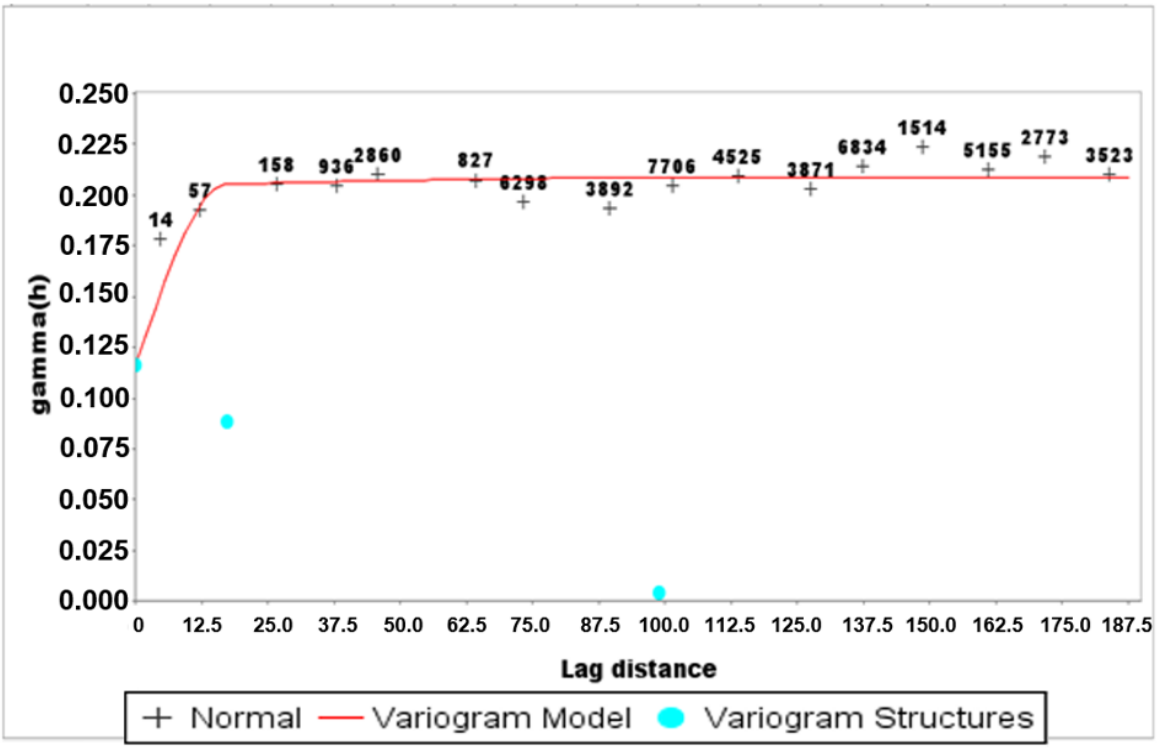

Figure 4.21 Indicator Variogram Across Strike Direction for 1.0g/t Cut-Off.

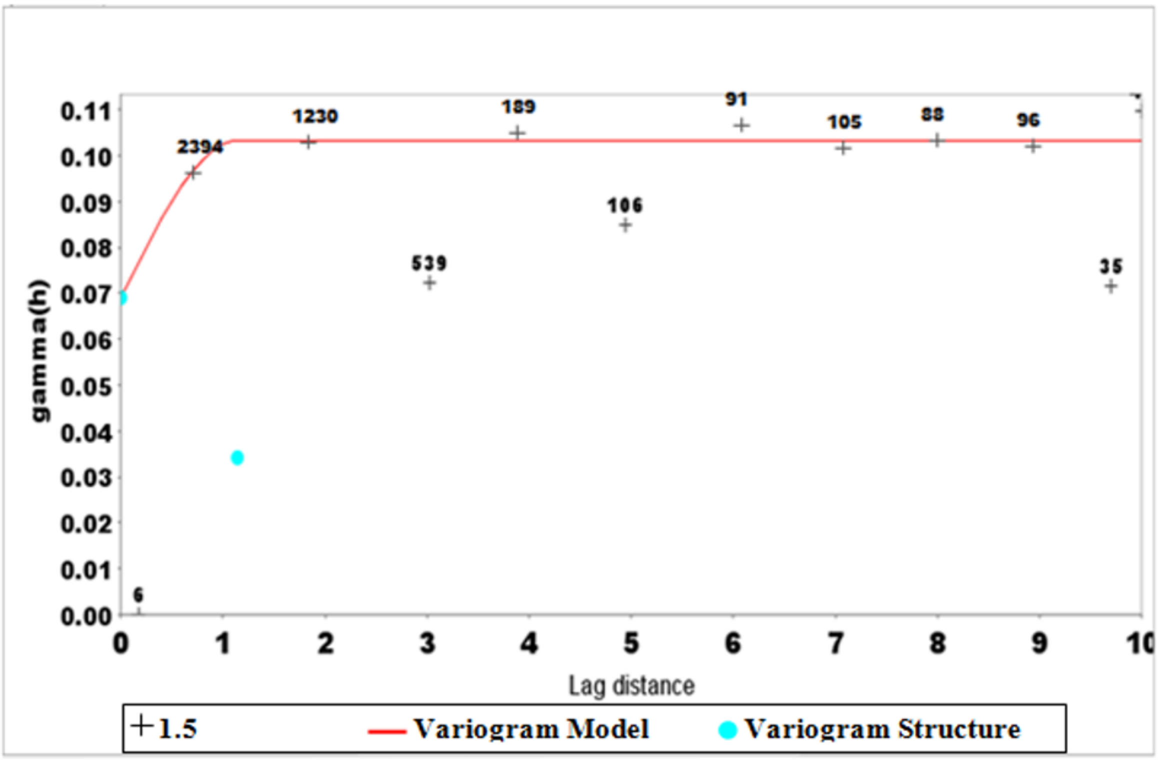

Figure 4.22 Indicator Downhole Variogram for 1.5g/t Cut-Off

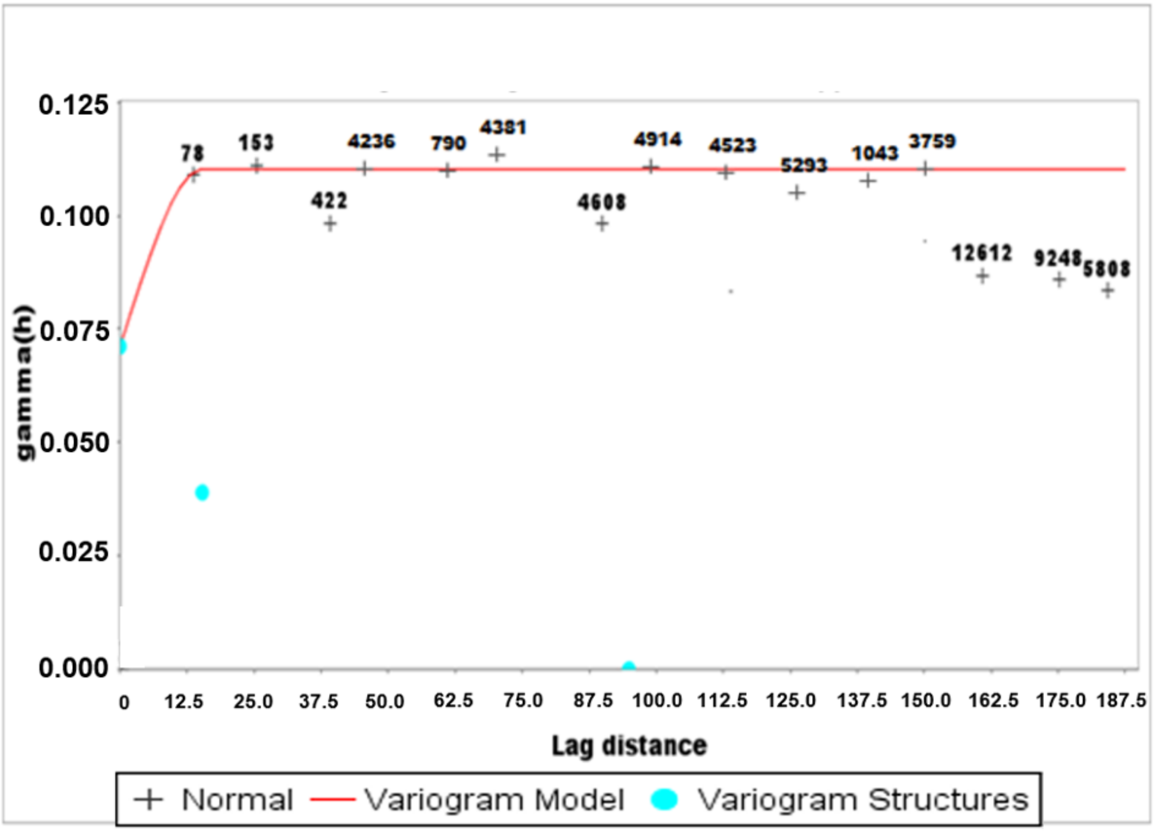

Figure 4.24 Indicator Variogram Along Strike Direction for 1.5g/t Cut-Off.

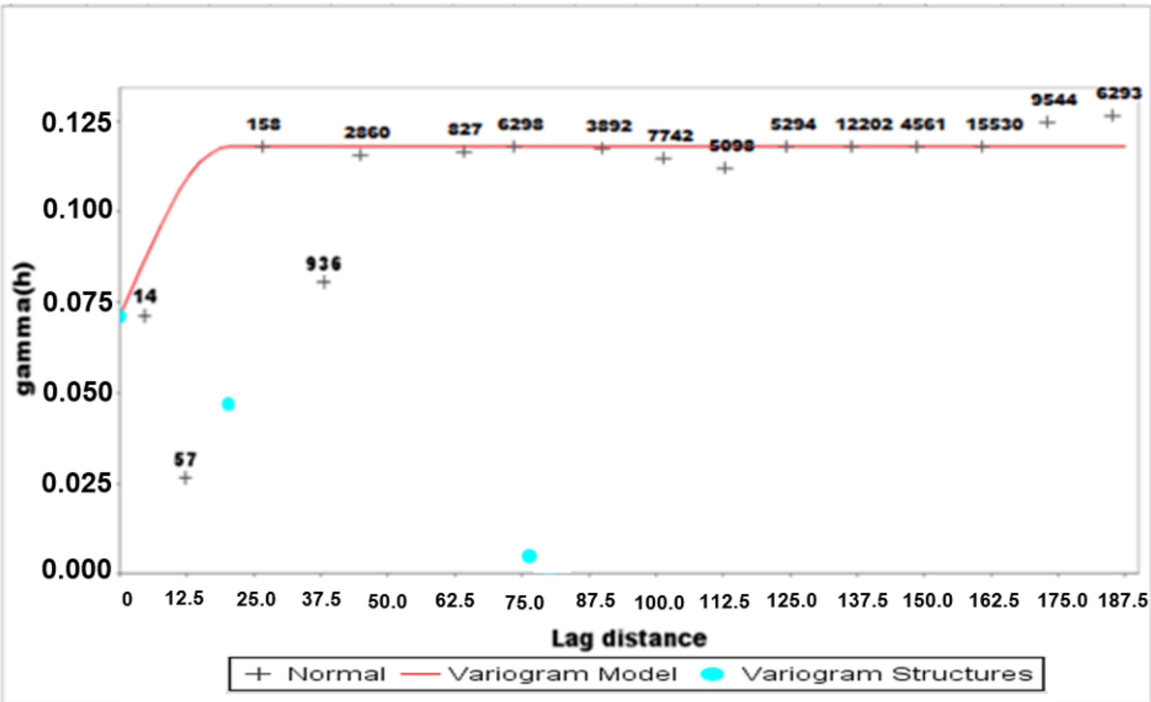

Figure 4.23 Indicator Variogram Across Strike Direction for 1.5g/t Cut-Off

Table 4.10 Afc1 Reef Indicator Variogram Parameters for MIK

Direction(m)	Indicator cutoff (g/t)	C_0	C_1	C_2	a_1	a_2	Model type
Downhole	0.5	0.6440	0.344		1.307		spherical
	1.0	0.1160	0.080		1.605		
	1.5	0.0720	0.034		1.144		
	2.0	0.0320	0.011		1.287		
	2.5	0.0200	0.006		1.706		
	3.0	0.0140	0.007		1.099		
	3.5	0.0110	0.007		1.811		
Along strike	0.5	0.6440	0.344	0.003	19.608	109.057	spherical
	1.0	0.1160	0.087	0.002	16.783	123.987	
	1.5	0.0720	0.039	0.006	18.924	96.016	
	2.0	0.0320	0.010	0.002	16.088	137.500	
	2.5	0.0200	0.009	0.001	15.987	140.006	
	3.0	0.0140	0.004	0.001	14.906	81.003	
	3.5	0.0110	0.006	0.003	16.888	67.260	
Across strike	0.5	0.6440	0.300	0.005	13.921	77.756	spherical
	1.0	0.1160	0.088	0.004	13.077	98.132	
	1.5	0.0720	0.047	0.003	13.29	76.311	
	2.0	0.0320	0.014	0.002	13.091	72.651	
	2.5	0.0200	0.009	0.003	13.08	85.679	
	3.0	0.0140	0.005	0.001	10.889	54.100	
	3.5	0.0110	0.005	0.002	13.002	54.303	

Table 4.11 Indicator Variogram Anisotropic Factors

Cut-off (g/t)	Along Strike or Major	Across Strike or Semi-Major	Down dip or Minor	$\frac{\text{Major}}{\text{Semi} - \text{Major}}$	$\frac{\text{Major}}{\text{Minor}}$
0.5	19.608	13.921	1.307	1.409	15.002
1.0	16.783	13.077	1.605	1.283	10.457
1.5	18.924	13.290	1.144	1.424	13.389
2.0	16.088	13.091	1.287	1.229	12.500
2.5	15.987	13.080	1.706	1.222	9.371
3.0	14.906	10.889	1.099	1.369	13.563
3.5	16.888	13.002	1.811	1.299	9.325

Cross -validation of variogram models

The "Variogram Validation" menu in Surpac was used to check whether semi-variogram model parameters of Ok and Indicator values were satisfactory or not. This involves point kriging using the parameters of the models. For each data point, a Kriged grade was estimated (predicted value) and compared with the actual grade value statistically. During the process, each sample value in the dataset was removed in turn and its value was re-estimated (Point kriged) from the remaining data using the spherical model to be tested. This was repeated for all the sample point locations. The summary statistics of spherical variogram model validation for both OK and Indicator values are shown in Tables 4. 12, 4.13 and 4.14 respectively

Table 4.12 Summary Statistics of OK Spherical Variogram Model Validation

Mean	0.00042
Variance	3.6026
Standard deviation	1.8981
Average square error	3.6625
Weighted square error	3.4121
No. of Assays	1141
Average Kriging variance	3.7398
Ratio of Average square error to Average Kriging variance	0.9693
Percentage of errors within two standard deviation	95.72 %,

Table 4.13 Summary Statistics of Indicator Spherical Variogram Model Validation

Mean	0.00039
Variance	2.8026
Standard deviation	1.7781
Average square error	3.4423
Weighted square error	3.2322
No. of Assays	1141
Average Kriging variance	3.6474
Ratio of Average square error to Average Kriging variance	0.9798
Percentage of errors within two standard deviation	96.82 %,

From Tables (4.12 and 4.13), the ratio of Average Square Error to Average Kriging variance are very close to one (1) which according to Davis (1986) and Annels (1991) are satisfactory for a good model. Additionally, the mean of the errors are all close to zero (0) as required for an unbiased model (Coombes *et al*., 1998). Relationship between the actual values and the estimated/predicted values shown in Figures 4.25, 4.26 and 4.27 have correlation coefficients approximately one (1) indicating good models according to Dowd (1992) and Sinclair & Blackwell (2002).

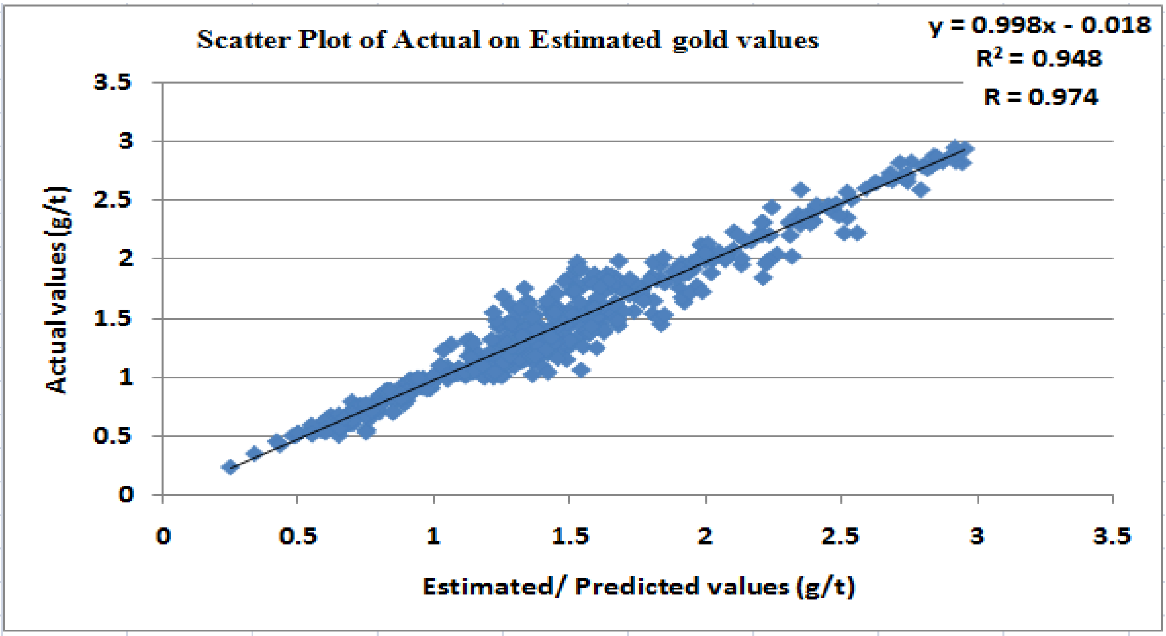

Figure 4.25 Scatter Plot of Actual on Predicted (Kriged) Values of OK Semi-Variogram Spherical Models

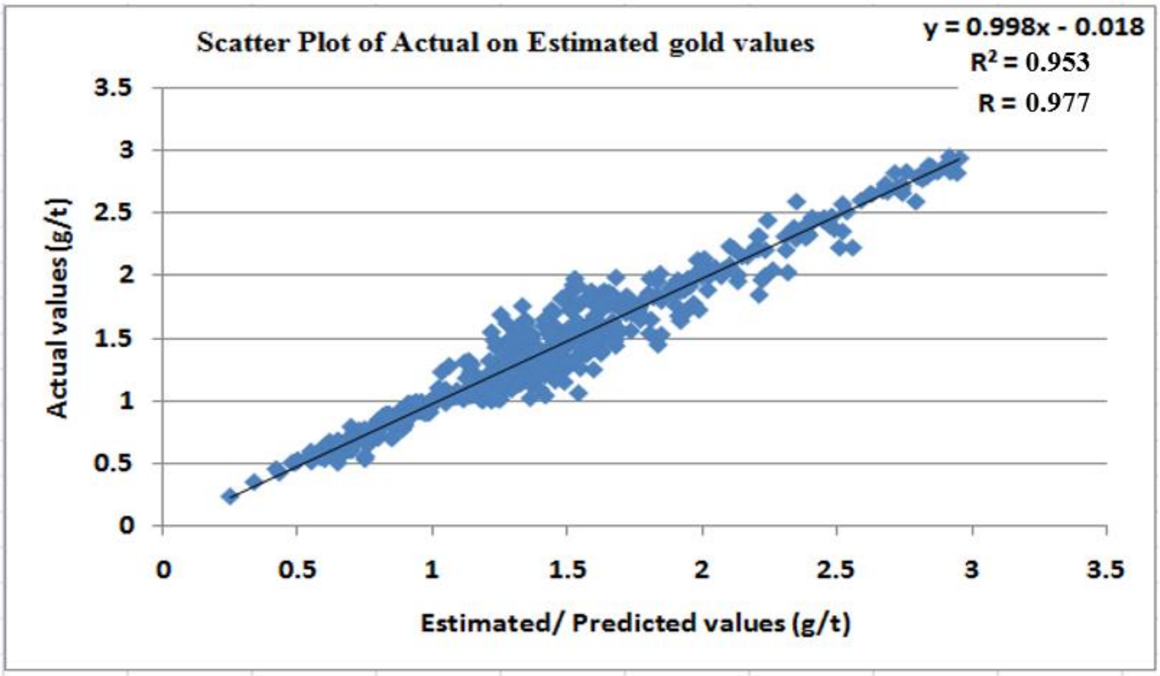

Figure 4.26 Scatter Plot of Actual on Predicted (Kriged) Values of IK Semi-Variogram Spherical Models.

4.5 Block Modelling

A block model was generated from the orebody wireframe model using the "Surpac Block Model Tool" Menu. The block modelling parameters are presented in Table 4.14. The parent cell size of 10 m x 10 m x 3 m corresponding to the average drill hole spacing along strike in the Y-direction and across strike in the X-direction of the orebody and the current mining bench of 3 m in the vertical dimensions (Z-direction) respectively was used.

Table 4.14 Summary of Afc1 Ore Block Model Parameters.

BLOCK MODEL NAME:	**Thesis_work_Afc1_Reconciliation_2018**		
Block Model Geometry			
Minimum Coordinate	Y = 15900 N	X = 3000 E	Z = -9 m
Maximum Coordinate	Y = 9500 N	X =6200 E	Z = 81 m
User Block size	Y = 10 N	X = 10 E	Z = 3 m
Minimum Block size	Y = 10 N	X = 10 E	Z = 3 m
	Dip = 0	Plunge = 0	Bearing = 0

Attributes	Description
Material type	Ore and waste material considered
Density	Specific Gravity of the material
Constraints Used	**Description**
Reef constrained	Ore zones within the solids defined by the wireframe
Topo constrained	DTM of the topography of the area
Cut-off grade	Ore cut-off grade within the ore zones solid wireframe

A total of 89 672 blocks were created in the orebody wireframe model. Each block cell was filled with attributes which contain information or properties used in assessing the Afc1 orebody. All the attributes were created using "Surpac Block Model Attribute Tool". A full description of the attributes used for this work is found in Appendix 2

Attributes were extracted from the area shown by the mined survey boundary for 2013 as shown in Figure. 4.27. And further analysis were conducted to determine tonnage and grade.

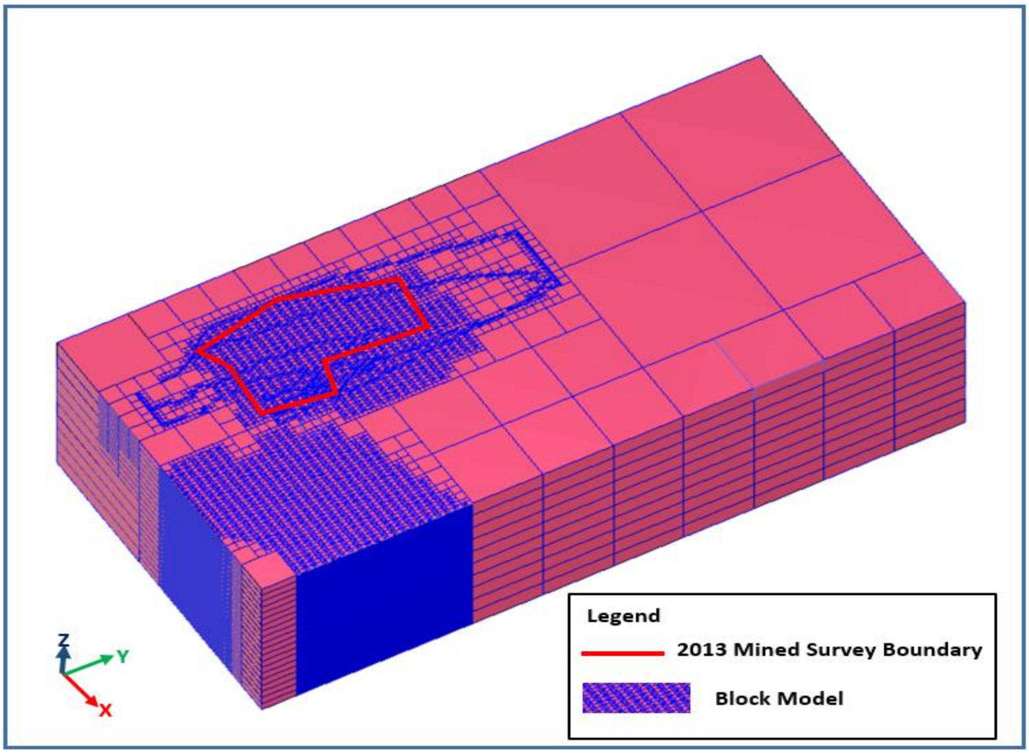

Figure 4.27 Area Mined from Kottraverchy Block Model in 2013

CHAPTER 5

RESOURCE ESTIMATION AND ANALYSIS

5.1 Resource Estimation

The resources were estimated using Ordinary Kriging (OK) and Multiple Indicator Kriging (MIK).

5.1.1 Grade estimation using the OK Method

Ordinary Kriging (OK) was used to estimate grades into the block model using "Surpac Block Model Estimation Menu Tool". A full description of the attributes used for this work is found in Appendix 3 whiles the parameters used for the OK are detailed in Table 5.1.

Table 5.1 Estimation Parameters used for OK

Parameters	**Description / Values**
Major Radius / Intermediate Radius	1.30
Major Radius / Minor Radius	42.15
Sill	0.984
Nugget	0.578
Structure Type	Spherical
Variogram Model Type	Nested Spherical
Maximum No. of Samples	20
Minimum No. of Samples	3
Dip	58 ^{o}
Strike	27 ^{o}

Validation of OK Models

OK block models were validated graphically to appreciate the accuracy of the grade interpolations. Cross-sectional and scatter plot techniques were adopted where drill hole composite grades were superimposed on the OK block models. Figures 5.1, 5.2, 5.3 and 5.4 are samples of cross-sectional views and scatter plots along 11500 N along strike and 4200 E across strike directions of the orebody respectively whiles the rest of the plots are found in Appendix 2.

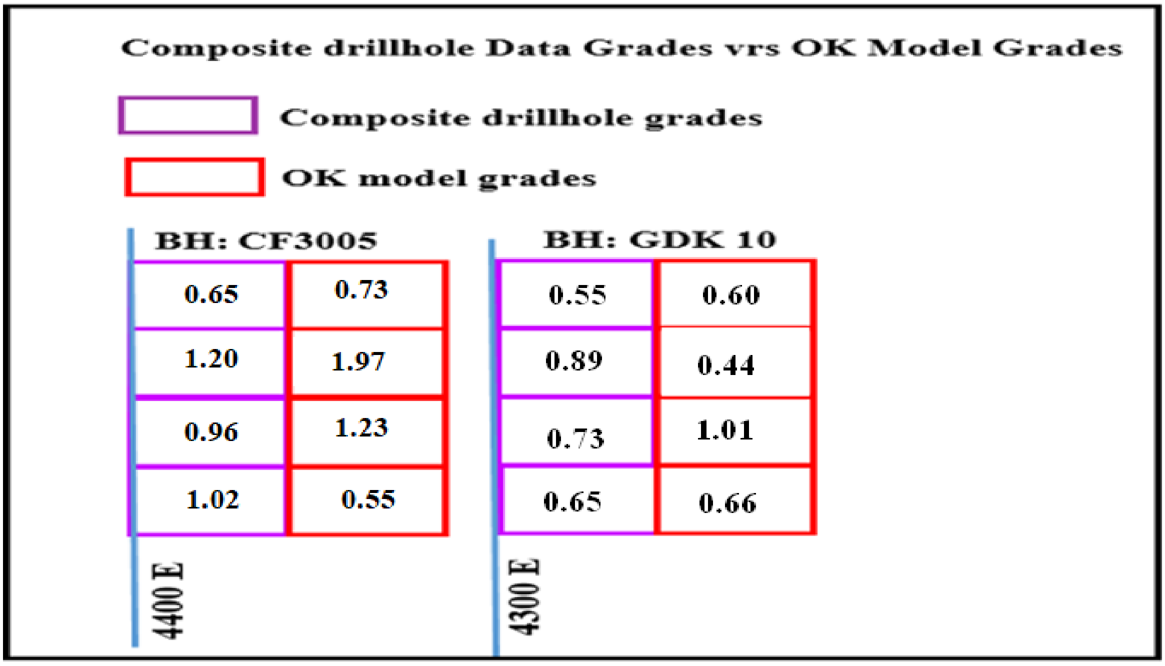

Figure 5.1 Cross –Sectional Views of Composite and OK Model Grades 11500 N Along Strike of the Orebody.

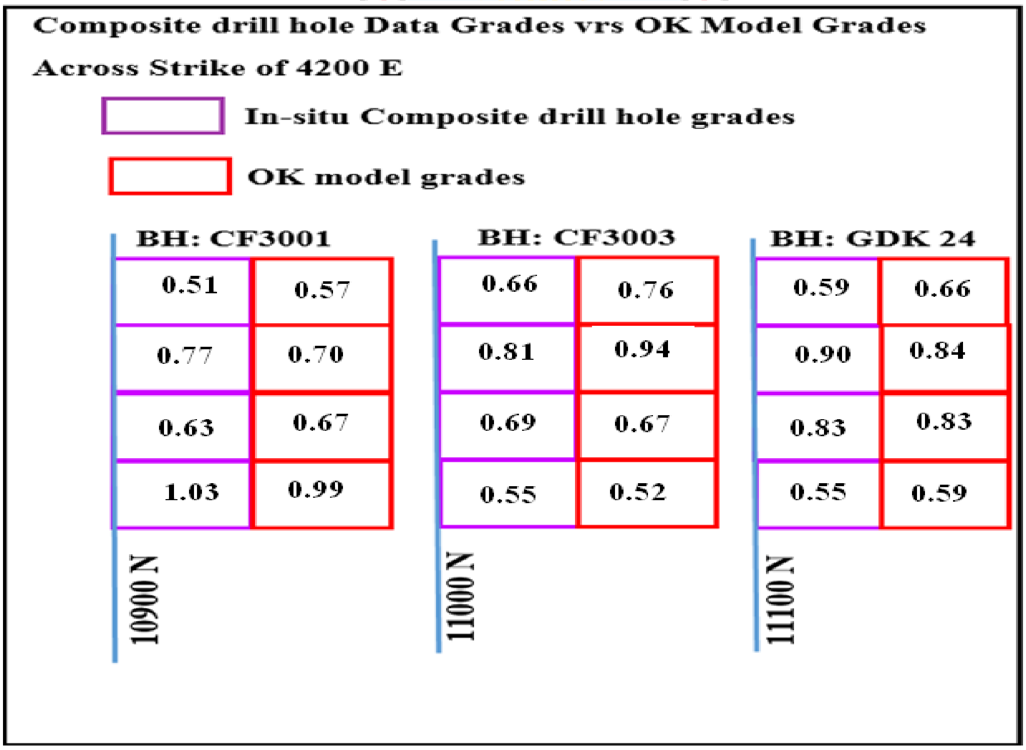

Figure 5.2 Cross –Sectional Views of Composite and OK Model Grades 4200 E Across Strike of the Orebody.

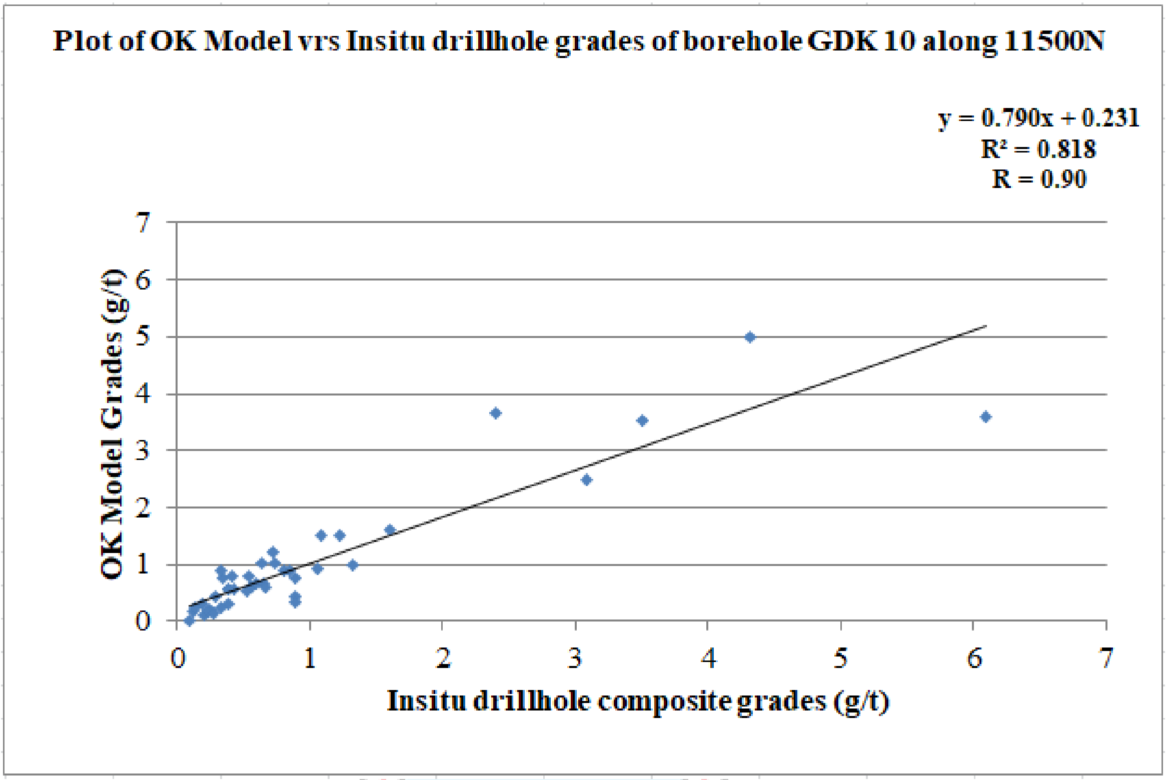

Figure 5.3 Scatter Plot of OK model and Composite Grades on 11500 N Along Strike of the Orebody.

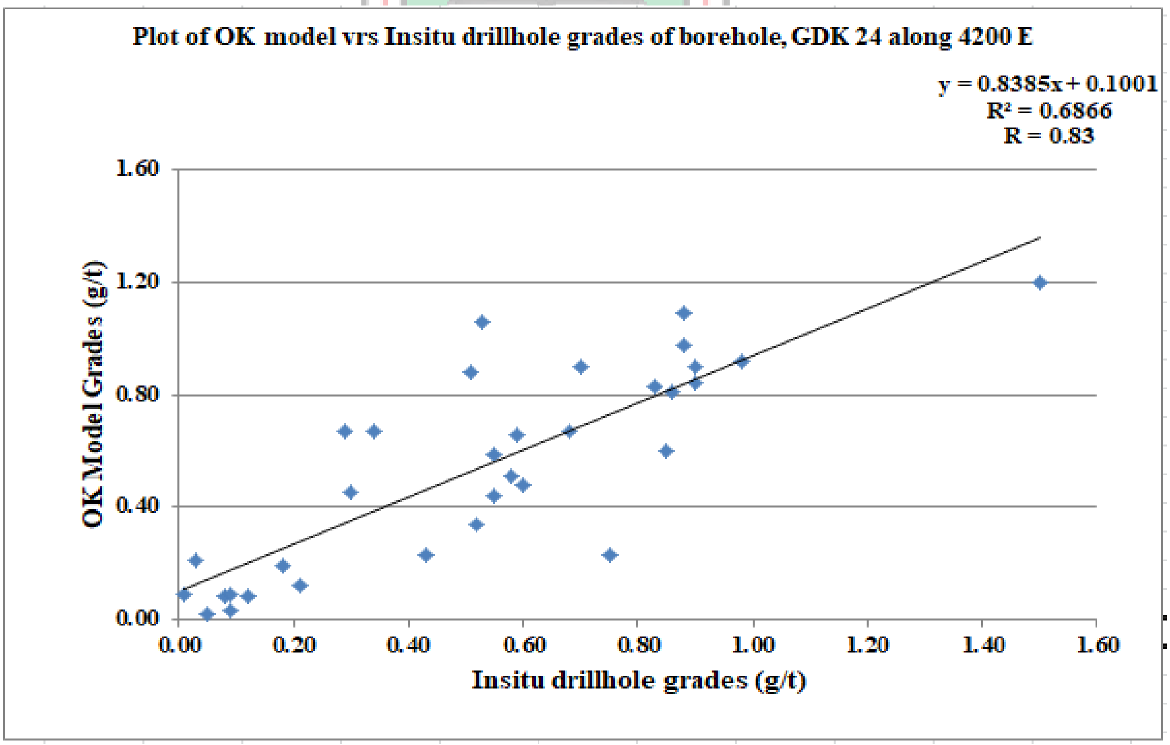

Figure 5.4 Scatter Plot of OK Model and Composite Grades on 4200 E Across Strike of the Orebody.

From the cross-sectional views (Figures 5.1 and 5.2), it could be deduced that the OK block models have a fair high positive grade correlation with the in-situ drillhole composite grades of boreholes CF3005, GDK10, CF3001, CF3003, and GDK 24 along and across strike respectively. The scatter plots (Figures 5.3, 5.4 and Appendix 3) further prove that OK showed fairly good positive relationship with the insitu grades with correlation coefficient of 0.87.

Resource estimates produced by OK at various block model cut-off grades are shown in Table 5.2

Table 5.2 OK Resource Estimates of AFc1 Reef

Cut-off grade	Tonnes, ore (t) above cut-off	Average Grade, (g/t) of ore above cut-off
0.5	102000.00	0.59
1.0	90000.00	0.60
1.5	85000.00	0.75
2.0	60000.00	0.79
2.5	28100.00	0.84
3.0	20440.00	0.89
3.5	12890.00	0.95

5.1.2 Resource Estimation by MIK

The grade estimation by Indicator Kriging was carried out using "Surpac Block Model - Estimation - Indicator Kriging Menu Tools". For each block, proportion of grades above the cut-off were estimated separately using the respective models.

For the purpose of this work, similar parameters used for OK were also used for MIK. A full description of the attributes used for this work is found in Appendix 3 whiles the parameters used for the MIK is detailed in Table 5.3

Table 5.3 Estimation Parameters used for MIK for various cut-offs

Parameters	Description and Values
Major Radius / Intermediate Radius	1.409, 1.283, 1.424, 1.229, 1.222, 1.369, 1.299
Major Radius / Minor Radius	15.002, 10.457, 13.389, 12.500, 9.371, 13.563, 9.325
Sills	0.988, 0.196, 0.106, 0.043, 0.026, 0.021, 0.018
Nugget	0.644, 0.116, 0.072, 0.032, 0.020, 0.014, 0.011
Structure Type	Spherical
Variogram Model Type	Nested Spherical
Maximum No. of Samples	20
Minimum No. of Samples	3
Dip	58 °, 58 °, 59 °, 46 °, 50 °, 49.5 °, 55 °
Strike	148 °, 148 °, 149 °, 136 °, 140 °, 139.5 °, 145 °
Cut-offs	0.5, 1.0, 1.5, 2.0, 2.5, 3.0, 3.5

Validation of MIK Models

Like the case of OK, MIK block models were also validated graphically to appreciate the accuracy of the grade interpolations. Cross-sectional and scatter plot techniques were also adopted where MIK block models were superimposed on the in-situ drill hole composite grades along and across strike of 11500N and 4200 E just like the OK validation.

Figures (5.5, 5.6 and 5.7) are samples of plots along strike of 11500 N and across strike of 4200 E directions of the orebody respectively having better grade correlations with the in-situ drillhole composite grades of boreholes CF3001, CF3003, CF3005 and GDK than that of OK. Again scatter plots of MIK showed a very good positive relationship with the insitu grades with correlation coefficient of 0.95

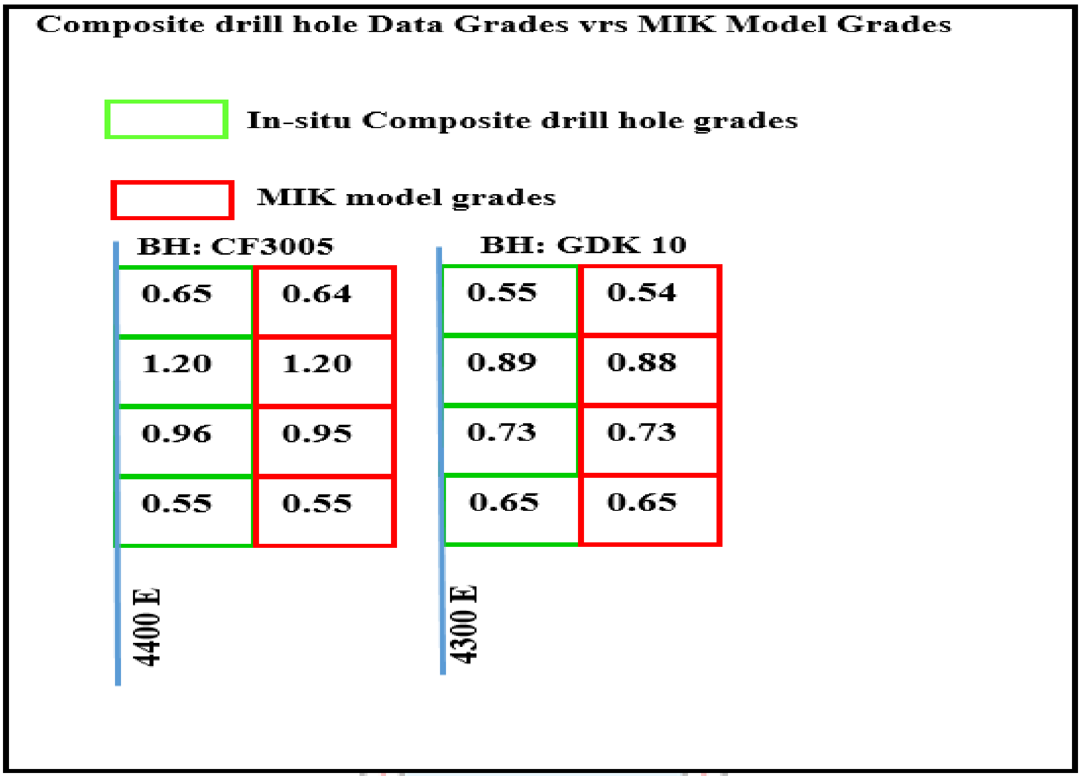

Figure 5.5 Cross –Sectional Views of In-situ Drillhole Composite and MIK Model Grades of 11500 N Along Strike Direction of the Orebody.

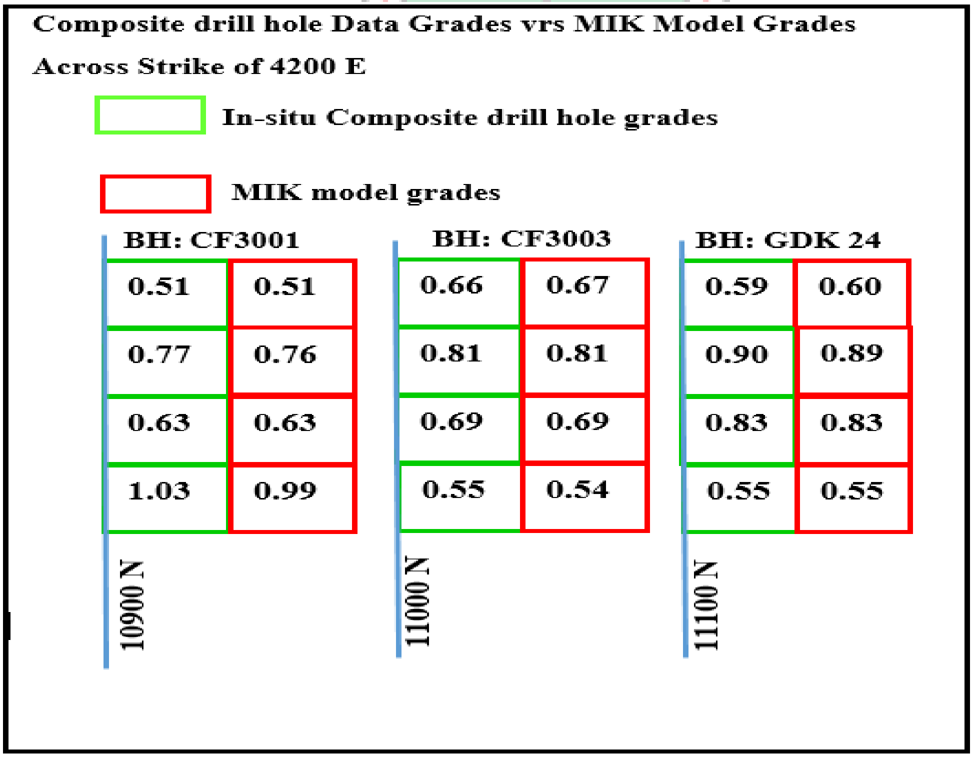

Figure 5.6 Cross –Sectional Views of In-situ Drillhole Composite and MIK Model Grades of 4200 E Across Strike Direction of the Orebody.

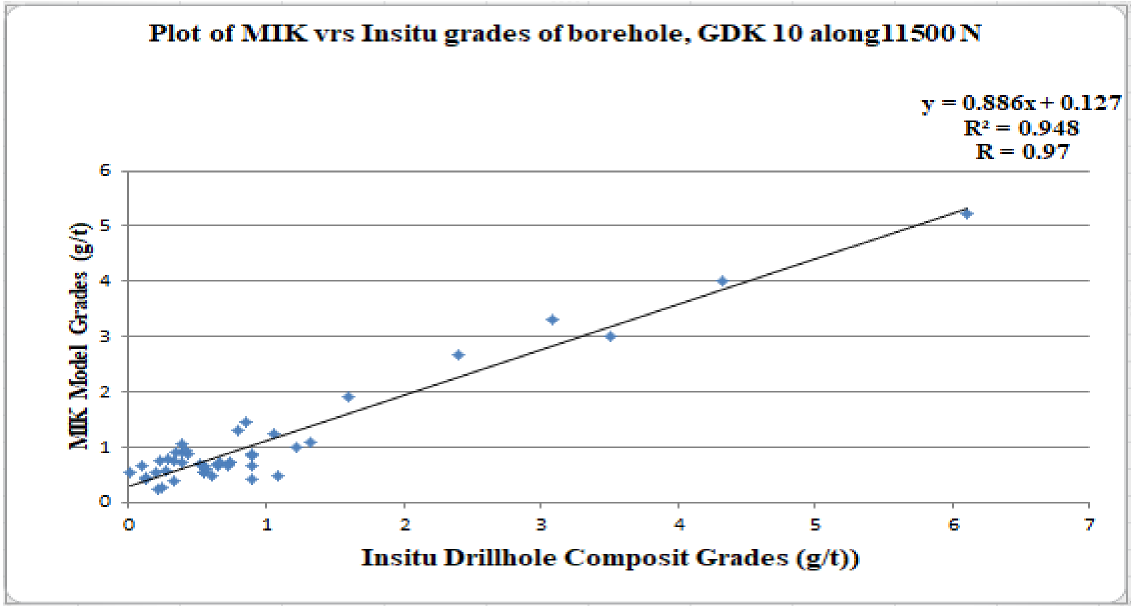

Figure 5.7 Scatter Plot of MIK model and Composite grades on 11500 N along strike of the Orebody.

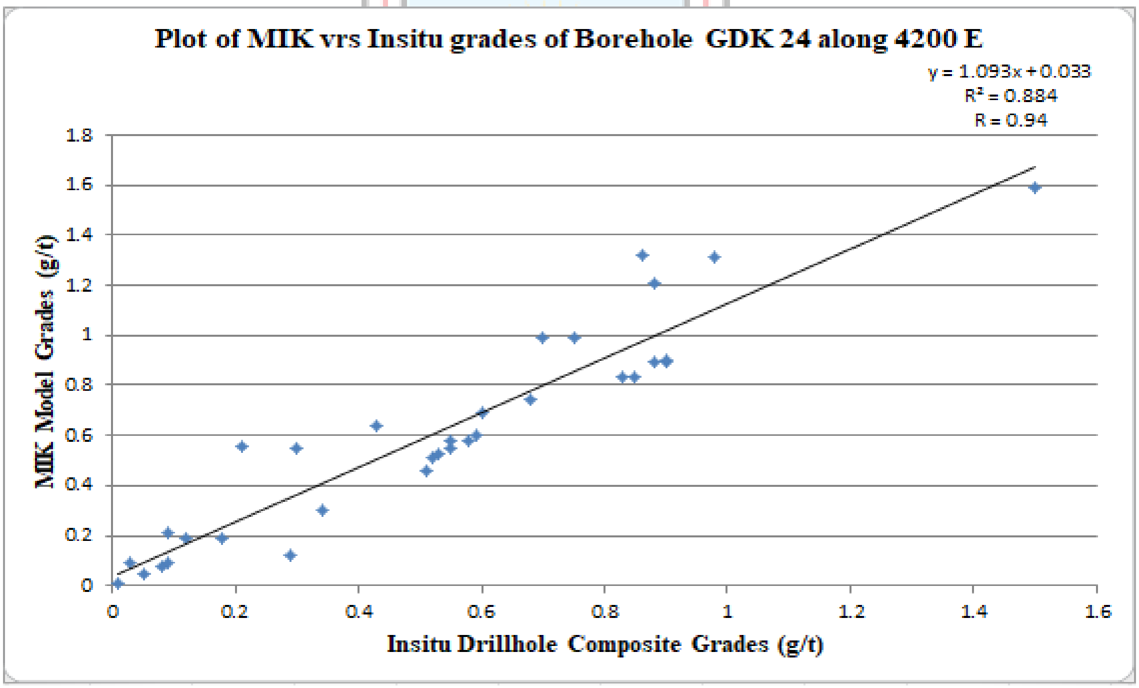

Figure 5.8 Scatter Plot of MIK model and Composite grades on 4200 E across strike of the Orebody.

Resource estimates produced by MIK at various cut-off grades are shown in Table 5.4

Table 5.4 MIK Resource Estimates of AFc1 Reef

Cut-off grade	Tonnes, ore (t) above cut-off	Average Grade, (g/t) of ore above cut-off
0.5	110050.00	0.52
1.0	97525.00	0.50
1.5	90000.00	0.60
2.0	76550.00	0.64
2.5	33006.00	0.75
3.0	24159.00	0.77
3.5	15421.00	0.88

5.2 Results and Discussions

5.2.1 Introduction

The results of OK and MIK estimates constrained within the Afc1 reef zone of 7 benches (between 75 m to 57 m) benches were considered and compared with the actual tonnages and grades mined from Kottraverchy AFc1 reef for a period of 12 months (between January - December, 2013). The values of tonnages and grades obtained from the two estimators and the actuals are shown in Table 5.5.

Table 5.5 Bench by Bench Average Grades and Tonnages of OK, MIK estimates and the Actuals mined from Pit.

Benches	Actuals mined from Pit		Models			
			OK		MIK	
	Tonnes, Ore (t)	Average Grade (g/t)	Tonnes, Ore (t)	Average Grade (g/t)	Tonnes, Ore (t)	Average Grade (g/t)
75mRL	47,599	0.74	40,501	0.91	45,890	0.68
72mRL	44,088	0.73	39,270	0.87	46,420	0.75
69mRL	11,640	0.74	10,234	0.74	11,100	0.73
66mRL	8,660	0.59	3,442	0.80	9,020	0.64
63mRL	20,110	0.83	11,235	0.93	22,000	0.75
60mRL	28,000	0.75	19,341	0.93	26,895	0.76
57mRL	19,550	0.76	13,398	0.97	17,670	0.90

The OK and MIK estimate results are discussed under the following:

1. Comparison of estimates from the two methods and the drillhole composite grades in sections.

2. Statistical comparison of the two estimates and the actuals using curves and grade - tonnage curves.

3. Comparison of OK and MIK estimates and actuals using grade-tonnage curves.

1. Comparison of OK and MIK block estimates and drillhole composite (in-situ grades)

Visual inspections of cross-section through OK and MIK block models along strike and across strike directions as shown in Figures 5.1. 5.2, 5.3 and 5.4 indicates that MIK block estimates are closer to the in-situ drillhole composite grades than those of OK. It therefore appears to be more satisfactory.

2. Statistical comparison of OK and MIK Block Estimates

The distribution of OK and MIK estimates and the actual grades and tonnages in each benches are presented in Figures 5.9 and 5.10.

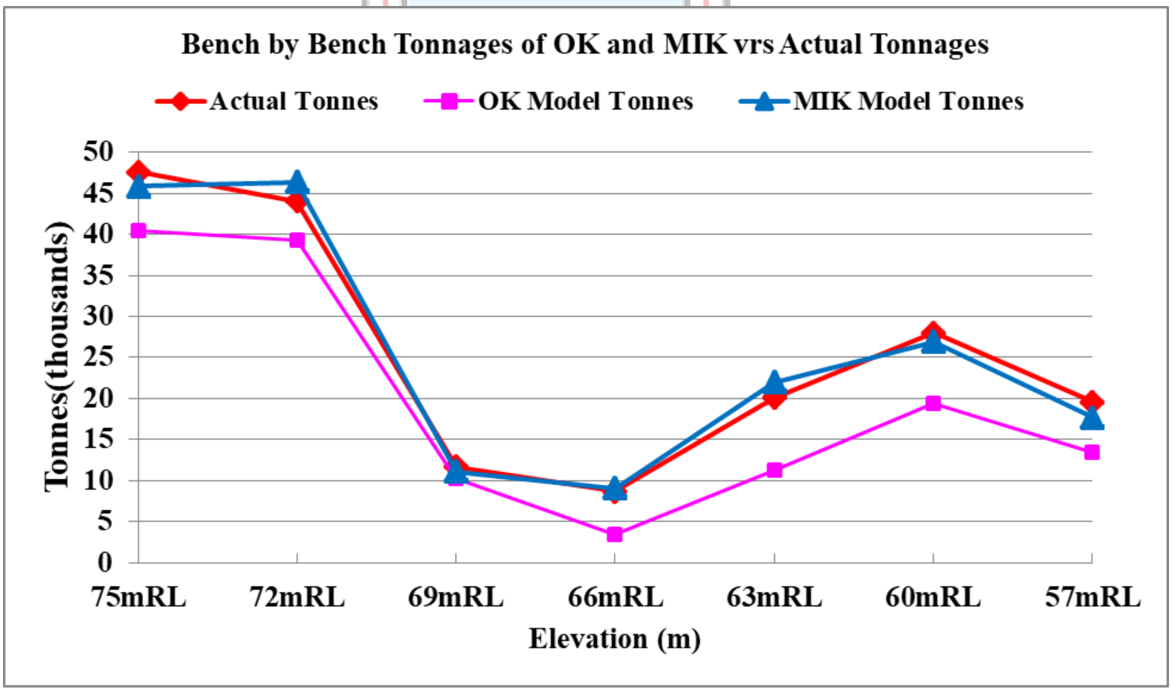

Figure 5.9 Bench by Bench Model Tonnages of OK and MIK Method Against Actual Tonnes of AFC1-Reef.

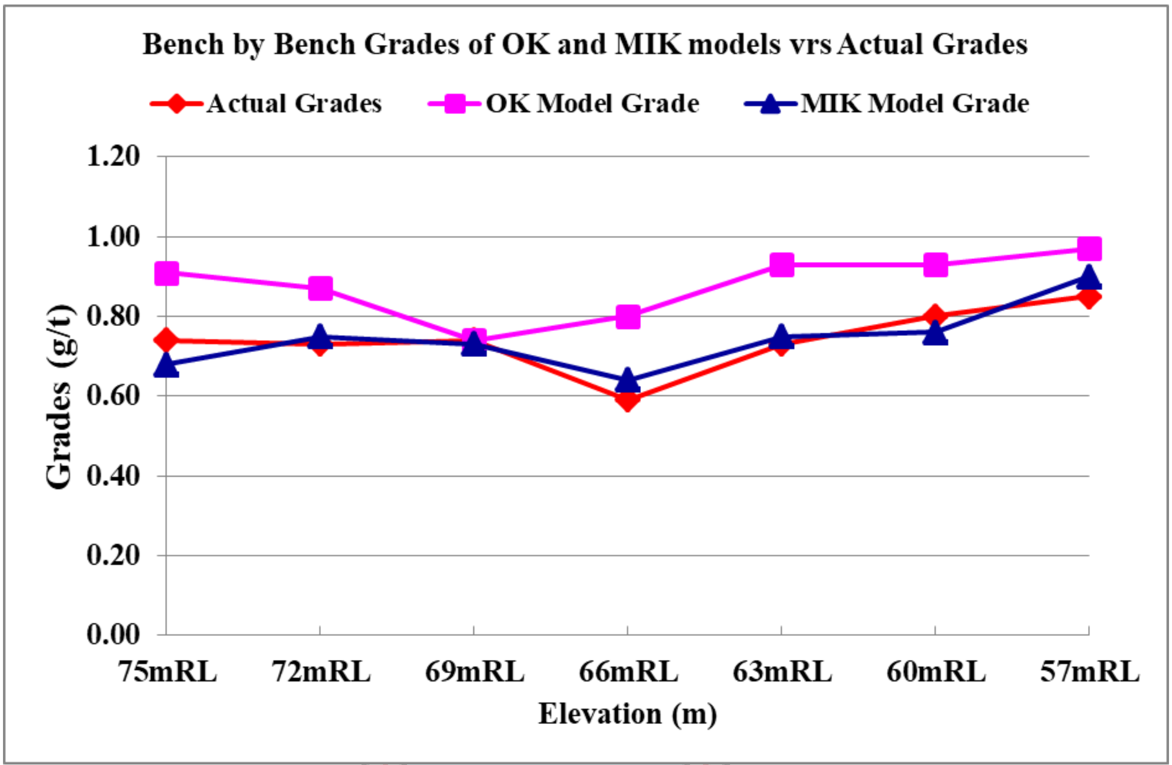

Figure 5.10 Bench by Bench Model Grades of OK and MIK Method against Actual Grades of AFC1-Reef.

It is again obvious that MIK estimates and the actual grades and tonnages are relatively better correlated than OK. Estimates on 75 m bench, 72 m bench, 63 m bench to 57 m bench indicate that OK consistently underestimate tonnes and over estimate grades as compared to the actuals (Table 5.5 and Figures 5.9 - 5.10).

Additionally, Regression and correlation analysis was performed to statistically assist in selecting the better estimation method between OK and MIK. Some of the scatter plots of OK and MIK estimates against actuals were plotted and Figures 5.11 and 5.12 show their respective plots.

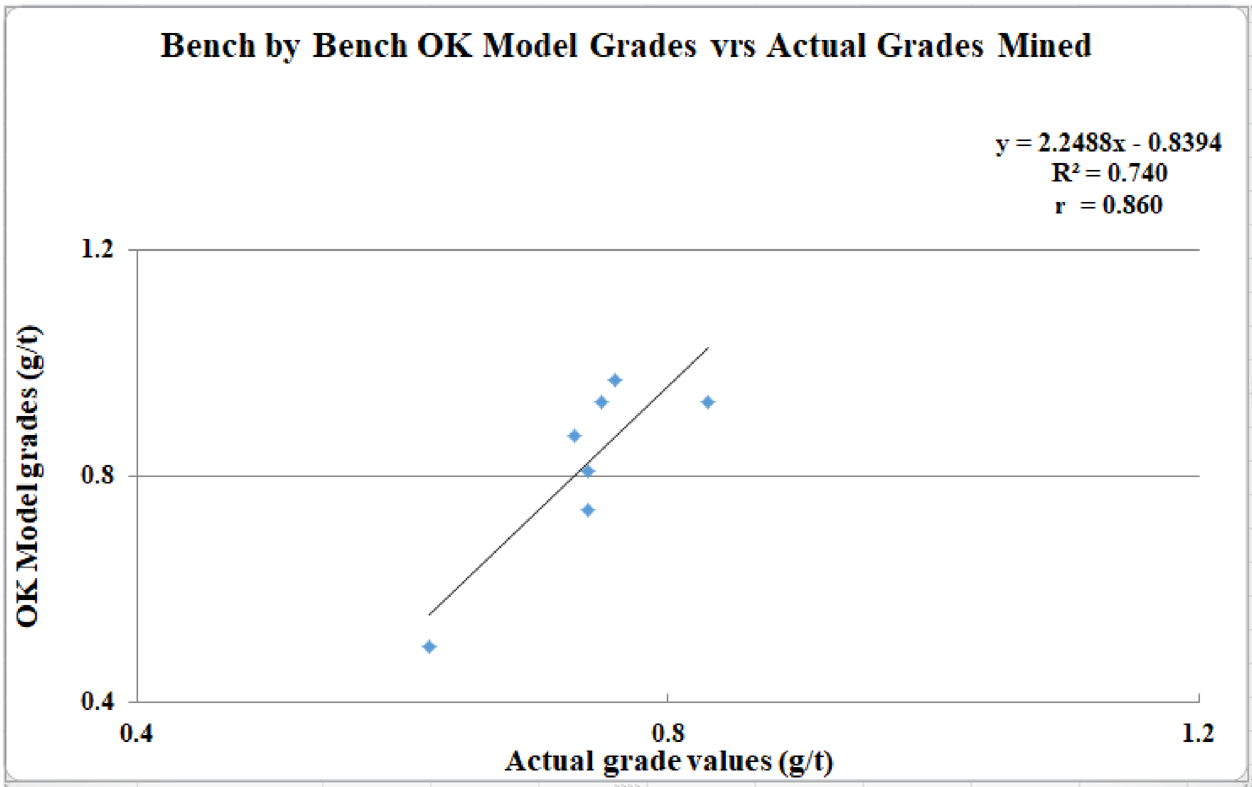

Figure 5.11 Scatter Plot of Bench by Bench O.K on Actual Grades of AFC1-Reef Zone

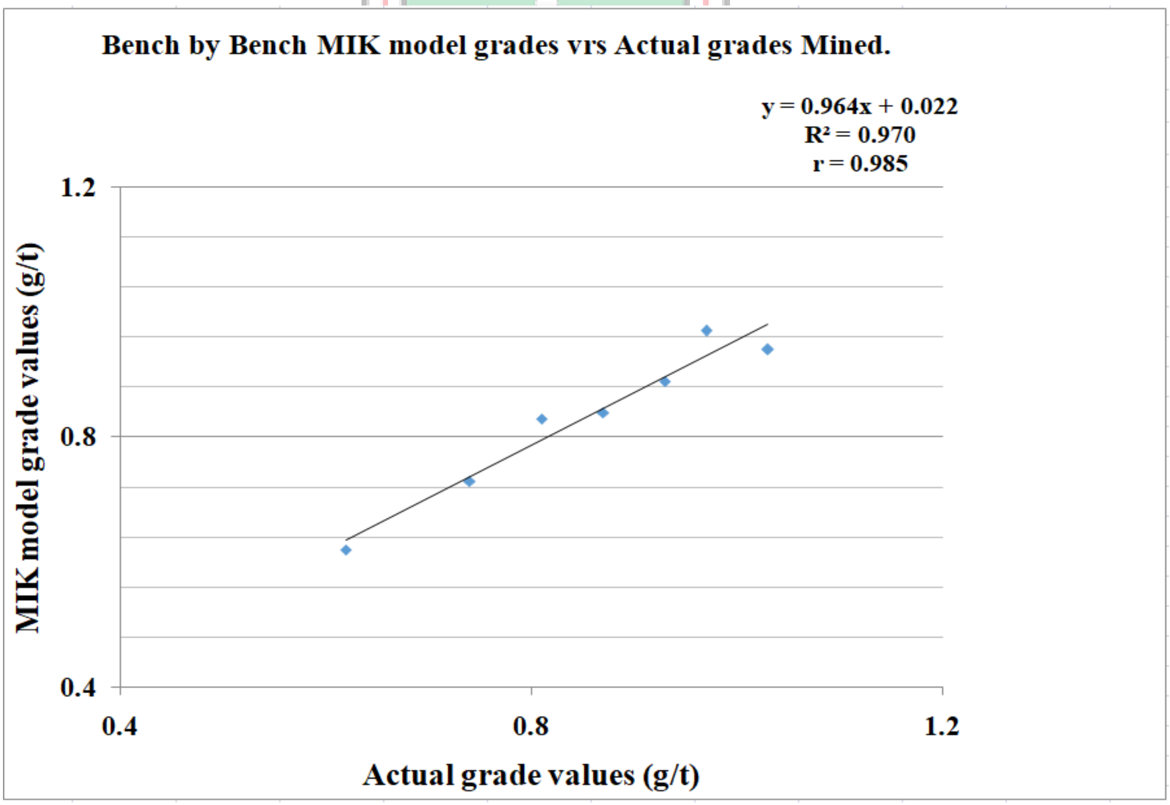

Figure 5.12 Scatter Plot of Bench by Bench MIK on Actual Grades of AFC1 -Reef Zone

Even though both OK and MIK show good positive relationship with the actuals with nearly 45 ^{o} curves, MIK shows better correlation coefficients than OK.

3. Comparison of OK and MIK Estimates and the actuals using grade -tonnage curves.

Grade tonnage relationship curves were plotted at different cut-off grades for both OK and MIK model estimates as shown in Figure 5.13.

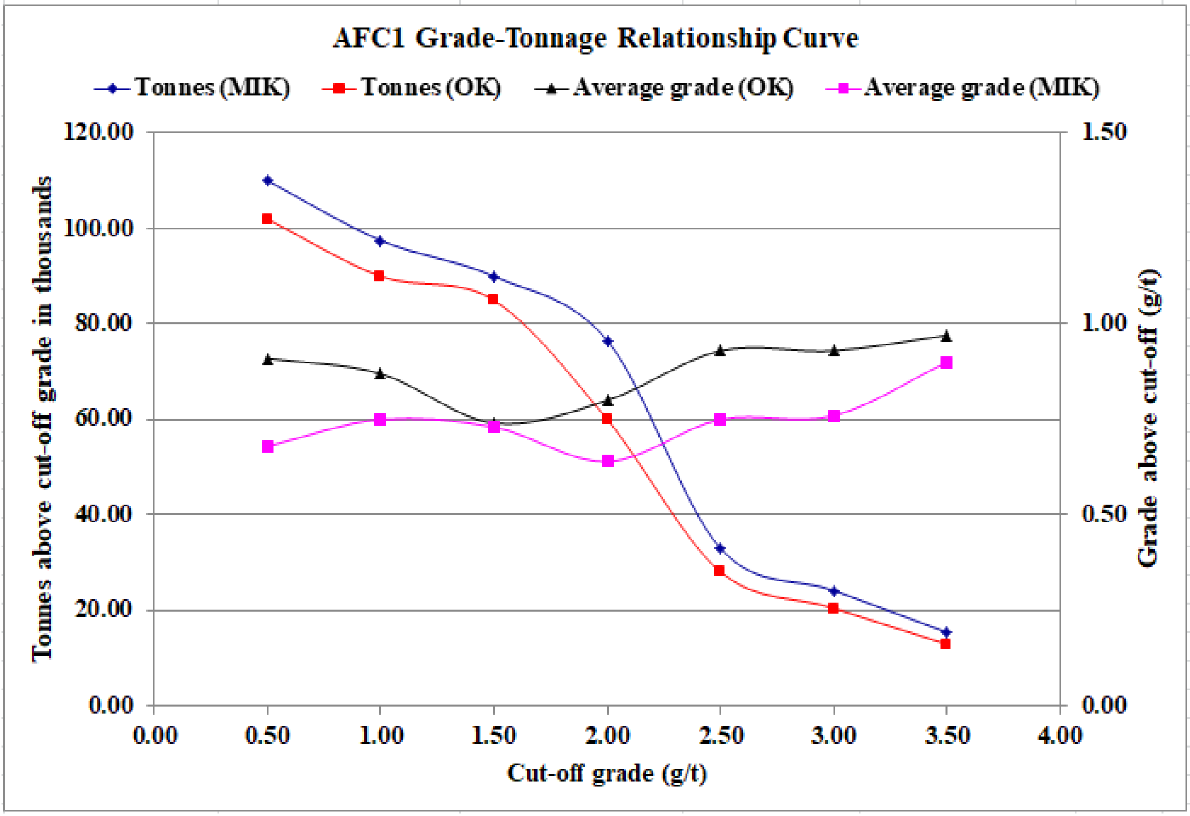

Figure 5.13 Grade-Tonnage Relationship of AFC1 Reef Zone

Generally, at any given cut-off (Figure 5.13), it can be deduced that OK consistently provides lower estimate of tonnage at higher average grade than those of MIK. This shows how MIK is able to provide recoverable tonnages in the cases when the distribution data is highly skewed whiles OK does not (Sinclair and Blackwell, 2002). This may have accounted for the reconciliation challenges of AFc1 reef at Kottraverchy pit.

5.2.2 Reconciliation.

Ordinary Kriging (OK) and Multiple Indicator (MIK) estimates were reconciled with the actual ore mined to assess the performance of the two methods. Figures 5.14 and 5.15

show the summary of OK and MIK estimates and the actual ore mined (AFC1Reef zone) from Kottraverchy pit between the periods of January, 2013 to December, 2013.

From Figure 5.14 and 5.15, it is again argued that MIK and actual mine production tonnage and average grade reconcile better than OK. Hence MIK is a preferred estimation method to OK for AFc1 reef at Kottraverchy pit.

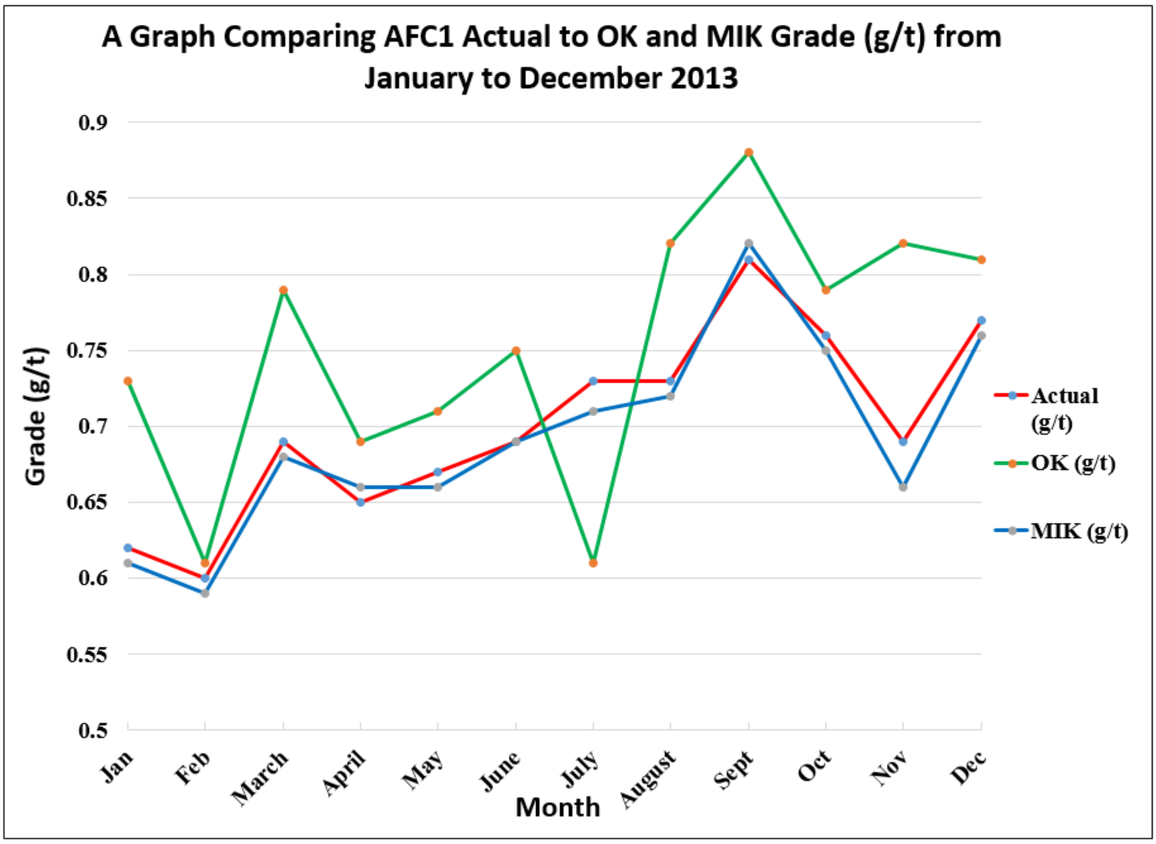

Figure 5.14 A Graph Comparing AFC1 Actual to OK and MIK Grade (g/t) from January to December 2013

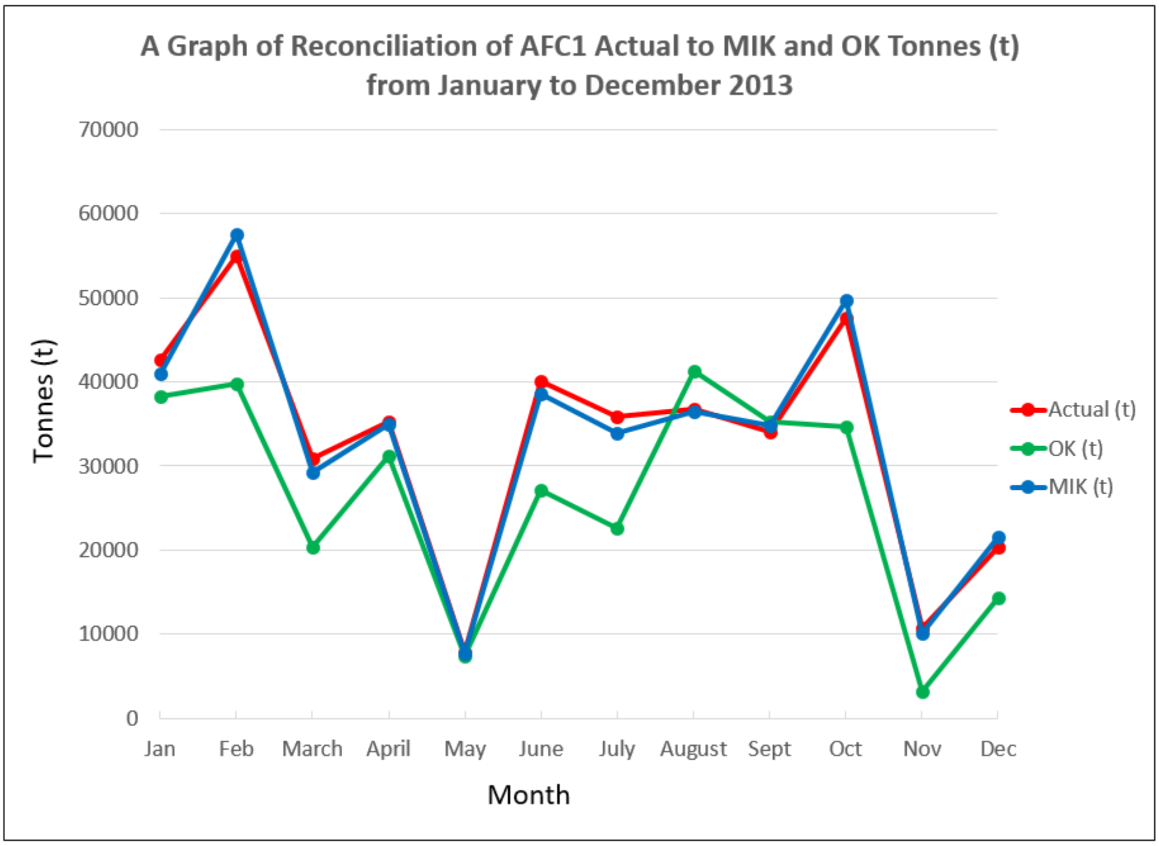

Figure 5.15 A Graph Comparing AFC1 Actual to OK and MIK Tonnes (t) from January to December 2013

CHAPTER 6

CONCLUSIONS AND RECOMMENDATIONS

6.1 Conclusions

From the studies the following conclusions can be drawn:

- Cross validation of OK and MIK indicate that MIK is a more appropriate estimation method for Afc1 reef at Kottraverchy as its grades are closer to the insitu grades.

- Comparative statistics of block estimates indicate that MIK compared better with the actuals for both grades and tonnages than OK; and OK consistently underestimates tonnage but overestimate grades.

- A comparison of the grade-tonnage curves, of OK and MIK estimates showed that OK consistently provides lower estimate of tonnage at higher average grade than MIK. This phenomenon could have accounted for the consistent reconciliation challenge.

- It is therefore suggested that MIK is a good estimator of the ore reefs than OK.

6.2 Recommendations

The following recommendations are made from the studies;

- MIK can be conveniently used in solving reconciliation challenges in the Afc1 reef and other similar reefs in the Tarkwaian deposit.

- A study could be re-conducted taking into consideration the structural data of the study area when the data is available in the future.

- The estimates would have been better if the wireframe could have incorporated geological structures if the data were available.

REFERENCES

Adjei, D. (2015), "Comparative Resource Estimation of Pepe Orebody Using Inverse Distance Weighting Method and Ordinary Kriging Method. A Case Study", *Unpublished MSC Thesis Work*, University of Mines and Technology, Tarkwa, pp. 18 - 42.

Al-Hassan, S. (2015), "Mineral Resource Estimation", *Unpublished MSC Modular Lecture Notes*, University of Mines and Technology, Tarkwa, 70pp.

Allibone, A., Jonathan, T., Greg, C., Mike, E., and Philip, U., (2002), "Timing and Structural Controls on Gold Mineralization at the Bogoso Gold Mine, Ghana, WA" *Economic Geology,* August 2002, vol. 97, pp. 949-969.

Annels, A.E. (1991), "Mineral Deposit Evaluation", *A practical Approach*, Chapman and Hall, London, England, 436p.

Anon. (2018a), "esri", *https://pro.arcgis.com/en/pro-app/help/analysis/geostatistical-analyst/how-inverse-distance-weighted-interpolation-works.htm*. Assessed: January 23, 2019

Anon. (2018b), "Investopedia", *http://investopedia.com/terms/a/assay.asp*. Accessed: December 16, 2018

Anon. (2017), "911Metarlurgist", *http://www.911metarlurgist.com/blog/fire-assay*. Accessed: October 22, 2018

Anon. (2013), "Tarkwa Goldmine Technical Short Form Report", www.goldfields.com.za. Accessed: December 3, 2018.

Anon. (2011), "Goldfields Ghana Limited, Goldfields Ownership, Annual Technical Report". *http://www.goldfields.com.za/ops_int_tarkwa.php.* Accessed: November 14, 2018

Anon. (2009), "Mineral Resources and Mineral Reserves Overview 2009", *http://www.goldfields.com/reports/rr_2009/tech_tarkwa.php*. Accessed: December 3, 2018

Anon. (2004), "*Advanced Surface and Solid Modelling*", Gems Training manual. 30 pp.

Anon. (2002), "*Advanced Block Modelling*", Gems Training Manual, Version 3.0, Perth, Australia, pp. 5-20

Armando, S. M. (2011), "A Discussion on Current Quality-Control Practices in Mineral Exploration", *AMEC International Ingenieria y Construcciones Limitada*, Chile, pp. 597-610

Barnes, R. J. (1991), "Teachers' Aid: The Variogram Sill and the Sample Variance", *Mathematical Geology*, 23, No.4, pp. 673 – 678.

Boamah, O. E. (2015), “Comparison of Ordinary Kriging and Multiple Indicator Kriging Estimation of Asuadai Deposit at Adansi Gold Ghana Limited”, *Unpublished MSC Thesis Work*, University of Mines and Technology, Tarkwa, pp. 21 - 58

Bronshtein, I.N. (2004), "*Handbook of Mathematics*", Fourth Edition, New York, Springer-Verlag, pp. 25-34.

Bruce, A. K. (1990), "Surface Mining”, *Society for Mining, Metallurgy and Exploration,* Second Edition, Vol. 2, United States of America, p. 8

Bruce, L. B. and O'Connell, B. (2003), “*Business Statistics in Practice”*, McGraw Hill Publications, London, 864p.

Caldwell, J. A. (2007), "Quality Assurance Quality Control Technical Review Report", *Geological Survey Bulletin, Australia*, Vol. 45, pp. 65-76.

Cameron, K, and Hunter, P. (2002), *“Using Spatial Models and Kriging Techniques to Optimize Long-Term Ground-Water Monitoring Networks”, A Case Study*, Environmetrics, 13, pp. 629–656

Clark, I. (2001), “*Practical Geostatistics*”, Geostocos Limited, Alloa Business Centre, Whins Road, Aloa, Central Scotland FK10 3SA pp. 275

Clarke, I. (1980), “*The Semi-Variogram in Geostatistics*”, Mousset-Jones, P. edition, McGraw Hill, New York pp. 17-40

Coombes, J., Thomas G.J., Gifford M., and Jepson L. (1998), "Assessing the Risk of Incorrect Prediction - A Nickel/ Cobalt, Case Study", *Proceedings AUSIMM Mine to Mill Conference*, The Australian Institute of Mining and Metallurgy, Melbourne, pp. 63- 68

David, M. (1988), "*Handbook of Applied Advanced Geostatistical Ore Reserve Estimation, in Developments in Geomathematics*", Series 6, Elsevier Service Publishers, New York, 216 pp.

Davis, C.D. (1986), "*Statistics and Data Analysis in Geology*, John Wiley & Sons, New York, 646 pp.

Davis B.M. (1987), “Uses and Abuses of Cross Validation in Geostatistics,” *Mathematical geology*, vol., 19 No. 3 pp. 230-248.

Dohm, G. C. (1980), "Circular Analysis-Open Pit Optimisation", *Mineral Exploration,* California, pp. 300 - 306.

Dominy, S.C., Annels, A. E. and Noppe, M. (2002), “Errors and Uncertainty in Ore Reserve Estimates - Operator Beware", *In proceedings Underground Operators Conference*, pp. 120 – 122.

Dowd, P.A. (1992), "Geostatistical Ore Reserve Estimation - A case study on a Disseminated Nickel Deposit. Case Histories in Mineral Deposits Evaluation", *Geological Society Special Publication,* London, (Annels, A.E. ed.), pp. 243 – 256.

Dzigbodi-Adjimah, K., and Gawu, S. K. Y. (1994), "Guides to Alluvial Gold Exploration in Ghana", *Ghana Mining Journal,* Vol. 14, No. 3, p. 3.

Eisenlohr, B.N. and Hirdes, W., (1992), "The Structural Development of The Early Proterozoic Birimian and Tarkwaian Rocks of South West Ghana, West Africa", *Journal of African Earth Sciences,* Vol. 14 No. 3, pp. 313 – 325.

Fitton, G. (1997), "*X-Ray Fluorescence Spectrometry; Modern Analytical Geochemistry: An Introduction to Quantitative Chemical Analysis for Earth, Environmental and Material Scientists",* Gill, R. (ed.), Addison Wesley, Longman Publication, UK, pp. 21.

Fosu, F., (2012), "Ore Resource Estimation of Pampe Gold Deposit Ghana", *Unpublished MSc Thesis*, University of Mines and Technology, Tarkwa, 90 pp.

Fytas, K. Chaouai, N. E. and Lavigne, M. (1990), "Gold Deposit Estimation using Indicator Kriging", *CIM Bulletin, Canadian Institute of Mining and Metallurgy*, Vol. 83, No. 934, pp. 77-83.

Glacken, I.M. (1996), "Resource Classification: Use and Abuse of the Kriging Variance", *Datamine Annual Conference*, p. 3-13.

Glacken, I. M. and Snowden, D. V. (2001), "Mineral Resource Estimation in Mineral Resource and Ore Reserve Estimation", *The AusIMM Guide to Good Practice*, *Ed*: A C Edwards, pp 189-198.

Goovaerts, P. (1997), "Geostatistics for Environmental Applications, Quantitative Geology and Geostatistics, *Proceedings of the Second European Conference on Geostatistics for Environmental Applications*, Valencia, Spain, Vol. 10, pp. 18 - 20

Hackman, B. A. (2012), "Resource Estimation Using Multiple Indicator Kriging at the Ricebeat Gold Project", *Unpublished MSc Thesis,* University of Mines and Technology, Tarkwa, pp. 1-105.

Harry, A. G. (2006), "A Comparative Study at Wassa Mines", *Unpublished Msc Thesis Report*, University of Mines and Technology (UMaT), Tarkwa, p. 35.

Hayslett, H.T. (1990), "*Statistics Made Simple"*, Heinemann Professional Publishing Ltd., Oxford, 246p.

Hellman, A. and Schofield, H. (2011), "Recoverable Resource Estimation for Obotan Ghana", *Unpublished Technical report*, Adansi Gold Project pp. 1-35.

Hirdes, W. and Nunoo, B., (1994), "The Proterozoic Paleoplacers at Tarkwa Gold Mine, SW Ghana: Sedimentology, Mineralogy and Precise Age Dating of the Main Reef and West Reef, and Bearing of the Investigations on Source Area Aspects" *BGR Geol. Jb D100*, Hannover, pp. 247 – 311.

Hirdes, W., Davis, D.W. and Eisenlohr, B.N. (1992), "Reassessment of Proterozoic Granitoid Ages in Ghana on the Basis of U/Pb Zircon and Monazite Dating", *Precambrian Research*, pp 56, 89-96.

Hohn, M. E. (1988), "*Geostatistics and Petroleum Geology",* Published by Van Nostrand Reinhold, New York, 264 pp.

Isaaks, E. H. and Srivastava, R.M. (1989), "*An Introduction to Applied Geostatistics",* Oxford University Press, Oxford (Publishers), 561pp.

Journel A.G. and Huijbregts C. J. (1978), "*Mining Geostatistics"*, New York: Academic Press, 600p.

Journel, A. G. and Huijbregts, C. J. (1991), "*Mining Geostatistics",* Academic Press, London, pp. 306 – 307.

Junner, N.R., Hirst, T. and Service, H. (1942), "Tarkwa Goldfields", *Memoir,* No. 6, Gold Coast Geological Survey, 5p.

Karpeta, W. P. (2001), "The Structural Evolution of the Tarkwaian basin": *A Review of the Geology, Mining and Exploration of the Tarkwa mine Area*, Bastillion Limited, 40p.

Karpeta, W. P (2000), "A Review of the Geology, Mining and Exploration of the Tarkwa Mine Area", *Tarkwa Goldmine - Case Study*, Bastillion Limited, pp. 15, 40.

Kennedy, B. A. (1990), "Surface Mining" Second Edition, *Society for Mining, Metallurgy and Exploration* Port City Price, Inc. Baltimore Maryland, USA, 1194p.

Kesse, G.O. (1985), "*The Mineral and Rock Resources of Ghana",* A. A. Balkema Publishers, Rotterdam, pp. 89 – 200.

Krige, D. G. (1999), "Essential Basic Concepts in Mining Geostatistics and Their Links with Geology and Classical Statistics", *South African Journal of Geology*. 1991 102(2), pp. 147 – 151.

Kwofie, J. G. (1993), "An integrated Approach to Orebody Modeling for Mine Planning and Design", *Unpublished, PGD Thesis*, UST School of Mines, Tarkwa, pp. 9 – 20.

Kock, S. G. and Link, R. F. (1970), "*Statistical Analysis of Geological Data*", John Wily & Sons Inc., New York, pp. 180- 205.

Lasme, T.D. (2014), “Comparative Mineral Resource Estimation of Pit 8 at Anglogold Ashanti Iduapriem Mine – A Case Study”, *Unpublished MSc Geological Engineering*, University of Mines and Technology, Tarkwa, 90pp.

Leube, A., Hirdes, W., Mauer, R. and Kesse, G.O. (1990)’ “The Early Proterozoic Birimian Supergroup of Ghana and Some Aspects of Its Associated Gold Mineralization”, *Precambrian Research*, 46, https://doi.org/10.1016/0301-9268(90)90070-7 p.139-165.

Marjoribanks, R. W. (1997), "*Geological Methods in Mineral Exploration and Mining*", 9th Edition, Springer Science and Business Media Publications, 27A Oxford Street, ISBN 978-94-011-5822-0, Perth WA 6152, Australia, pp. 115

Marshal, D. (1987), “*Statistics for Geoscientists”*, Pergamon Press, Oxford, pp. 119.

Noble, A. C. (1992), "SME Mining Engineering Handbook for Mining and Metallurgy", *Exploration*, Inc. Littleton, Colorado, pp. 344 – 358.

Oberthur, T., Vetter, U., Davis, D.W. and Gyapong, W. (1998), “Age Constraints on Gold Mineralisation and Paleoproterozoic Crustal Evolution in the Ashanti Belt of Southern Ghana”, *Precambrian Research*, Vol. 89, pp. 129-143.

Olea, R. A. (1999), “Geostatistics for Engineers and Earth Scientists*”, Step by Step Mathematical Development of Key Concepts, with clearly Documented Numerical Examples*, Kluwer Academic Publishers, pp. 269 -299.

Osei, S. (2015), “Comparative Resource Estimation of Ajopa Deposit at Anglogold Ashanti Iduapriem Limited Using Indicator Kriging and Inverse Distance Weighting Methods” – A Case Study, *Unpublished MSC Geological Engineering*, University of Mines and Technology, Tarkwa. 132pp.

Raymond, G. F. (1982), "Geostatistical Production of Grade Estimation in Mount Isa's Copper Orebodies", *Proc. Aust. Inst. Min. Mettall.*, No. 284, pp. 17 - 39.

Rendu, J.M. (1981), “*An Introduction to Geostatistical Methods of Mineral Evaluation”,* published by South African Institute of Mining and Metallurgy, Johannesburg, 102 pp.

Royle, A. G. (1993), "Cutting High Assays in the Vicinity of Stopping Blocks”, *International Journal of Earth Sciences*, *Unpublished Report*, London, 13 p.

Royle, A. G. (1992), "A Personal Overview of Geostatistics; In Case Histories and Methods in Mineral Resource Evaluation”, *Geological Society Special Publication*, London, (Annels, A. E., ed.), no. 63, pp. 233 - 241.

Sestini, G. (1973), "Sedimentology of a Paleoplacer; The Gold Bearing of Tarkwaian of Ghana: Ores in sediments”, *International Union of Geological Sciences*, Series A, No. 3, pp. 269 – 278.

Shaw, W.J. (1997), "Validation of Sampling and Assaying Quality for Bankable Feasibility Studies", *The Resource Database Towards 2000*, AusIMM Illawara branch, Wollongong, Australia pp.69-79.

Shepard, D. (1968), "A Two-Dimensional Interpolation Function for Irregularly-Spaced Data", *Proc. 23rd National Conference*, ACM, pp. 517-524.

Sides, E. J. (1997), "Geological Modelling of Mineral Deposits in Mining", *International Journal of Earth Sciences (Geologische Rundschau)*, Springer- verlag Berlin Heidelberg, pp. 342 – 353

Sinclair, A. J. and Blackwell, G. H, (2004) "*Applied Mineral Inventory Estimation*", Press Syndicate of the University of Cambridge. The Pitt Building, Trumpington Street, Cambridge, United Kingdom. ISBN 0-521-79103-0 hardback. pp. 181-233.

Sinclair, A. J. and Blackwell, G. H, (2002), "*Applied Mineral Inventory Estimation*", Published by Cambridge University Press, United Kingdom; 381pp.

Sinclair, A. J. (1998), "Geological Controls in Resource/Reserve Estimation", *Exploration Mining and Geology*, Vol. 7, pp. 29 - 44.

Smedley, P. L., (1996), "Arsenic in Rural Groundwater in Ghana", Journal *of African Earth Sciences*, 22, pp. 459–470.

Snowden, V. (1999), "Practical Interpretation of Mineral Resource and Ore Reserve Classification Guidelines", MSC, FAusIMM, CP Geo, MGAA, *Mineral Resource and Ore Reserve Estimation, The AusIMM Guide to Good Practice (Monograph 23)*, pp. 11- 12.

Stephenson, P. R. (2002), "What Does it mean for Today's Mining Geologist?", *Proceedings of the International Mining and Geology Conference, Australasian Institute of Mining and Metallurgy*, Melbourne, pp. 68.

Strogen, P. (1991), "The Sedimentology and Structure of the Tarkwaian, Western Region and its Relevance to Gold Exploration and Development", *In Proceedings of the International Conference of the Geology with Special Emphasis on Gold*, pp. 34 - 45.

Thomas, G. and Snowden, V. (1990), "A Practitioner's Implementation of Indicator Kriging", *Proceedings of a One Day Symposium: Beyond Ordinary Kriging*, Perth Western Australia Geostatistical Association of Australasia, October 30th, 1990, pp. 1-10.

Vann, J. And Guibal D. G, (2001), "Beyond Ordinary Kriging – An Overview of Non-Linear Estimation in Mineral Resource and Ore Reserve Estimation", – *The AusIMM Guide to Good Practice* (Ed, A C Edwards) pp. 12-15.

Webster, R, and Oliver, M. A. (1993), *"How Large a Sample Is Needed to Estimate the Regional Variogram Adequately", GeostatisticsTroia '92 , ed.* A. Soares, Kluwer Academic Publishers, Dordrecht, Vol. 1, pp. 155-166.

Whitelaw, O. A. L., (1929), "Geological and Mining Features of the Tarkwa-Aboso Goldfields". *Gold Coast Geological Survey,* Memoir No. 1, pp. 12-17.

Wright A. J., (1997), "The Tarkwa Project" *World Gold Conference, Australasian Institute of Metallurgy Publication Series* pp. 189-197.

Zhu, S., Hack, R., Turner, A.K., and Hale, M. (2003), "Assessing Uncertainty of Mineral Grade Estimation". *A tin/zinc deposit case study*, http://www.iamg.org/meetings/Proceedings-2003/Zhu.pdf, Accessed November 20, 2018

APPENDICES

APPENDIX 1

QAQC Plots of Assay Values

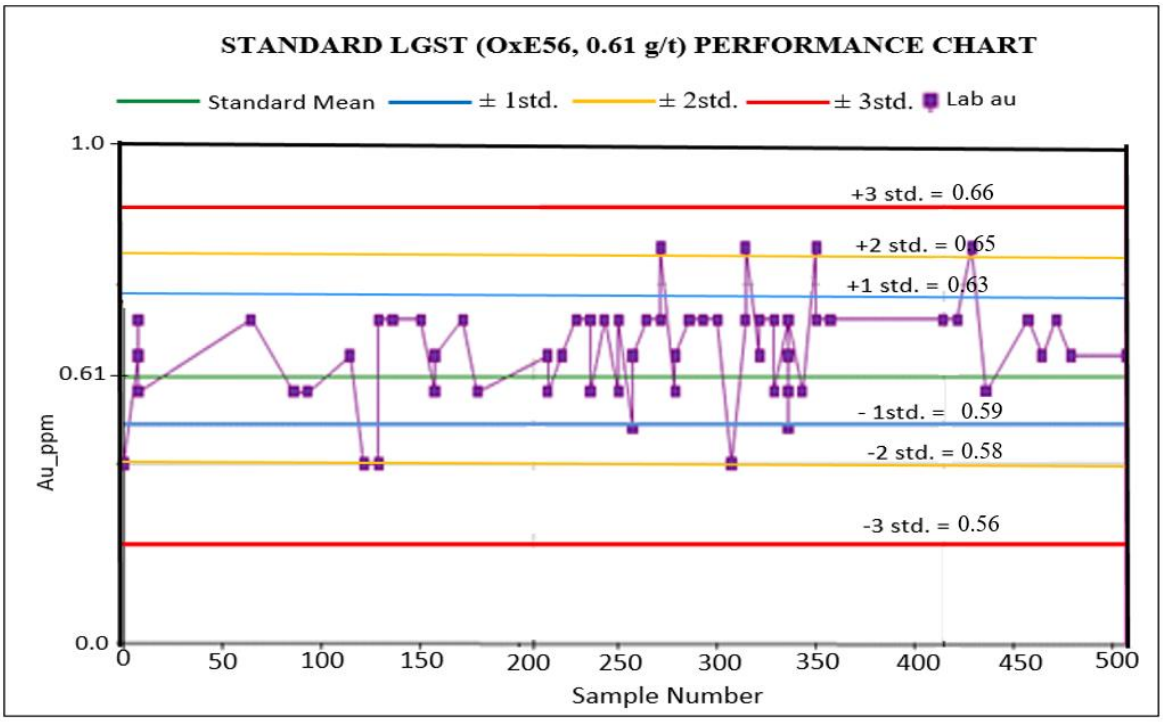

Plots of Assay Results of LGST OxE56 (0.61 g/t) against ±3 Standard Deviation.

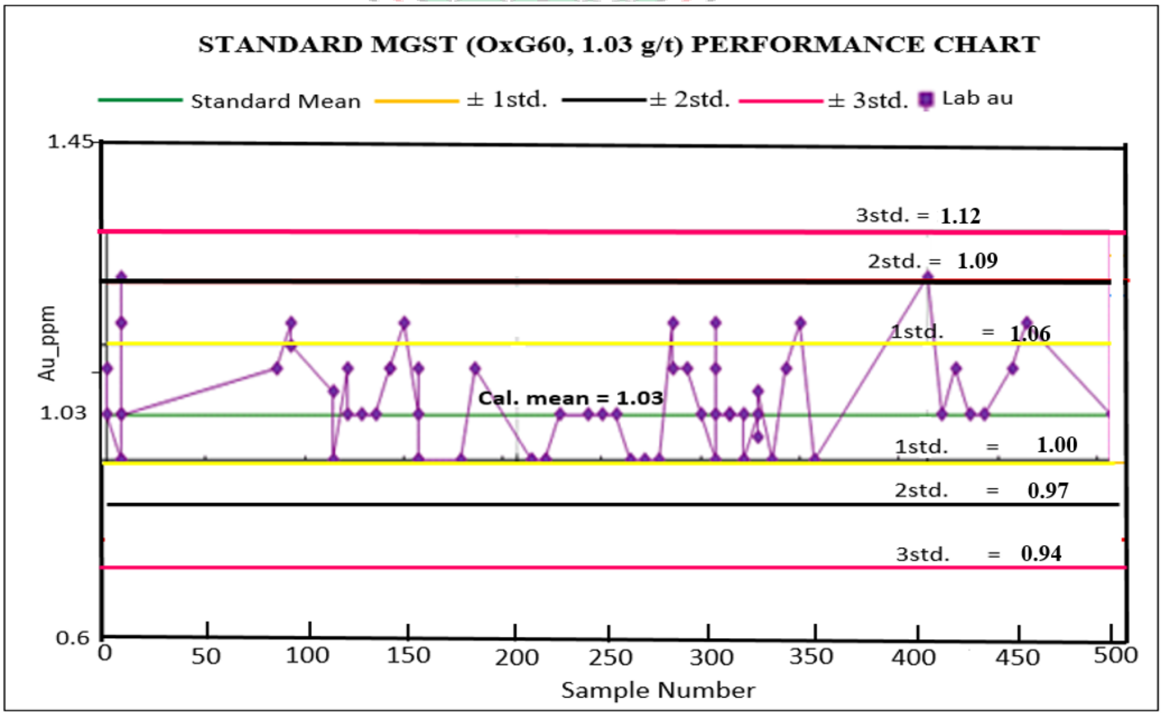

Plots of Assay Results of MGST OxG60 (1.03 g/t) against ±3 Standard Deviation.

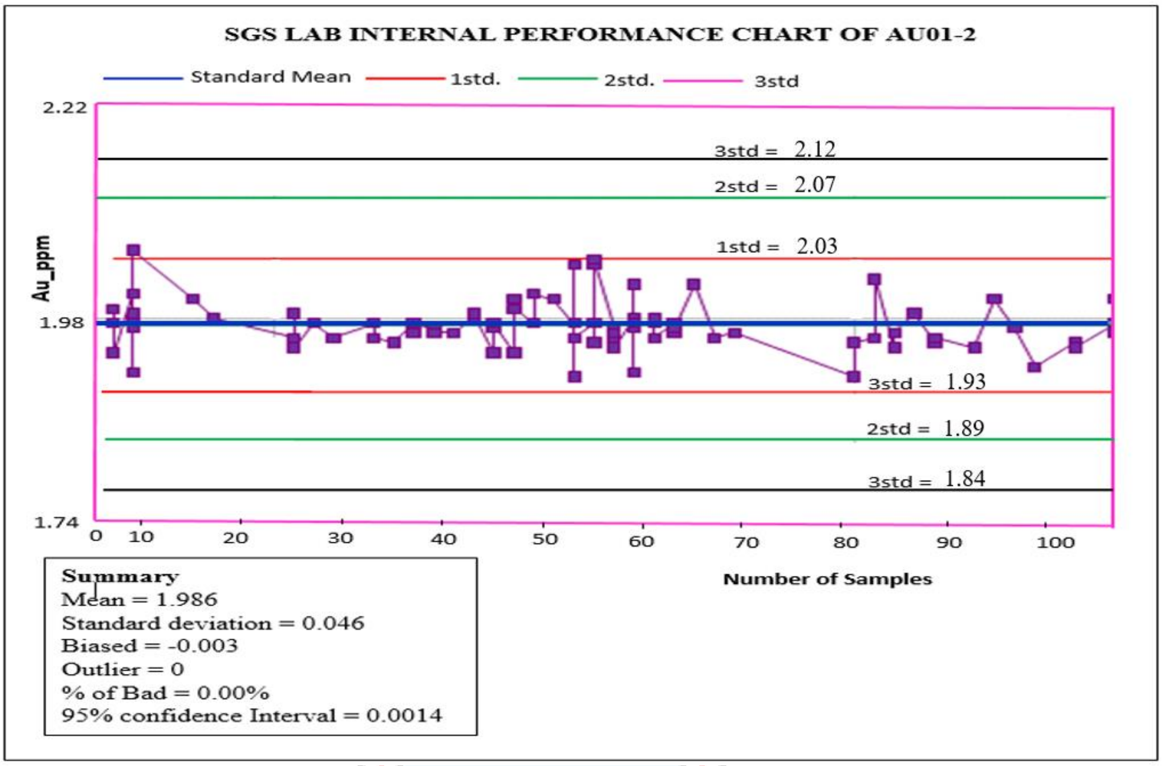

Plots of SGS Lab Internal Performance against Detection Limit

Combination of Diamond Drill and Reverse Circulation Data Samples

Summary of Input Data Statistics for the Orebody

Table 4.5 Summary of Input Data Statistics for the Orebody

Data	No. of Samples	Min. (g/ t)	Max. (g/ t)	Mean (g/ t)	Variance (g/ t)^2	Standard dev. (g/t)
RC	6289	0.01	60.12	1.25	1.53	1.24
DD	500	0.01	18.15	1.18	1.82	1.35

The null, Hypothesis and the claim was identified as

$$\mathrm{Ho}: \sigma^2_{\mathrm{RC}} = \sigma^2_{\mathrm{DD}} \text{ (claim)}$$

$$H_1 : \sigma^2_{RC} \neq \sigma^2_{DD}$$

Critical value: The hypothesis that the two variances are equal is rejected if the

$$F > F_{0.05}(n_{RC} - 1, n_{DD} - 1)$$

where $(n_{RC} - 1)$, $(n_{DD} - 1)$ are degree of freedom of the sample RC and DD respectively.

n_{RC} = 6, 289 σ^2_{RC} = 1.53 μ_{RC} = 1.25 s^2_{RC} = 1.53

n_{DD} = 500 σ^2_{DD} = 1.82 μ_{DD} = 1.18 s^2_{DD} = 1.82

where: n_{RC}, n_{DD} = number of samples of RC and DD respectively

σ^2_{RC}, σ^2_{DD} = population variances of RC and DD respectively

μ_{RC}, μ_{DD} = sample mean of RC and DD respectively

s^2_{RC}, s^2_{DD} = sample variances of RC and DD respectively

The calculated value, F = $\frac{\sigma^2_{RC}}{\sigma^2_{DD}} = \frac{1.53}{1.82}$ = 0.84

At 5% level of significance and for two tailed test, the tabulated value,

$F_{0.025}(6289-1,$ 500-1) $= F_{0.025}(6288,499)$ was obtained from statistical table as $F_{0.025}(\infty, \infty)$ = 1.00

APPENDIX 2

Variogram Models

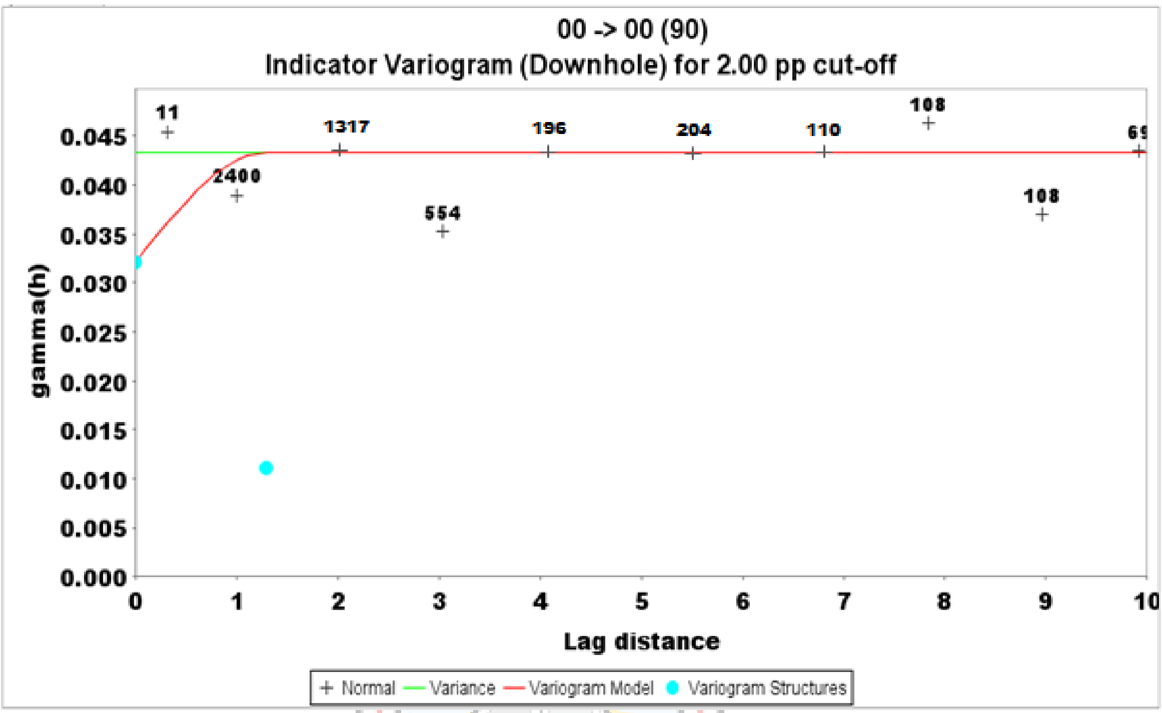

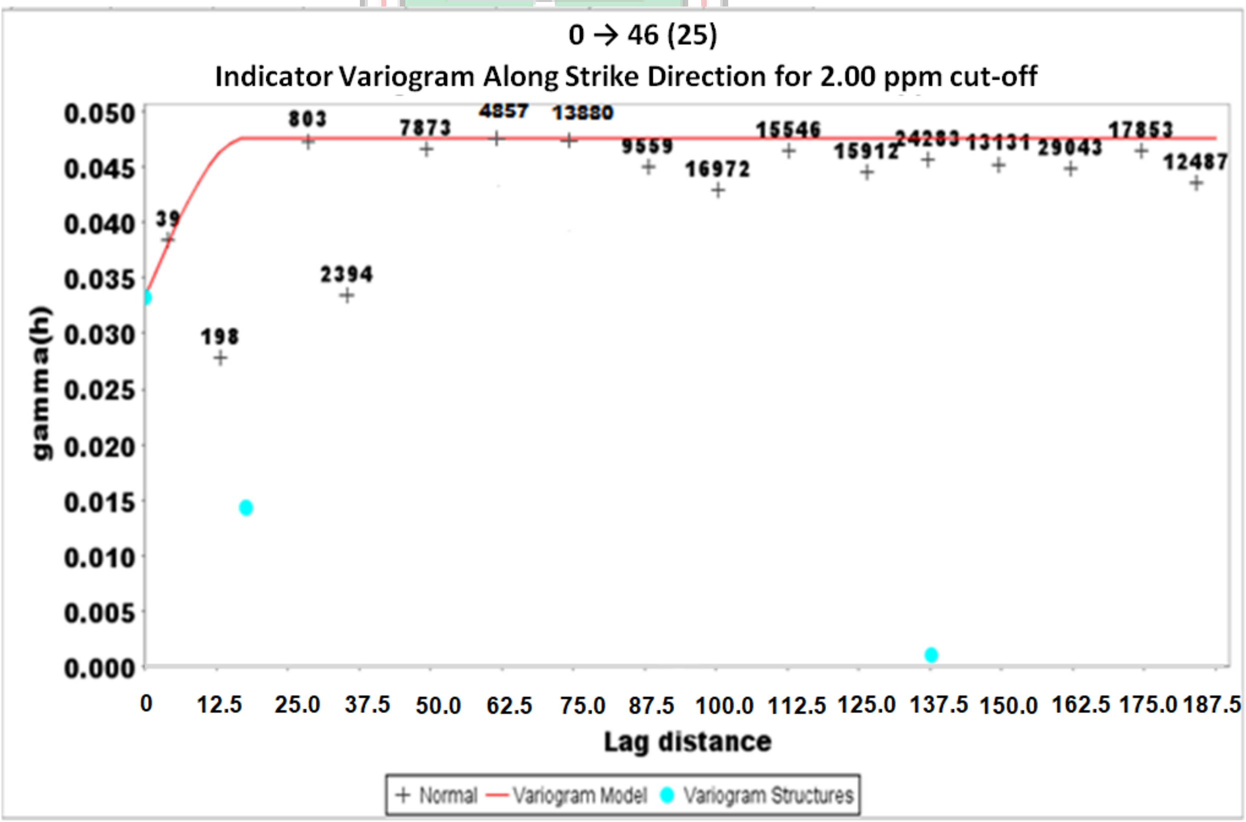

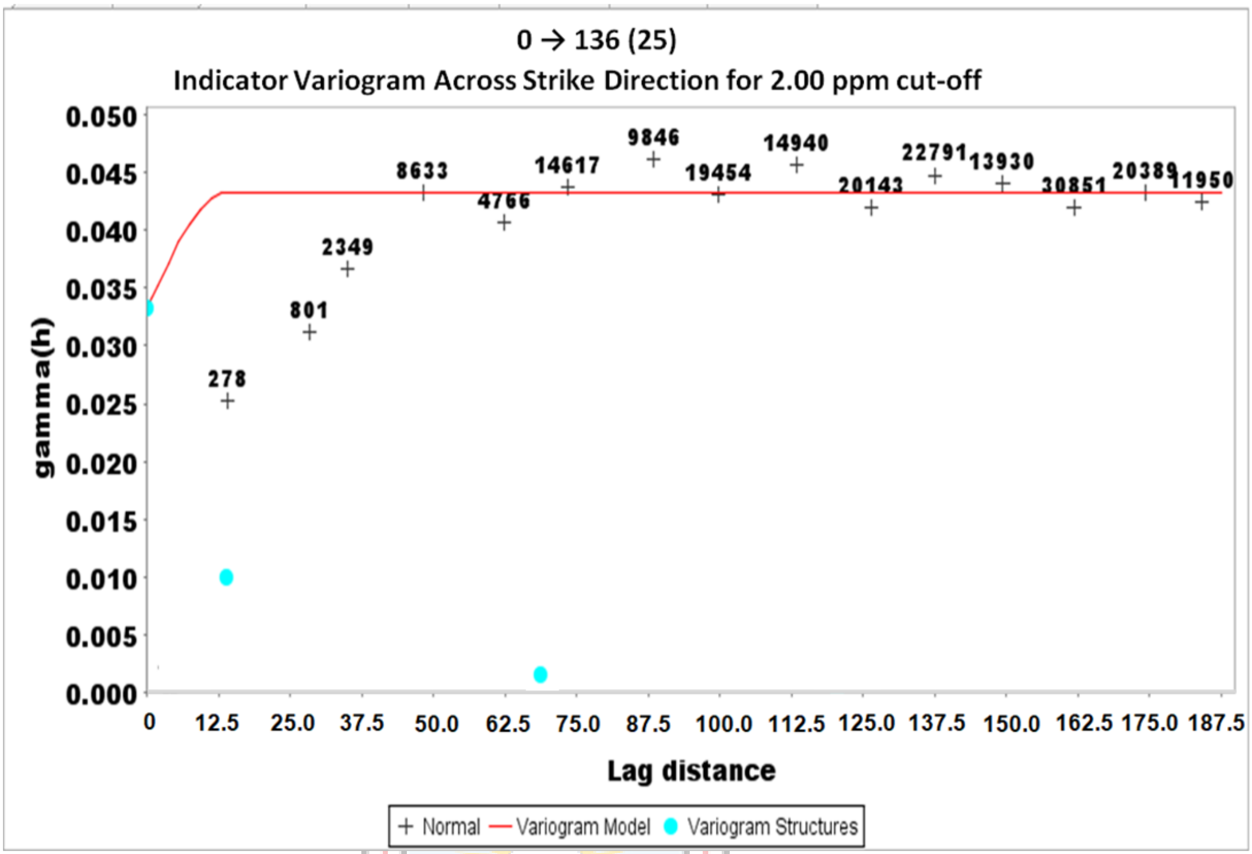
0 → 136 (25)
Indicator Variogram Across Strike Direction for 2.00 ppm cut-off
gamma(h)
0.050
0.045
0.040
0.035
0.030
0.025
0.020
0.015
0.010
0.005
0.000
0
12.5
25.0
37.5
50.0
62.5
75.0
87.5
100.0
112.5
125.0
137.5
150.0
162.5
175.0
187.5
Lag distance
278
801
2349
8633
4766
14617
9846
19454
14940
20143
22791
13930
30851
20389
11950
Normal
Variogram Model
Variogram Structures

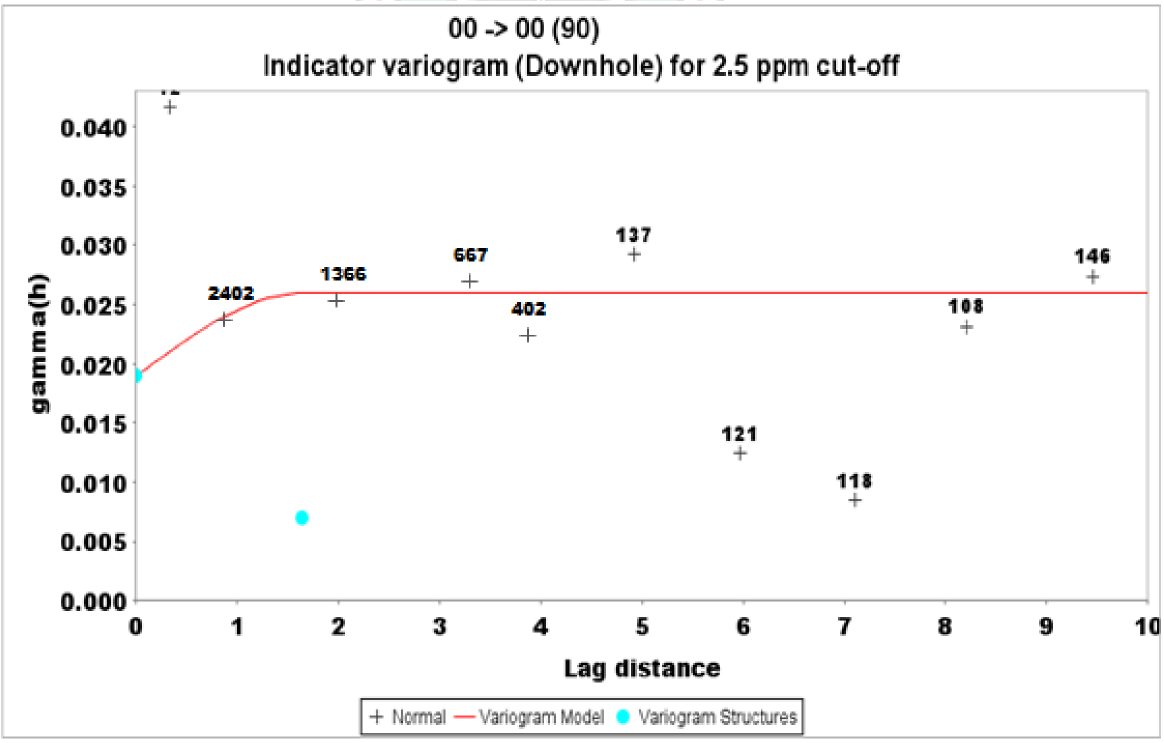
00 -> 00 (90)
Indicator variogram (Downhole) for 2.5 ppm cut-off
gamma(h)
0.040
0.035
0.030
0.025
0.020
0.015
0.010
0.005
0.000
0
1
2
3
4
5
6
7
8
9
10
Lag distance
2402
1366
667
402
137
121
118
108
146
Normal
Variogram Model
Variogram Structures

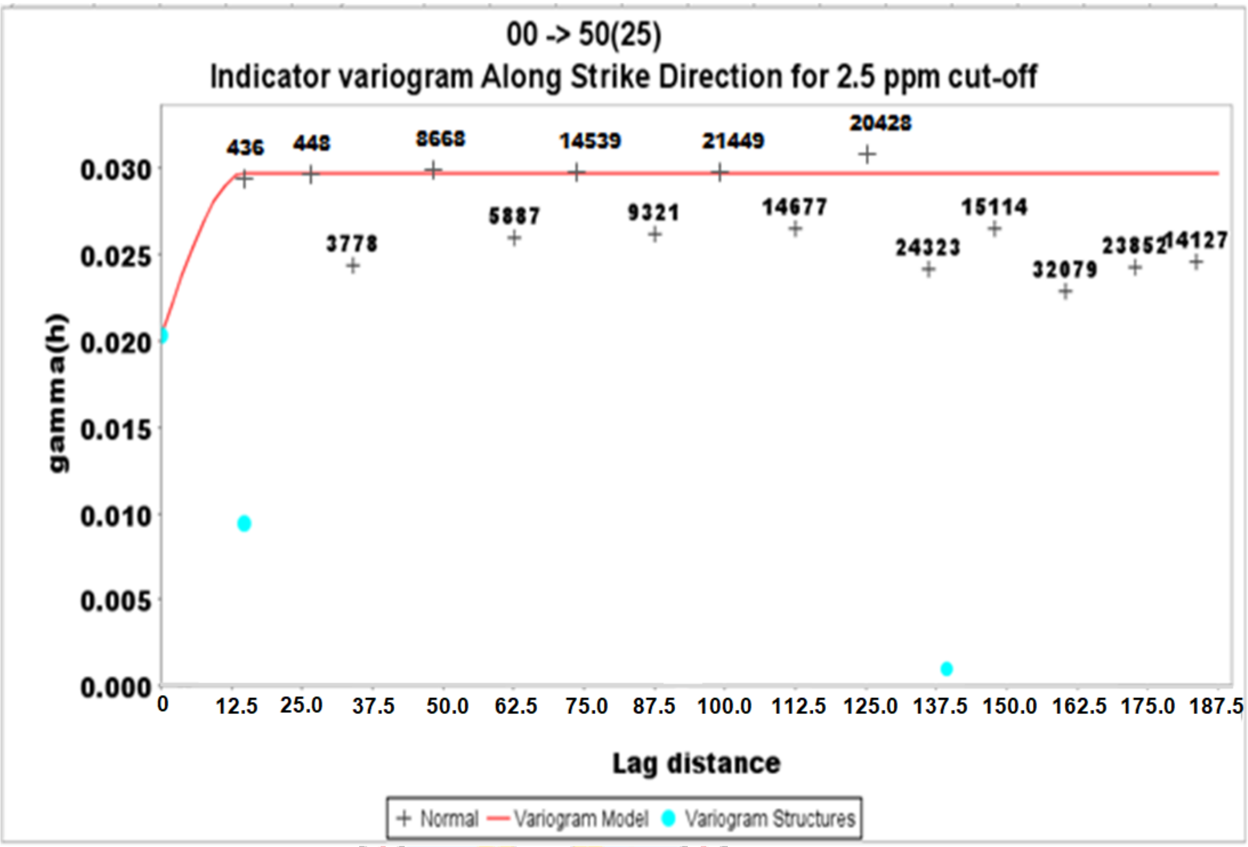
00 -> 50(25)
Indicator variogram Along Strike Direction for 2.5 ppm cut-off
gamma(h)
Lag distance
Normal
Variogram Model
Variogram Structures

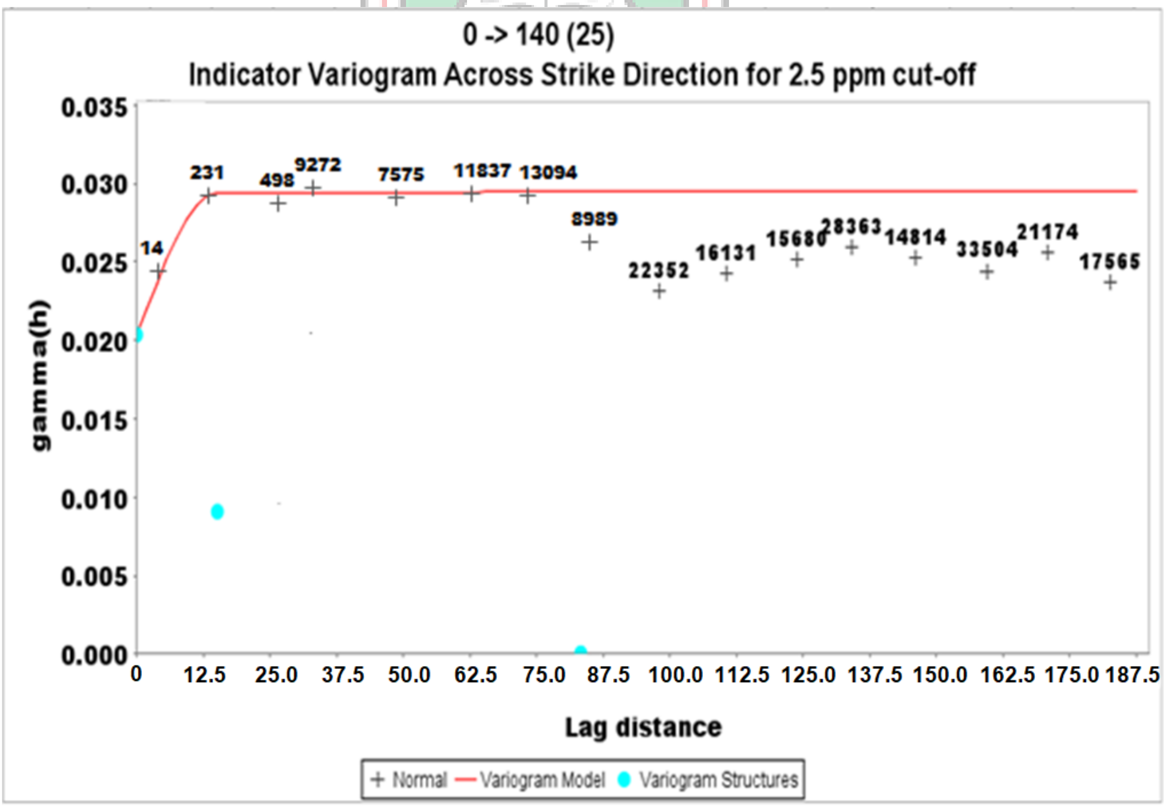
0 -> 140 (25)
Indicator Variogram Across Strike Direction for 2.5 ppm cut-off
gamma(h)
Lag distance
Normal
Variogram Model
Variogram Structures

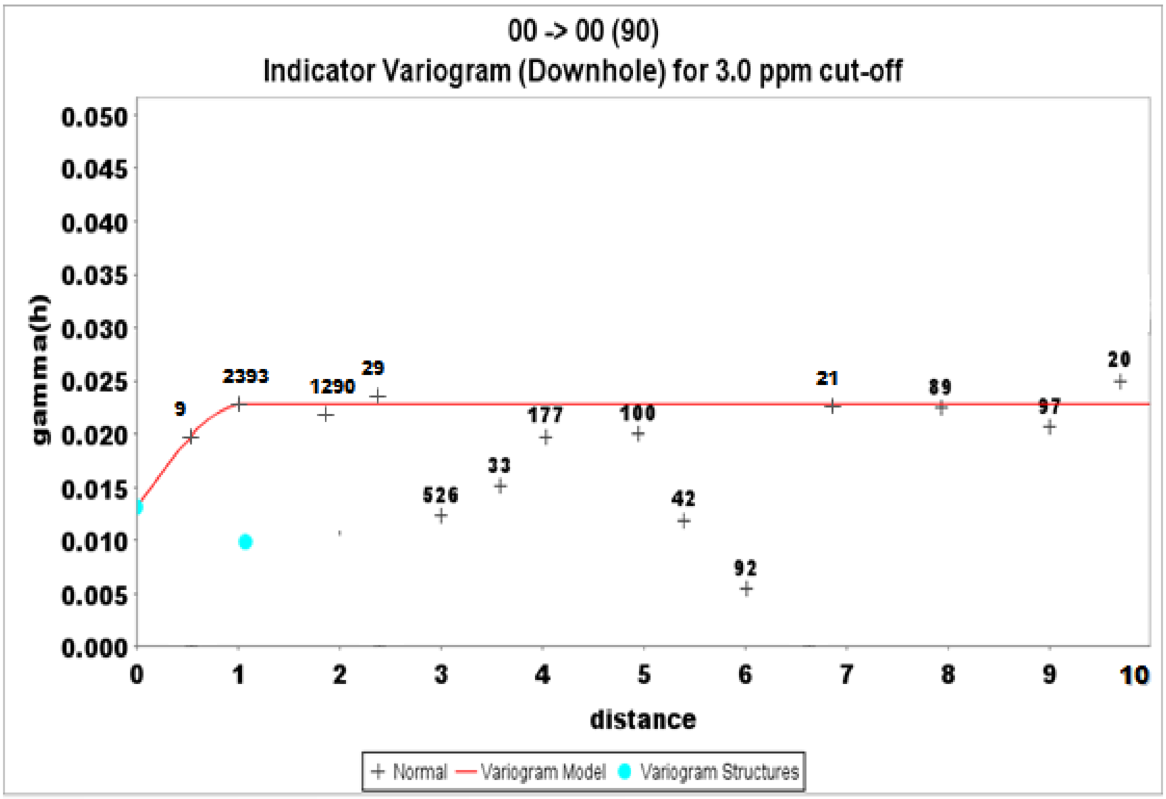

00 -> 00 (90)
Indicator Variogram (Downhole) for 3.0 ppm cut-off
gamma(h)
0.050
0.045
0.040
0.035
0.030
0.025
0.020
0.015
0.010
0.005
0.000
9
2393
1290
29
526
33
177
100
42
92
21
89
97
20
0
1
2
3
4
5
6
7
8
9
10
distance
Normal
Variogram Model
Variogram Structures

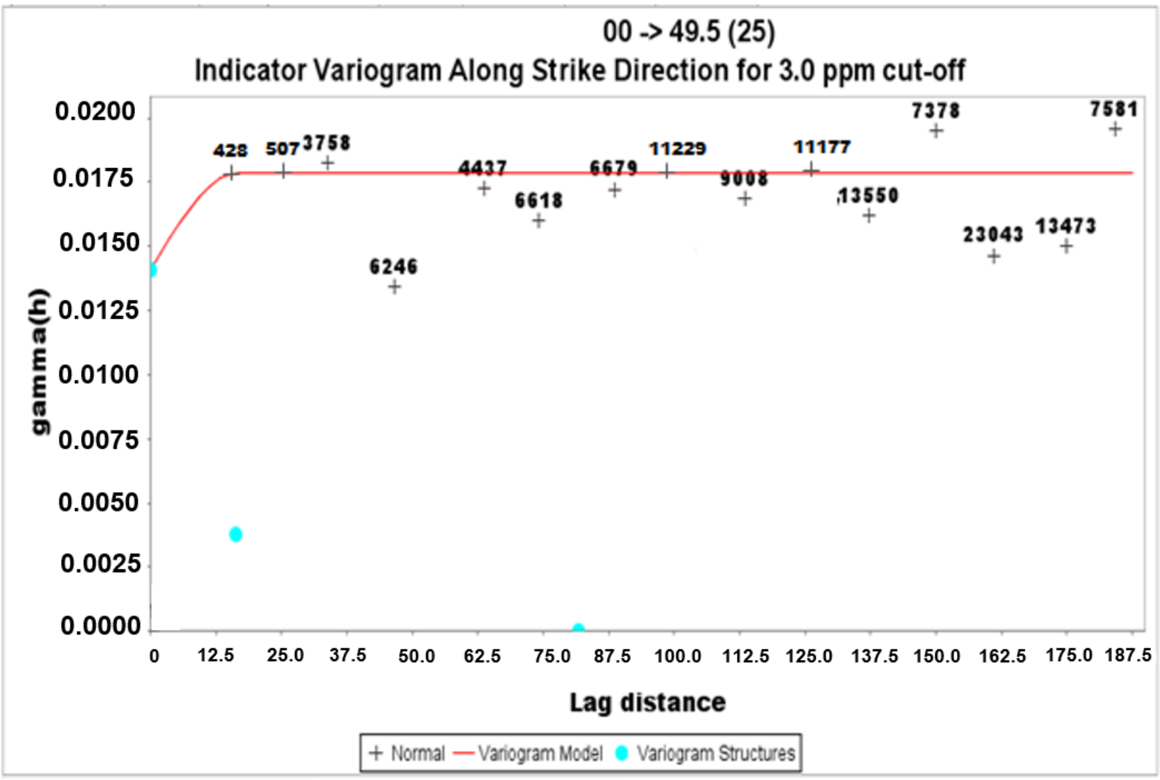

00 -> 49.5 (25)
Indicator Variogram Along Strike Direction for 3.0 ppm cut-off
gamma(h)
0.0200
0.0175
0.0150
0.0125
0.0100
0.0075
0.0050
0.0025
0.0000
428
507
3758
6246
4437
6618
6679
11229
9008
11177
13550
7378
23043
13473
7581
0
12.5
25.0
37.5
50.0
62.5
75.0
87.5
100.0
112.5
125.0
137.5
150.0
162.5
175.0
187.5
Lag distance
Normal
Variogram Model
Variogram Structures

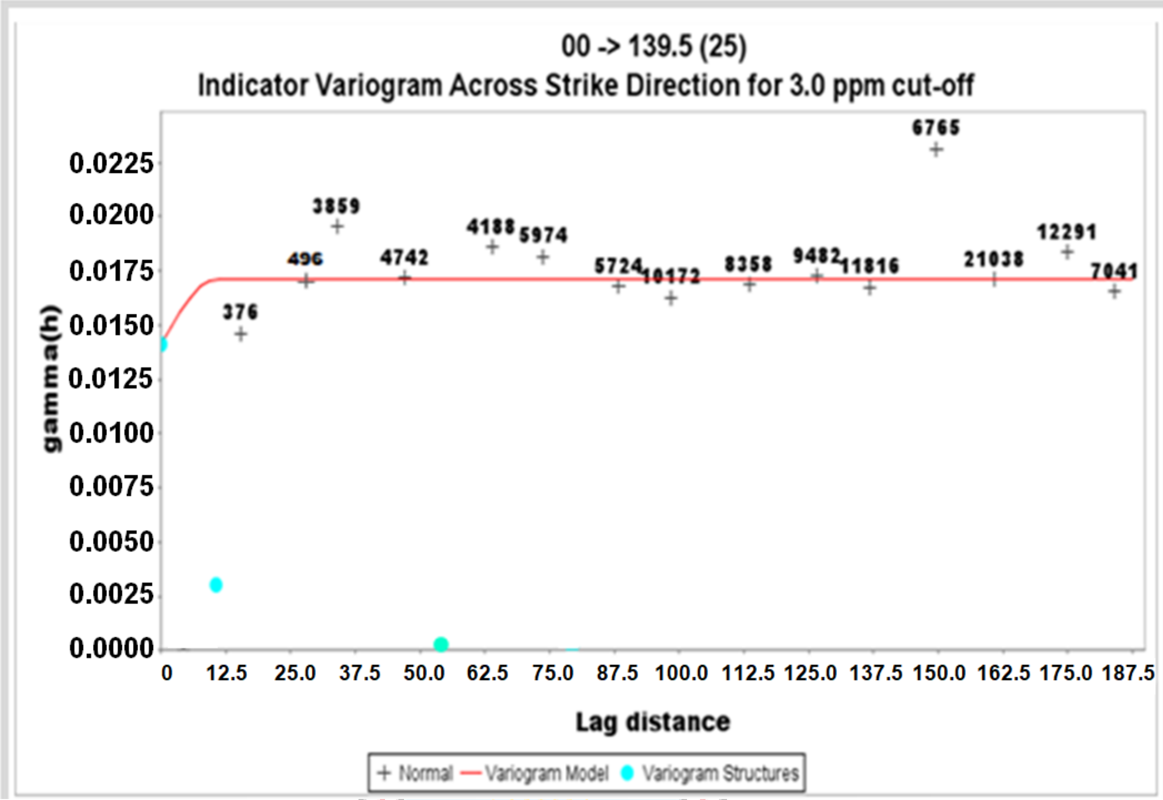
00 -> 139.5 (25)
Indicator Variogram Across Strike Direction for 3.0 ppm cut-off
gamma(h)
0.0225
0.0200
0.0175
0.0150
0.0125
0.0100
0.0075
0.0050
0.0025
0.0000
0
12.5
25.0
37.5
50.0
62.5
75.0
87.5
100.0
112.5
125.0
137.5
150.0
162.5
175.0
187.5
Lag distance
6765
3859
4188
5974
12291
496
4742
5724
10172
8358
9482
11816
21038
7041
376
Normal
Variogram Model
Variogram Structures

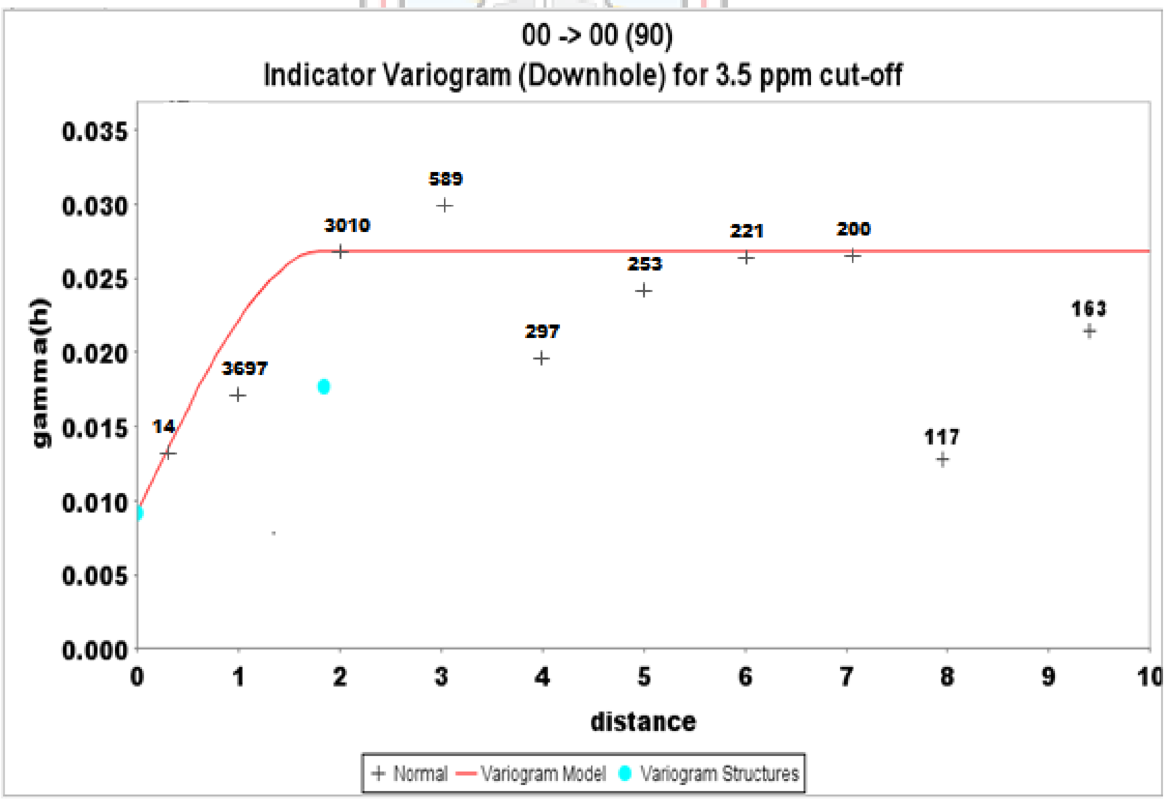
00 -> 00 (90)
Indicator Variogram (Downhole) for 3.5 ppm cut-off
gamma(h)
0.035
0.030
0.025
0.020
0.015
0.010
0.005
0.000
0
1
2
3
4
5
6
7
8
9
10
distance
589
3010
221
200
253
163
297
3697
14
117
Normal
Variogram Model
Variogram Structures

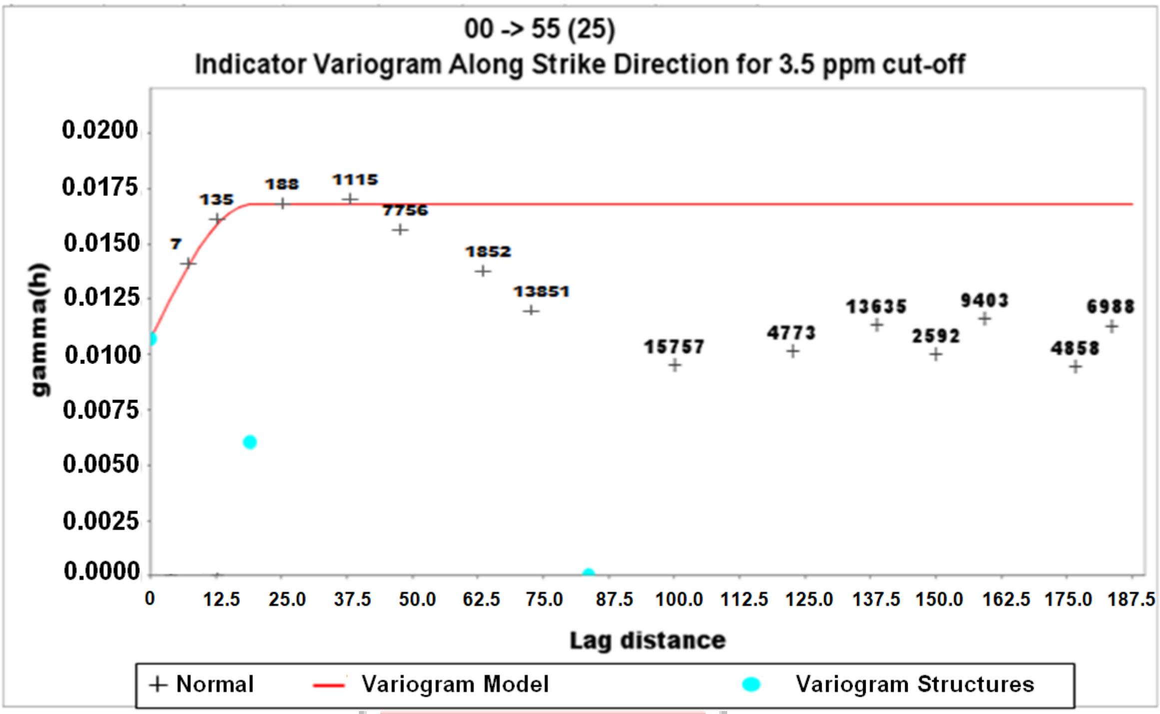

00 -> 55 (25)
Indicator Variogram Along Strike Direction for 3.5 ppm cut-off
gamma(h)
Lag distance
Normal
Variogram Model
Variogram Structures

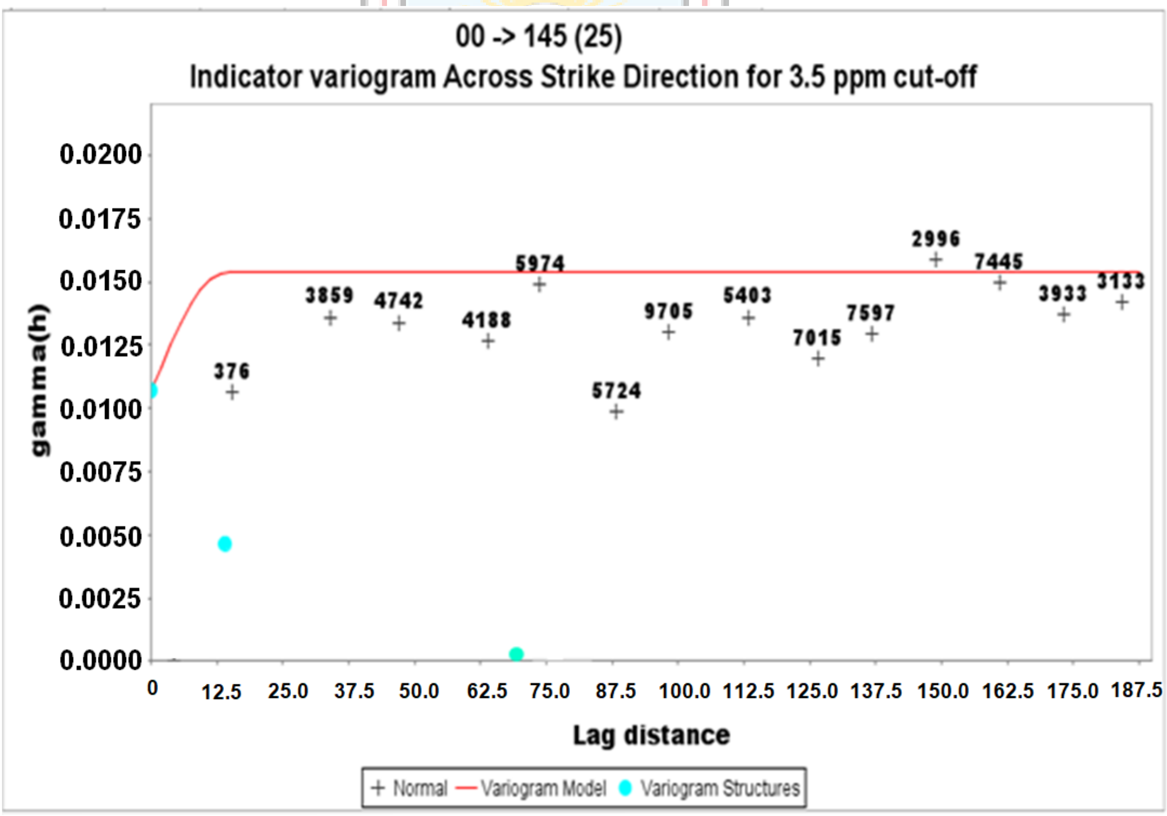

00 -> 145 (25)
Indicator variogram Across Strike Direction for 3.5 ppm cut-off
gamma(h)
Lag distance
Normal
Variogram Model
Variogram Structures

APPENDIX 3

OK Block Model Attributes

Attribute Name	Type	Decimals	Description
material	character		Material type
resource	real	1	Inferred, indicator and measured
sg	Float	1	Specific gravity of rocks
Pcode	real	1	Porosity code
nsamp	Integer		Number of samples
krig_efficiency	Float	1	Kriging efficiency
Kvar	Float	1	Kriging variance
avdis	Float	1	average anisotropic distance to samples
ndis	Float	1	Anisotropic distance to the nearest sample
au	real	1	gold grade
reef	character		Reef type
nsamp	Float	1	number of samples used for block estimate

MIK Block Model Attributes

Attributes Name	**Description**
_ikb#au#0.000_value	average grade of the entire block
_ikb#au#0.50_value	average grade of the block above the cut-off of 0.5
ikb#au#0.5_fraction	percentage/fraction of the block above the cut-off of 0.5
_ikb#au#1.00_value	average grade of the block above the cut-off of 1.00
ikb#au#1.00_fraction	percentage/fraction of the block above the cut-off of 1.00
_ikb#au#1.5_value	average grade of the block above the cut-off of 1.5
_ikb#au_0.5_fraction	percentage/fraction of the block above the cut-off of 1.5
_ikb#au#2.0_value	average grade of the block above the cut-off of 2.0
_ikb#au_2.0_fraction	percentage/fraction of the block above the cut-off of 2.0
_ikb#au#2.5_value	average grade of the block above the cut-off of 2.5
_ikb#au_2.5_fraction	percentage/fraction of the block above the cut-off of 2.5
_ikb#au#3.0_value	average grade of the block above the cut-off of 3.0
_ikb#au_3.0_fraction	percentage/fraction of the block above the cut-off of 3.0
_ikb#au#3.5_value	average grade of the block above the cut-off of 3.5
_ikb#au_3.5_fraction	percentage/fraction of the block above the cut-off of 3.5
_ikc#au#0.5	Proportion of the block below cut-off of 0.5
_ikc#au#1.00	Proportion of the block below cut-off of 1.00
_ikc#au#1.50	Proportion of the block below cut-off of 1.50
_ikc#au#2.00	Proportion of the block below cut-off of 2.00
_ikc#au#2.50	Proportion of the block below cut-off of 2.50
_ikc#au#3.00	Proportion of the block below cut-off of 3.00
_ikc#au#3.50	Proportion of the block below cut-off of 3.50

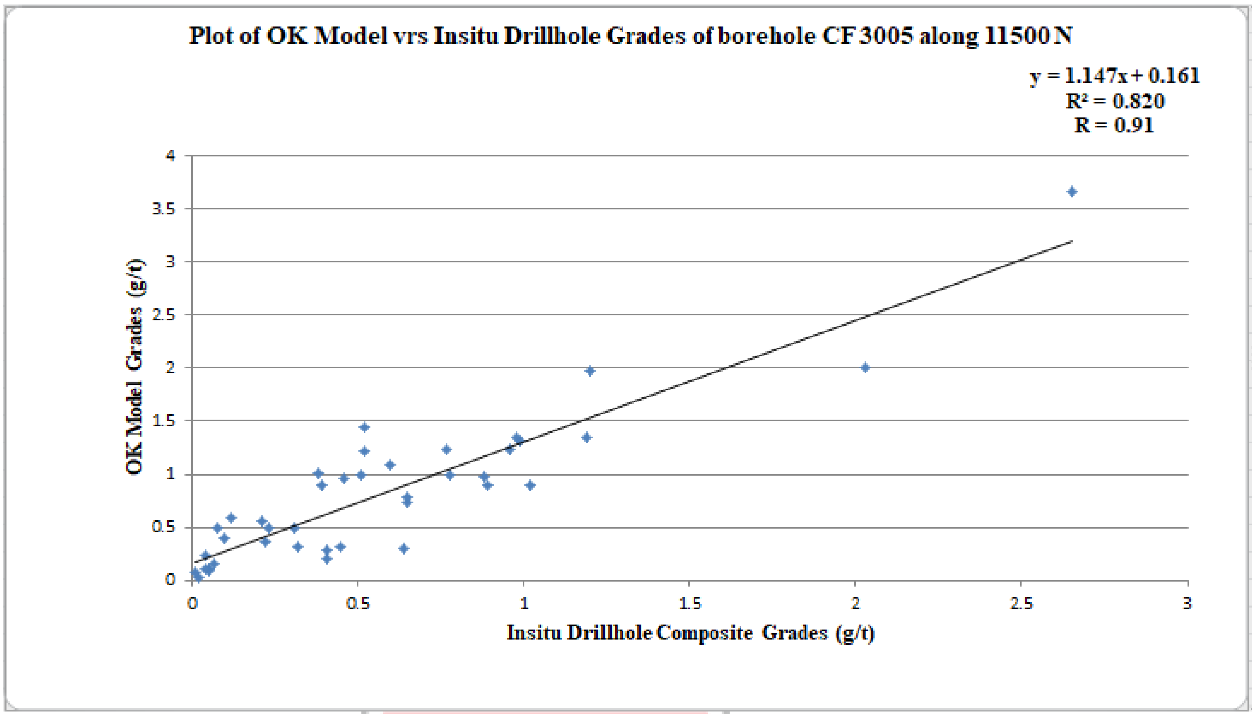

Scatter plot of OK vrs insitu grades of borehole CF 3005 along strike of the orebody.

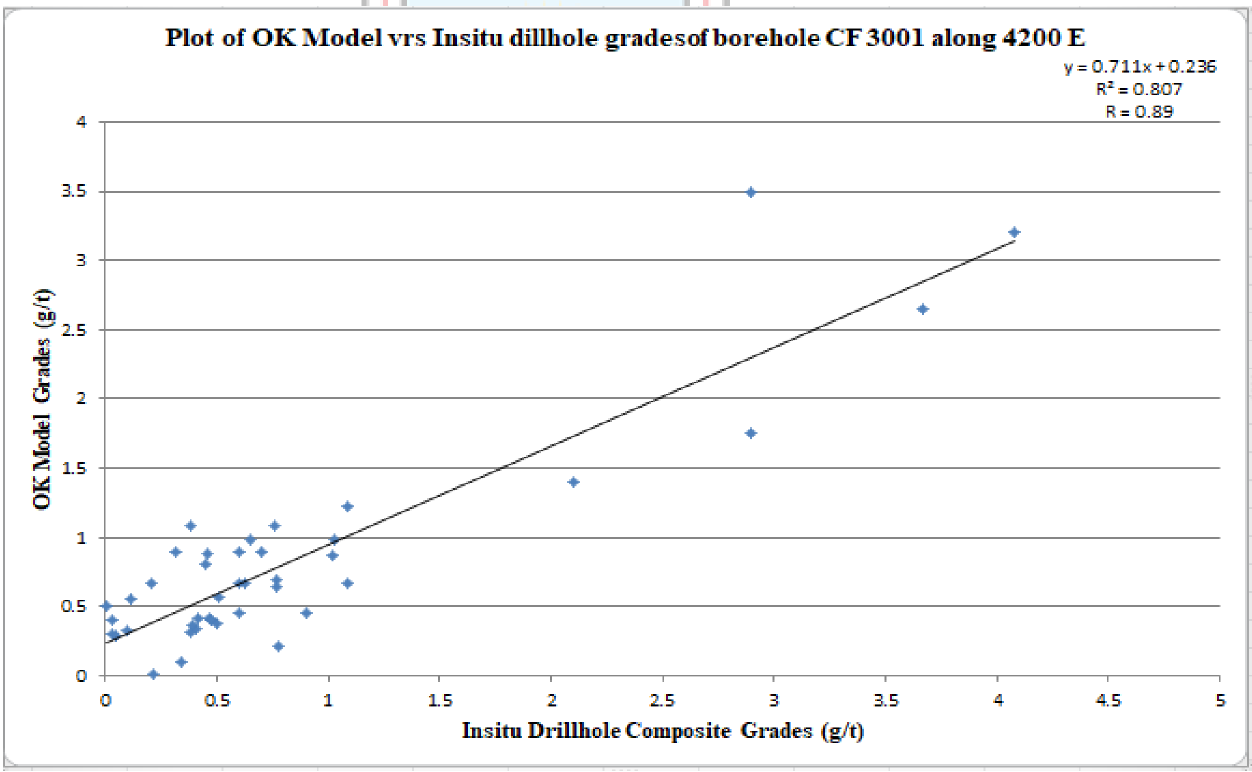

Scatter plot of OK vrs insitu grades of borehole CF 3001 across strike of the orebody

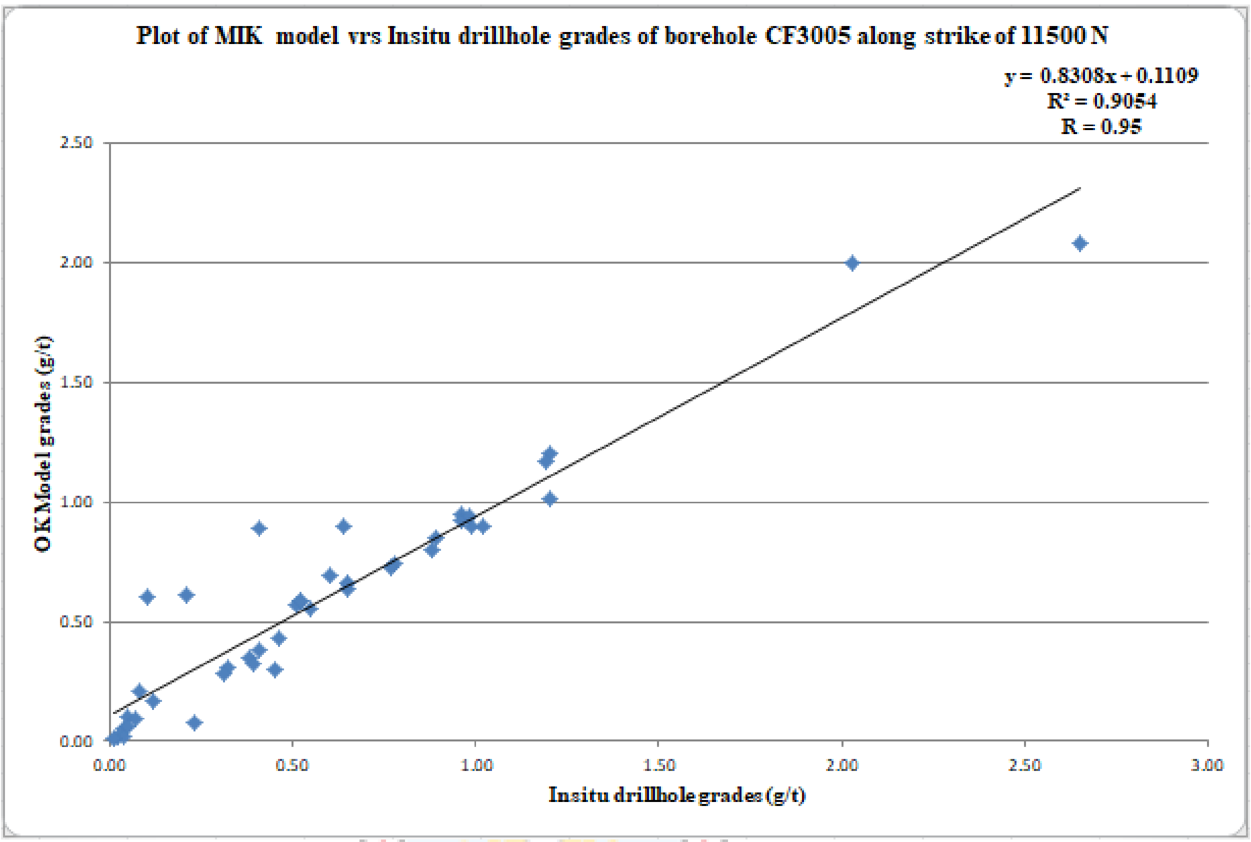

Scatter plot of MIK vrs insitu grades of borehole CF 3005 along strike of the orebody

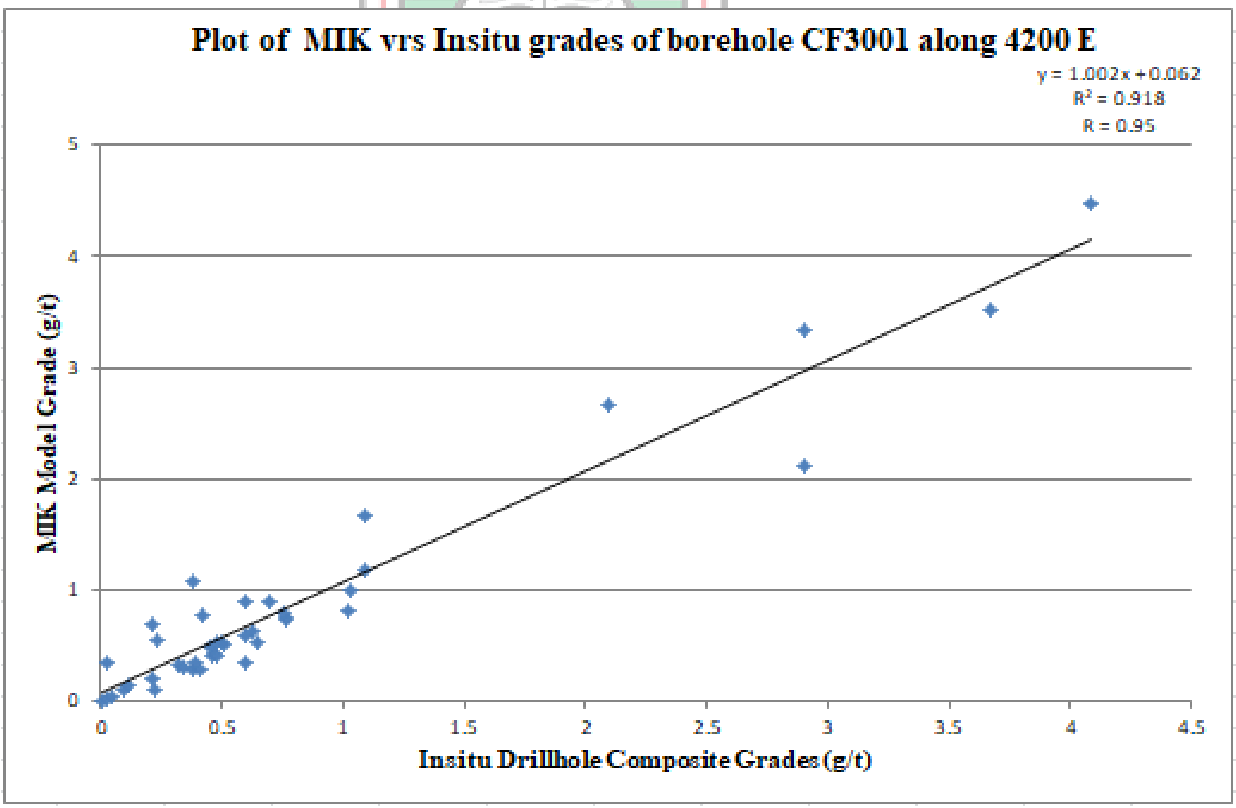

Scatter plot of MIK vrs insitu grades of borehole CF 3001 across strike of the orebody

Table 5.6 Results of Actual vrs OK and MIK Model Estimates from Kottraverchy Pit (AFC1 Reef Zone) from January, 2013 to December, 2013.

	Actual Mine Production			**OK Model**			**MIK Model**		
Month	Tonnes, ore (t)	Average grade (g/t)	Tonnage (t) x grade (g/t)	Tonnes, ore (t)	Average grade (g/t)	Tonnage (t) x grade (g/t)	Tonnes, ore (t)	Average grade (g/t)	Tonnage (t) x grade (g/t)
Jan	42617	0.62	26422.54	38250	0.73	27922.50	41020	0.61	25022.2
Feb	55041	0.60	33024.60	39734	0.61	24237.74	57525	0.59	33939.75
March	30893	0.69	21316.17	20337	0.79	16066.23	29250	0.68	19890
April	35326	0.65	22961.90	31230	0.69	21548.70	34992	0.66	23094.72
May	7896	0.67	5290.32	7500	0.71	5325.00	7739	0.66	5107.74
June	40107	0.69	27673.83	27183	0.75	20387.25	38552	0.69	26600.88
July	35796	0.73	26131.08	22580	0.61	13773.80	33855	0.71	24037.05
August	36811	0.73	26872.03	41220	0.82	33800.40	36477	0.72	26263.44
Sept	34022	0.81	27557.82	35248	0.88	31018.24	34837	0.82	28566.34
Oct	47648	0.76	36212.48	34655	0.79	27377.45	49677	0.75	37257.75
Nov	10664	0.69	7358.16	3252	0.82	2666.64	10100	0.66	6696
Dec	20340	0.77	15661.80	14380	0.81	11647.8	21592	0.76	16409.92
Total	**397161**		**276482.73**	**315569**		**235771.75**	**395616**		**272855.79**
Average		**0.696**			**0.747**			**0.690**	
	Weighted Average Grade = $\frac{\sum(\text{Tonnes x grade})}{\sum(\text{Tonnes})} = \frac{276482.73}{397161.00}$ **= 0.70**			**Weighted Average Grade** = $\frac{\sum(\text{Tonnes x grade})}{\sum(\text{Tonnes})} = \frac{235771.75}{315569.00}$ **= 0.75**			**Weighted Average Grade** = $\frac{\sum(\text{Tonnes x grade})}{\sum(\text{Tonnes})} = \frac{272855.79}{395616.00}$ **= 0.69**		

Index

A
AAS (atomic absorption spectrometer), 15
accumulation, 9, 25
accuracy, 17, 50, 54, 79, 83
Actual Grades of AFC1 -Reef Zone, 89
Actual Grades of AFC1-Reef Zone, 89
actual grade value, 75
actual mining production figures, 48
actual production values, 4
actuals, validation scatter plot of, 43
adjoining sections, 59
AFC1, 48, 63, 77, 89
Afc1 Ore Block Model Parameters, 77
Afc1 orebody, 78
AFC1-Reef, 87–88
AFc1 Reef Cut-off grade, 86
Afc1 Reef Indicator Variogram Parameters for MIK, 74
Afc1 Reef Omni-directional Variogram, viii, 64
AFc1-reef Values, 62
AFC1Reef zone, 91
AFC1 Reef Zone, 86, 90, 114
AFC1-Reef Zone, 62, 89
AFC1 resource analysis, 61
alternations, 9
analysis
  chemical, 17
  direction variation, 48
  statistical, 4, 22, 48, 58–59, 97
analysis protocols, 54
analytical results, 50
ancillary equipment, 14
Angular bisector methods, 24
angular bisectors, 24
angular tolerance, 64, 68
Anisotropic distance, 110
anisotropic ratios, 25, 69
  geometric, 25
anisotropies, 41
Anisotropy in grade continuity, 41
annual rainfall, 8
anticlines, 12
  north-east plunging, 12
aplite, 11–12
application, 25, 31
  mineral estimation, 41
applied model, 38
aqua regia, 17
aqua regia digest, 15
area
  catchment, 8
  complex, 14
  eastern, 8
  project, 56, 59
  total, 5
area range, 7
argillites, 10
  graded, 11
arithmetic, 18–19
arrangement, 17
artisanal workings, 5
assay data, 50, 57
  drill-hole, 50
assaying, 17–18, 39, 49
  reliable, 17
assaying process, 17
assay results, viii, 17, 50, 55, 101
assays, 17–18, 48, 52–53, 55, 75
atomic absorption spectrometer (AAS), 15
attributes, 18, 29, 46, 66, 78–79, 82
average anisotropic distance, 110
average depth, 48
average drill hole spacing, 68, 77
average grade, 31, 86, 90–91, 93, 114
average Kriging variance, 42, 75–76
average mining width, 48

B
Banket formation, 7
Basal reef, 11
basins, 9
batches, 50
batch rejection, 54
belts, 9
benches, 86–88
Bench MIK on Actual Grades of AFC1, 89
Bench Model Grades, 88
Bench Model Tonnages, 87

bench ore blocks, 15
better grade correlations, 83
Birimian lithology, 10
Birimian mafic volcanics, 9
Birimian metasedimentary rocks, 9
Birimian metavolcanic rocks, 9
Birimian rocks, 9
blank samples, coarse, 50
block, 4, 16, 25–33, 35, 46, 78, 82, 111
block cell, 78
block centre, 25
block estimates, 93, 110
block grade, 27–28, 33–34
  probability of, 34–35
block mode, 46
block model cut-off grades, 82
block models, 43, 46–47, 66, 77, 79, 82
block size, 48
borehole, 112–13
boreholes, surrounding, 60
boundary, lower, 19
Breccia reef, 11
bulk, 20
bullion bars, 15
burn farmland, 8

C

carbonate, 11
  ferrious, 12
Carbon movement, 15
carried interest, free, 5
chlorite, 9, 11–12
chloritoid, 9, 11
  whithout, 11
class, 19, 67–68
climatic condition, 8
closed string, 45
collars, 15, 48–49
  missing, 50
colour, 8, 10, 12
colour banding effects, 11
commencement, 14, 16
commonality, 22
composite grades, 79, 81–83, 85–87
composites, viii, 61, 80
composite samples, 61
computation, 67
concession boundary, 8
conditional expectation, 28
configuration, 16
conglomerates, 11, 14
constant, 18, 37, 40–41
  perfect regression, 43
construction, 45
contamination, 18, 50
  monitor, 50
contamination index, 50
contemporaneous, 9
continuity, 26
  major, 66
  maximum, 64
control, 36
  spatial, 25
control points, 45
convectional Carbon-In-Leach, 15
core logging, 18
core samples, half, 52
correlation, 40
  auto, 40
  fair high positive grade, 82
correlation analysis, 88
correlation coefficient, 43, 76, 82–83
  better, 90
  good, 52
covariance, 23, 27–28, 40, 62
creation, 3, 46
crusher, 15
  primary jaw, 15
  secondary cone, 15
  toggle jaw, 15
crushers, primary, 15
curves, 37–38, 87, 90
  cumulative, 30
  cumulative probability, 30
  frequency distribution, 18, 21
  grade/tonnage, 29
  grade-tonnage, 87, 93
  grade tonnage relationship, 90
cut-off grades, 29–31, 67, 78, 85, 90
  economic, 59
  selected, 30
  upper, 63

cyanide solution, 15
hot caustic, 15
cyclone overflow, 15

D

data
drill hole, 43, 58, 61
interpreting, 18
lithology, 55
logging, 46
point, 42
retrieved, 3
secondary, 48
structural, 48, 93
time, 48
data array, 42
database, 17
company’s, 48
database section, 48
data distribution, 18, 28
data pairs, 35
data points, 26, 39, 45, 75
adjacent, 45
data processing, 3–4, 55
data sets, 19, 22, 29, 61
data support, 29
data validation, 3, 49
data values, surrounding, 42
data variance, total, 40
data variation, 18
deficiencies, 3
deformation, 9
deformational fabrics, 9
degree line, 42–43
degrees of freedom, 22–23, 102
delimitation, 24
dendritic growth, 12
density, 48, 78
deposit, 1, 3, 11–12, 18, 25, 36, 43–44, 46, 48, 63
design capacity, 15
detection, 18
visual, 18
difference, 3, 25, 35, 40, 59
absolute, 53
digital terrain model (DTM), 44, 46
digitisation, 4
digitised wireframe string, viii, 59
digitising, 59
dilution, 1, 14
dip, 7, 12, 48, 66, 69, 77, 79, 83
steep, 66
dip angles, 12
directional, 68
direction perpendicular, 41
drill hole, 48, 79
drillhole, 55, 86–87
drill hole, in-situ, 83
drillhole collars, 55
drillhole data, 30
composited, 63
drillhole database, 55
drillhole layout, 48–49
drillhole spacing, 48
drilling, 15, 18, 58
drilling types, 58
drill rigs, 14
duplicates, coarse, 17

E

electro wining cell, 15
elevation, 7–8
ellipse, 25
search, 25
ellipse axes, 25
equidistant, 29
equivalence, 58
equivalency, 22
errors, 17–18, 26, 49, 60, 75–76, 95
absolute, 42
data compilation, 39
human, 17
measurement, 39
minimising, 26
minimum estimation, 27
systematic, 26
estimated values, 26, 42–43
assigned, 46
best, 27
estimates grade, 43
estimation, 3, 15–17, 25, 27–28, 63–64, 82
grade/tonnage, 18

estimation errors, 26
estimation location, 33
estimation method, 1, 4, 25, 93
  better, 88
  non-linear, 26, 28
  preferred, 91
estimation model, 18
estimation problems, 62
estimation procedures, 35, 41
estimation variance, 27
estimators, 26, 44, 86
  good, 93
evaluation, 17, 50
excessive smoothing, 25
experimental variograms, 38, 68
exploration, early, 16
extension, 36, 44
extraction, 3, 14

F

faults, 60, 65
  large thrust, 12
  major, 60
  major thrust, 9
  minor, 9
  reverse, 12
felsic dykes, 9
fertility, poor, 8
fitting, 38, 42
folds, open, 11
footwall quartzite, 11
forest, secondary, 8
fossil placer, 11
fraction percentage/fraction, 111
freedom, 22–23, 102
function, 27, 30, 35
  exponential distance, 24
  probability density, 20

G

Gaseous oxygen, 15
generation, 22, 58
geological boundaries, 46
geological continuity, 18
geological influence, 16
geological interpretation, 46, 59
geological logging, 52
geological mapping, 18
geological models, 14, 46
  conceptual, 46
geological phenomenon, 40
geological structures, 3
  incorporated, 93
geological supervision, close, 14
geological zones, 46
geologic explanation, 41
geologic interpretation, 43
geologists monitor, 14
geology, 7, 15, 48, 95, 97, 99
geometric support, 18
geophysical anomalies, 16
geostatistical, 94
geostatistical analyses, 3
gold, 1, 11, 14–15, 17, 28, 50, 98–99
  aid, 15
  metallic, 15
  open-pit, 14
  underground, 5
gold-barren phyllite, 50
gold concentration, 14
gold deposits, 61–62
gold grades, 17, 31, 110
gold mineralisation, 61
  noneconomic, 10
gold-rich solution, 15
gold value, known, 54
grade conditions, 34
grade continuity, 41
grade control, 15
grade control information, 14
grade estimation, 3, 79, 82, 98
grade interpolations, 4, 79, 83
grade interval, 34–35
Grade Interval Mean Grade Median Grade, 32
grade map, 29
grade resource estimates, 46
grades, 1–3, 15–16, 18–20, 24–25, 27–31, 33–36, 43–44, 46, 60, 82, 84, 86–88, 90, 93, 114
  actual, 3, 87–88
  cut-of, 29

estimate, 79, 88
expected, 34
extreme, 34
high, 18, 29, 54, 59, 63
in-situ, 87
interval, 34
low, 9, 29, 40, 54
maximum, 35
median, 34
medium, 54
model and composite, 81
sample, 31
unknown, 26
grades and tonnages, 1, 16, 93
grade threshold, 67
grade variability, 39
gravity, 78, 110
greenish-grey feldspathic quartzite, 10
greenish-to-pale-grey, 12
grid pattern, 15
grits, 10
ground, 16, 18
groups, 5, 22, 29, 58
super, 10
guides, 59, 96

H

high grade ores, 32
high-grade outlier samples, 63
high grade samples, 63
histogram scale, 29
historical classified resource cut-offs, 32
holes, 15, 48, 56, 61
inclined, 15
linking drill, 24
vertical, 15
horizontal planes, 43, 68
hydrated iron oxides, 8
hydrogen peroxide, 15
hydrothermal activity, 9
hydrothermal alterations, 14

I

improvement, 3
inconsistencies, 49–50
independence, attained, 5
indicator cut-offs, 32
indicator interval, 31
indicator transform, 28
indicator variable, 3, 28–29, 68
indicator variogram models, 69
influence
climatic, 8
disproportionate, 63
information, 4–5, 16–17, 42–43, 78
gathered, 48
spatial, 36
surface mapping, 46
information input, 36
information processor, 36
intercalated argillite layers, thin, 12
intercepts, 43, 60
drillholes, 45
interruption, major, 8
intersection form, 24
interval errors, 49
isoclinal folding, 9
isotropic, 41
issued shares, 5

K

kriging, 3, 26–30, 35, 96
kriging coefficient, 27
kriging efficiency, 110

L

laboratory, 17, 50, 52–54
analytical, 17
lacustrine deposit, 11
lag distance, 35
maximum, 64, 68
lag spacing, 64, 68
lenticular orebodies, 44
level, 16, 40, 58–59, 103
given, 22–23
linear drift, 37
linear methods, 3, 28
linear model, 36
link attributes, 25
lithological, 49
lithologic model, 36
lithology, 9, 18, 40, 48

loaded carbon, 15
low grade samples, 63

M
magnetite, 11–12, 14
magnetite banding, distinct, 12
mapable units, 9
material
  grained, 11
  homogeneous, 54
  mineral, 14
material type, 78
matrix, 14, 28
matrix form, 27
measurement observations, 36
measures
  autocorrelation, 23
  quality control, 17
metamorphic, 14
metamorphism, regional, 9
meta-sediments, 9
meta-volcanics, 9
methods
  analytical, 50
  cross-sectional, 24
  polygonal, 24
  sectional, 24
  sensible, 44
  standard, 17
  triangular, 24, 45
  t-test, 58
micro-variability, 40
middle value, 19
mined survey boundary, 78
mineral deposits, 16, 37, 41, 99
  sedimentary, 14
mineralisation, 14, 16, 24–25, 40, 44, 65–66
  plane of, 41
mineralised corridors, 49
mineralogical domains, 61
mineral resource, 3, 25, 48, 96, 99
mineral resource estimation, 3–4, 18, 22–24, 94, 96
mineral resource evaluation, 36, 98
minerals, 17, 94
  assessor, 14
  common, 9
mines, 5, 94, 96–98
minimum, bearest, 26
minimum value, 62
mining, 1, 5, 14–15, 95–99
mining area, 8
mining bench, 77
mining bench height, 48
mining company, 17
mining concession, 5
mining operation, 15
mining projects, 16
modelled orebody geometry, 16
modelling, 3, 17–18, 30, 44–45
  horizontal directional variogram, 66
  sectional, 44
modelling methods, 44
modelling process, 43
modelling semi-variograms, 41
models, 15, 21, 25, 35–38, 41, 46, 75, 79, 81, 86, 114
  dimensional, 45
  good, 76
  satisfactory, 42
  sectional, 44
  single, 40
  solid, 43, 46
  string, 44–45
  unbiased, 76
modification, 46
moist semi deciduous forest, 8

N
natural log, 28
nearest samples, 25, 110
nearest waste dump, 15
nested structures, 40, 65
  depicted, 69
network, 45
  undulating patchwork form triangular, 44
non-linear transformation, 28
non-transitional models, 36
nugget effect, 36
nugget variance, 39–40, 64, 68
  high, 18

O

open pit, large-scale, 5
open pit operation, large, 1
operations, 5, 8
  underground, 5
ore, 1, 14–17, 24, 31, 82, 86, 98, 114
  actual, 90–91
ore blocks, 1, 24
ore body, 48
orebody, 14, 16, 24, 41, 43–44, 58, 64–66, 77, 79–81, 83–85, 98, 102, 112–13
orebody modelling, 43
orebody wireframe model, 77–78
ore cut-off grade, 78
ore deposits, 1, 38
ore reefs, 93
ore zones, 3–4, 59, 78
  constrained, 78
organic contents, low, 8
origin, 37–38
  fluvial, 10
orogeny, 9
  eburnean, 9
orthogonal directions, 41
outliers, 18, 23, 61–63
  effects of, 23, 29
  low grade, 18
overestimation, consistent, 26
oxide, 50
  manganese, 12
oxidizing agents, 15

P

parabolic, 37
parallel dissection, 44
parameters, 18, 23, 42, 75, 79, 82
  block modelling, 77
  flow, 12
  indicator variogram model, 69
  statistical, 23
patchwork quilt, 44
peakedness, 21
pebbles, 14
  packed, 14
  rounded quartz, 11
penetration, 16
perpendicular bisectors, 24
phylite, 11
Physical identification, 23
plane, 65
planimeter, 44
  digital, 24
planners, 14–15
point kriging, 75
polygons, 24
pophyroblasts, 11
populations, 8, 19, 22–23, 36, 58, 63
  identical, 59
  total, 29
power
  high, 25
  low, 25
power index, 25
precision, 17, 50, 53–54
  good, 52
  high, 52–53
predetermined upper limit, 23
prediction, 16, 95
preparation, poor, 18
probability estimation location, 34
probability function, 29
procedure, analytical, 16
processes, 4, 15–17, 75
  wireframe verification, 60
processing, 15, 49–50
pulp, 15, 50
pulp duplicates, 17
pulp samples, 50
pumping carbon, 15

Q

quality, 16–17, 50, 55
  control assaying, 17
  control sampling, 17
  poor, 18
  preparation, 17
quality resource model, high, 16
quartz, 9–10, 12
quartzite, upper, 11
quartz veins, 11

R
rainfall, high, 8
random component, 18
range, 8, 36–42
  longest, 41
  shortest, 41
reanalysing, 23
recognition, 1
recommendations, 4, 93
  following, 93
recorded measurements, 36
recoverable reserves, estimating, 1
recovery, poor, 18
reefs, 11–12, 14, 78, 93, 97, 110
  conglomerate, 11
  middle, 11
reference plane, 45
regionalisation, 40, 42
regionalised variance, 37, 39–40
regression line, 43
rehabilitation purposes, 14
relationship, 28, 36, 76
  good positive, 82–83, 90
  strong, 43
repetition, 12, 30
representation, 16, 36
  better, 34
  computer-based, 46
  graphical, 54
  spatial, 25
reserve estimations, 26
resource, 16, 24, 26, 79
  reliable, 17
resource block model, 46
resource estimation, 4, 16, 23, 26, 48, 56, 59, 79, 96
resource estimation methods, 3, 16, 24
resource work, 50
respective models, 29, 82
results, 4, 25–26, 29–30, 48, 50, 53, 58–59, 65, 86
reverse circulation. *See* RC
Reverse circulation holes, 49
ridges, 7
  pronounced, 7
risk, high, 16
rivers traverse, major, 8
road, 6, 95
rocks, 10, 110
  clastic metasedimentary, 9
  fresh, 14, 16
  stacked fluvial sedimentary, 11

S
sample data, 33
sample data set, 42
sample length, 61
sample location pattern, 27
sample locations, 27, 33
sample pairs, 35, 53
sample point locations, 75
sample points, 24
sample populations, 23, 63
sample precision, 52
sample preparation, 17
  laboratory's, 54
sample RC, 102
sample rifter, 15
samples, 15–20, 22–28, 30–32, 35, 40, 48, 50, 52, 54–56, 58–59, 61–63, 79, 83, 100, 102–3
sample sites, 24
samples krig, 110
samples ndis, 110
sample types, 58
sample variance, 20, 94, 103
sample variogram, 38
sampling
  geochemical, 16
  good, 16
sampling errors, 39
sampling interval, 40
sandstones, 10–11
  interbedded green, 11
sandstones/quartzites, 7
sandy, 11
scarp slopes, 7
search ellipsoid, 66
sectional interpretation, 15
sediments, 11, 98
  shallow water deltaic, 9
segments, 59

selection, 44, 61
selective mining method, 1
selective mining unit, 48
selective surface mining methods, 14
semi variance, 39
semi-variance, 35
semi-variogram analysis, 4
semi-variogram curve, 38
semi-variogram model analysis, 38
semi-variogram model parameters, 42, 75
  directional, 64
semi-variogram models, 29, 36, 40, 42, 69
  directional indicator, 68
semi variograms, 26
semi-variograms, 26, 28–29, 39–41, 64, 95
  experimental, 23, 40
  omni-directional downhole, 64
  theoretical, 36
sequence, 9, 11
  metamorphosed rock, 8
  thick, 9
sericite, 9, 11–12
shearing, 9, 65
short-term mining scheduling, effective, 15
silica impurities, 8
sill, 11, 36–42, 79, 83
  finite, 36
slope, 40, 43
soils, 8
solids, 59–60, 78
solid wireframe grade control model, 15
sorted large pebble conglomerate, 10
source, partial, 10
spatial component, 40
spatial continuities, 35
spherical model, 37–39, 69, 75
  schematic, 38
splitting process, good, 52–53
spot height string, 45
stage riffle splitter, 49
standard deviation range, 50, 55
statistical table, 59, 103
statistical tools, applying, 26
statistics, 18, 42, 58, 62, 75, 95
  classical, 18, 97
  classical parametric, 26
  conditional, 67–68
statistics for geoscientists, 98
statistics made simple, 96
statistics textbooks, 22–23
std, 55
steel wool, 15
stratigraphic, 9
stratigraphy, 9, 11
  schematic, 12
strike, 12, 48, 64, 66, 68–69, 77, 79–83, 85, 87, 112–13
strike length, 48, 59
strike perpendicular, 66
string, open, 45
string lines, 44
string menu, selected, 68
strings, 44–45, 59
  adjacent, 44
structural attritudes, 66
structural complexities, 36
structure, 36, 39–40, 43, 99
  geologic, 43–44
  long range, 65
  pitching fold, 7
  sedimentary, 10
  showing Nested, 41
  solid design, 46
structured discontinuities, 11
sub-angular grains, 12
submission point, 17
sub-population, 29
sub-populations, distinct, 63
succession, 37, 44
suitability, 21
Sulphide mineralisation, 14
surface, 5, 14, 44, 48
surface wireframe, 46
  down-hole, 48
  drill hole collar, 18
surveyors peg, 14
survey pickup, poor, 18
synclines, 8, 12
system
  braided fluvial, 12
  braided river, 11
  dimensional, 46

drainage, 8

T
tail, 20
skewed, 34
upper, 32
tangent, 37–38
tanks, 15
leach, 15
techniques
analytical, 17
following, 17
observation, 17
spatial interpolation, 28
tectonic, major, 9
temperatures, monthly, 8
terpolation-works.htm, 94
test, 22–23, 58–59
tailed, 59, 103
thickness, 10, 24–25, 40, 59
insignificant, 59
three-metre flitches, 14
threshold, 29–30, 68
given, 30
given indicator, 3
respective indicator, 33
threshold length, 61
threshold values, 30, 68
defined, 29
tie lines, 24
constructing, 24
tonnage curves, 87, 90
tonnage discrepancies, 1
tonnage reconciliation, 3
tonnages, 1, 3, 16, 43, 46, 78, 86–88, 93, 114
actual, 86
lower estimate of, 90, 93
production, 91
recoverable, 90
tonnes, 2, 86, 88, 114
cut-off grade, 82
top-cut value, upper, 63
topography, 7, 48, 78
topsoil, 14
triangles, 24, 45, 60
triangular lines, 46
triangular patches, 44
triangular plates, 45
triangulated surfaces, 60
tributaries, 8
tropical rain forest, 8

U
unbiased linear estimator, 27
best, 26
uncertainties, 16
underestimation, 26
underground, 5
univariate statistic, 62
upstream, recovered, 15

V
validation, 4, 42, 48, 50, 75, 79, 83, 93, 99
spherical variogram model, 75
valleys, 7
value average grade, 111
values, viii, 3, 19–20, 22–23, 25–26, 28–30, 32, 35, 39–40, 42, 54–55, 58–60, 63, 68, 75–77
actual, 42–43, 76
assay, 21, 49, 101
calculated, 59, 103
estimated/predicted, 76
extreme, 19, 28
gravity, 48
kriged, 30
measured, 25
negative, 20
pair, 53
predicted, 75
sample, 33, 40, 68, 75
single, 32
skewness, 20
table, 22–23
tabulated, 59, 103
zero, 20
variability, 20–21, 23, 26, 40
variable, 3, 26, 28
estimated, 25
real-valued random, 20
regionalised, 35, 40

transformed, 29
variable amount, 12
variance, 19–20, 22–23, 26–28, 35, 37, 40, 58, 62, 75, 102
identical, 58
kriging, 27, 96
population, 40, 103
variants, 26
variation, 8, 21
moderate-to-high grade, 62
varied tools, 25
variogram, viii, 27
experimental semi, 35
variogram analysis, 63
variogram curve levels, 40
variogram parameters, 48
variography map, 66
vegetation, 8
vertical dimensions, 48, 77
vertical samples, 48
vertices, 24
vicinity, 5, 8, 11, 30

W

waste, 1, 32
waste material, 15, 78
water, shallow, 10
weighted linear combinations, 26
Weighted square error, 75
weighting coefficients, 28
satisfactory, 27
weighting factors, 24, 27
weights, 25–28, 33
total, 27
wet season, 8
whiles, 20, 25, 58, 79, 82
polymictic, 11
skewed, 90
transition models, 36
wireframe, 3–4, 43, 58–59, 61, 63, 93
dimensional, 60
solid, 78
triangulated 3-dimensional, 59
wireframe model, 3, 46, 61
wire frames, 45
wireframe Topo, 78
work, 4, 17, 28, 38, 50, 53–54, 58, 77–79, 82
work Reverse Circulation, 16
circular, 41
continuous conglomerate, 14
elliptical, 41
mineralised, 59
poor, 37
shear, 40
transitional, 14